



LIBRARY  
Michigan State  
University

This is to certify that the  
dissertation entitled

INTEGRATION OF PHYSIOLOGICAL, METABOLIC AND  
GENETIC INFORMATION TO IDENTIFY THE MECHANISMS  
OF FREE FATTY ACID TOXICITY TO HEPATOMA CELLS

presented by

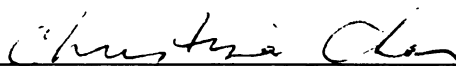
SHIREESH SRIVASTAVA

has been accepted towards fulfillment  
of the requirements for the

Ph.D.

degree in

Chemical Engineering and  
Materials Science



Major Professor's Signature

1/5/07

Date

**PLACE IN RETURN BOX** to remove this checkout from your record.  
**TO AVOID FINES** return on or before date due.  
**MAY BE RECALLED** with earlier due date if requested.

DATE DUE	DATE DUE	DATE DUE

**INTEGRATING PHYSIOLOGICAL, METABOLIC AND  
GENETIC INFORMATION TO IDENTIFY THE  
MECHANISMS OF FREE FATTY ACID TOXICITY TO  
HEPATOMA CELLS**

By

**SHIREESH SRIVASTAVA**

A DISSERTATION

Submitted to  
Michigan State University  
in partial fulfillment of the requirements  
for the degree of

DOCTOR OF PHILOSOPHY

Department of Chemical Engineering and Materials Science

2007



## **ABSTRACT**

### **INTEGRATING PHYSIOLOGICAL, METABOLIC AND GENETIC INFORMATION TO IDENTIFY THE MECHANISMS OF FREE FATTY ACID TOXICITY TO HEPATOMA CELLS**

By

**SHIREESH SRIVASTAVA**

The development of novel high-throughput techniques has made it possible to identify the global metabolic and genetic responses of the cells under a variety of conditions. The challenge is to efficiently analyze and relate the multi-source high-throughput data to generate novel information about cellular responses. The contributions of this thesis is the characterization of physiological, global metabolic and genetic alterations caused by different types of free fatty acids (FFAs) and tumor necrosis factor alpha (TNF- $\alpha$ ) in the context of lipotoxicity, and the development of systems-biology frameworks to integrate multi-source information.

In the first part of the research, the toxicity of different types of free fatty acids was investigated. Among the different types of FFAs, only saturated FFA (palmitate) was toxic to the cells. Interactive effects of palmitate and TNF- $\alpha$  were observed on the toxicity. The reactive oxygen species (ROS) mediating the palmitate-cytotoxicity were identified to be hydrogen peroxide and hydroxyl radicals. In the next part, the differences in the metabolism of the cells in response to different types of FFA were investigated by applying metabolic flux analysis (MFA). It was identified that palmitate reduced the synthesis of glutathione by reducing cysteine uptake, caused by a reduction in the levels of cystine transporter xCT. Supplementing cysteine to the cells reduced the toxicity significantly. The global genetic changes caused by exposure to FFAs and TNF- $\alpha$  were

identified by microarray analyses. Two novel methods were developed to integrate genomic and metabolic/ physiological information. In the first method, the genes that regulate multiple cellular responses were identified by the dual response genetic algorithm partial least squares (GA/PLS) analysis. This method identified that NADH dehydrogenase and mitogen activated protein kinases (MAPKs) regulate cytotoxicity and TG accumulation. These predictions were experimentally verified. Finally, a novel Bayesian regression mixture model-based framework was developed to incorporate the gene ontology (GO) information to select the genes that could discriminate between the subpopulations. It was identified that incorporation of prior information improved the classification of the genes. Important roles of lysosomal ATPases and adenylate cyclase in mediating the toxicity were identified by this analysis, which were experimentally validated. Thus, in this research, the multiple alterations responsible for mediating palmitate-toxicity to hepatoma cells were identified and novel frameworks were developed to integrate multi-source high-throughput information.

© COPYRIGHT

Shireesh Srivastava

2007

**DEDICATED TO MY FAMILY**

## **ACKNOWLEDGEMENTS**

This research would not have been possible without the support and help I received from so many people over the past five and a half years. It is likely that I may not explicitly name everyone who by his/ her actions made it possible for me to come this far. Yet, I solemnly remember their contributions to my research and my life.

The first person without whose constant patience, support and encouragement, I would have never completed my research, is my advisor Dr. Christina Chan. Her appreciation of my efforts, prompt and critical evaluation of my work, coupled with the intellectual freedom she provided, helped in my development as a researcher. I can only hope to follow the myriad of things I learned from her. I am also extremely grateful to every member of my Ph.D. advisory committee for taking time to participate in the committee. Their interest in my work, coupled with critical evaluation and support, vastly improved the quality of the research. My special thanks to Prof. Donald Jump for providing novel insights into my research, as well as for providing the cells when we lost ours to contamination and personally showing me how to do thin layer chromatography. I would also like to acknowledge the knowledge I gained by my interaction with Prof. Mark Worden, especially during the Advanced Biochemical Engineering class. I am confident that what I learnt in that class would continue to help me in the future, as it did in the current research. Prof. Dale, too was always supportive of my research. I would like to thank him for always taking time from his busy schedule to attend the committee meetings, asking pertinent questions and providing useful feedback. I am also grateful to Dr. S.P. Walton (Pat) for always being appreciative of my work and efforts and providing

useful suggestions. I would also like to thank Dr. Rong Jin of Computer Science department for interesting discussions on microarray data analysis.

The unwavering support and confidence of my family and friends made it possible for me to walk through the thick and thins of research. I am thankful to my parents for the hardships they bore to help me study whatever and wherever I wanted. My wife, Sheenu, had many contributions in making this research possible. I am thankful to her for all the technical, emotional (and dietary) support she provided. My brother, Aasheesh, was a constant source of knowledge, evaluation and inspiration.

I am very grateful to my friends and lab-members for their support and insightful discussions. My special thanks to Anish, Srivatsan, Sachin, Hemant, Joe, Xuerie, Zheng and Krishnan. Although it is difficult to name everyone here, I thank each of my labmates and friends for their encouragement.

Last, but not the least, I thank the Department of Chemical Engineering and Materials Science, the College of Engineering, the office of international student and scholars, council of graduate studies (COGS) and the graduate school for the financial support in the form of Food, Nutrition and Chronic Disease Fellowship and travel fellowships. Their contributions helped me present my research at the national and international levels.

# TABLE OF CONTENTS

<b>LIST OF TABLES .....</b>	<b>IX</b>
<b>LIST OF FIGURES .....</b>	<b>X</b>
<b>LIST OF ACRONYMS.....</b>	<b>XIII</b>
<b>CHAPTER 1. INTRODUCTION.....</b>	<b>1</b>
<b>CHAPTER 2. IDENTIFICATION OF THE REACTIVE OXYGEN SPECIES CAUSING THE CYTOTOXICITY OF PALMITATE TO HEPATOMA CELLS AND THE RELATIONSHIP OF THE CYTOTOXICITY TO MITOCHONDRIAL PERMEABILITY TRANSITION .....</b>	<b>10</b>
2.1 INTRODUCTION .....	10
2.2 MATERIALS AND METHODS.....	12
2.3 RESULTS .....	18
2.5 DISCUSSION .....	33
<b>CHAPTER 3. APPLICATION OF METABOLIC FLUX ANALYSIS TO IDENTIFY ALTERED FLUXES ASSOCIATED WITH THE TOXICITY OF PALMITATE.....</b>	<b>41</b>
3.1 INTRODUCTION .....	41
3.2 MATERIALS AND METHODS.....	43
3.3 RESULTS .....	55
3.4 DISCUSSION .....	80
<b>CHAPTER 4. IDENTIFICATION OF GENES THAT REGULATE MULTIPLE CELLULAR PROCESSES/ RESPONSES IN THE CONTEXT OF LIPOTOXICITY TO HEPATOMA CELLS.....</b>	<b>86</b>
4.1 INTRODUCTION .....	86
4.2 MATERIALS AND METHODS.....	88
4.3 RESULTS .....	93
4.4 DISCUSSION .....	109
<b>CHAPTER 5. INTEGRATING THE ONTOLOGY INFORMATION AND EXPRESSION DATA TO IDENTIFY GENES THAT REGULATE METABOLIC AND PHENOTYPIC FUNCTIONS .....</b>	<b>116</b>
5.1 INTRODUCTION .....	116
5.2 MATERIALS AND METHODS.....	121
5.3 RESULTS AND DISCUSSION.....	129
5.4 DISCUSSION .....	137
<b>CHAPTER 6. CONCLUSIONS AND FUTURE DIRECTIONS .....</b>	<b>142</b>
6.1 CONCLUSIONS .....	142
6.2 FUTURE DIRECTIONS .....	143
<b>APPENDIX .....</b>	<b>146</b>
1. TABLE OF METABOLIC FLUXES FOR DAY 1 .....	146
2. VALUES OF THE METABOLIC FLUXES FOR DAY 2 .....	149
3. VALUES OF THE METABOLIC FLUXES FOR DAY 3 .....	152
4. MATLAB PROGRAM USED FOR FLUX CALCULATIONS .....	155
5. MATLAB PROGRAM USED FOR GROSS MEASUREMENT IDENTIFICATION ACCORDING TO WANG AND STEPHANOPOULOS .....	157
6. MATLAB PROGRAM USED FOR THE PERTURBATION ANALYSES .....	161
<b>BIBLIOGRAPHY .....</b>	<b>163</b>

## LIST OF TABLES

Table 3.1 List of the metabolic reactions included in the MFA model ..	47
Table 3.2 List of intracellular metabolites.....	50
Table 3.3 List of measured extracellular fluxes .....	52
Table 3.4 Ratio of change in the intracellular to extracellular lactate levels. ....	59
Table 3.5 Ranked list of Pearson's correlation coefficient of the metabolic fluxes with cytotoxicity.....	61
Table 4.1. The cytotoxicity of various treatments.....	92
Table 4.2. Top genes identified for TG accumulation. GA/PLS analysis was conducted to identify genes related to intracellular TG accumulation. ....	93
Table 4.3. Effect of various treatments on the expression of selected genes based on the microarray data.....	111
Table 4.4. KEGG pathway represented by the genes identified for TG, LDH and (TG + LDH).....	112
Table 4.5. Enriched GO categories identified by the GOTM analyses.....	113
Table 4.6. Top genes identified for cytotoxicity (LDH release) by GA/PLS analysis.....	97
Table 4.7. Top genes selected for TG+LDH by dual response GA/PLS.....	101
Table 4.8. Effect of inhibition of NADH dehydrogenase on the cytotoxicity of palmitate and TG accumulation. ....	115
Table 5.1 The ranks of the three genes, adenylate cyclase 9 (AC9) and lysosomal ATPases (ATP6V0A1 and ATP6V1G1) as a function of Sc and Tau .....	131



## LIST OF FIGURES

Figure 2.1a Toxicity of different types of fatty acids.....	18
Figure 2.1b. Concentration-dependence of saturated fatty acid toxicity.....	19
Figure 2.2a Increased ceramide synthesis in response to palmitate, and inhibition by Fumonisin B1 (FB1).....	21
Figure 2.2b. Effect of inhibition of ceramide synthesis on the toxicity of palmitate.....	22
Figure 2.3a Levels of reactive oxygen species (ROS) in the cells following exposure to palmitate.....	23
Figure 2.3b Release of hydrogen peroxide into the medium following palmitate exposure. ....	24
Figure 2.3c Effects of scavengers of H <sub>2</sub> O <sub>2</sub> and hydroxyl radical on the oxidized status of the cells.....	25
Figure 2.3d Effects of scavengers of H <sub>2</sub> O <sub>2</sub> and hydroxyl radical on palmitate-toxicity.....	26
Figure 2.4a Mitochondrial potential after exposure to fatty acids or hydrogen peroxide for 24 h.....	28
Figure 2.4b Effect of hydroxyl radical scavengers and the MPT inhibitor on the mitochondrial potential.....	29
Figure 2.4c Effect of the inhibition of MPT on the cytotoxicity.....	29
Figure 2.5a Effects of inhibiting mitochondrial complexes I and III on mitochondrial potential loss .....	32
Figure 2.5b Effects of inhibiting mitochondrial complexes I and III on the cytotoxicity of palmitate.....	33
Figure 3.1 a. Cytotoxicity of various treatments.....	55
Figure 3.1b Activation of caspase-3 by palmitate .....	56
Figure 3.2 Measured flux through the synthesis of triglycerides in response to FFAs.....	56
Figure 3.3 a. Profile of intracellular lactate levels in response to various treatments.....	58
Figure 3.3 b. Profile of extracellular lactate levels in response to various treatments.....	58

Figure 3.4 Results of MFA analysis, depicting major intracellular fluxes on day 1 .....	81
Figure 3.5 Results of MFA analysis, depicting major intracellular fluxes on day 2.....	82
Figure 3.6 Results of MFA analysis, depicting major intracellular fluxes on day 3.....	83
Figure 3.7a Measured flux of release of total ketone bodies (acetoacetate + beta-hydroxybutyrate) by the cells.....	63
Figure 3.7b Effect of inhibition of fatty acid beta-oxidation on the toxicity of saturated FFA.....	64
Figure 3.8a Calculated flux through ceramide synthesis.....	65
Figure 3.8b Intracellular C-16 ceramide levels in response to palmitate.....	66
Figure 3.8c Results of in silico perturbation studies for the effect of serine or palmitate on the flux of de novo ceramide synthesis.....	66
Figure 3.8d Effect of inhibition of ceramide synthesis on the levels of C-16 ceramide in the cells.....	67
Figure 3.8e Effect of inhibition of ceramide synthesis on the cytotoxicity of palmitate...	67
Figure 3.9a Calculated relative fluxes of GSH synthesis, as predicted by MFA.....	70
Figure 3.9b Measured relative levels of total intracellular GSH. Cells were treated with palmitate or oleate for 3 days. ....	70
Figure 3.9c Results of in silico perturbation studies on the effect of increasing uptake of amino acids on GSH synthesis.....	71
Figure 3.9d Effect of the treatments on the expression of gamma-glutamyl cysteine synthetase (GCS) heavy subunit. ....	72
Figure 3.9e Effect of the treatments on the expression of xCT (a subunit of cystine transporter).....	73
Figure 3.9f Effect of NAC supplementation on the cytotoxicity of palmitate .....	74
Figure 3.10a Effect of NAC supplementation on GCL levels in palmitate-treated cells.....	76
Figure 3.10b Effect of NAC supplementation on GCL levels in control medium.....	77

Figure 4.1 Intracellular accumulation of TG in response to various FFAs and TNF- $\alpha$	91
Figure 4.2a. Effect of palmitate on the transcript levels of SCD, measured by microarray and RT-PCR	94
Figure 4.2b. Effect of palmitate and oleate on the protein levels of stearyl-CoA desaturase (SCD)	95
Figure 4.3a. Effect of various treatments on the mitochondrial potential	99
Figure 4.3b. Activation of caspase-3 by palmitate treatment	99
Figure 4.4a. Effect of inhibition of various MAPKs on the cytotoxicity of palmitate	105
Figure 4.4b. Effect of inhibition of various MAPKs on the TG accumulation in response to palmitate	105
Figure 5.1a Cytotoxicity of the treatments	126
Figure 5.1b Profile of acetoacetate release by various treatments	127
Figure 5.2 Variation of the discriminating ability of the mixture model with the smoothing constant ( $\tau$ ) and the weight to GO ( $\lambda$ )	128
Figure 5.3a Discrimination of the cytotoxic conditions from the non-toxic conditions for $\lambda = 0.5$ , $\tau = 3$	129
Figure 5.3b Discrimination of the ketogenesis for $\lambda = 0.5$ , $\tau = 3$	129
Figure 5.4 Effect of inhibitor of lysosomal ATPase, bafilomycin (Bfl) on the toxicity of palmitate	132
Figure 5.5 Effect of increasing cAMP levels on the caspase-3 activation by palmitate	133

## LIST OF ACRONYMS

1. 1400W – N-(3- (Aminomethyl)benzyl)acetamidine dihydrochloride
2. 2-MA – 2 Mercaptoacetate
3. AC – Adenylate Cylcase
4. AG – Aminoguanidine hydrochloride
5. ALT – Alanine Aminotransferase
6. AM-H2-DCFDA – 6-carboxy-2',7'-dichlorodihydrofluorescein diacetate, di(acetoxymethyl ester)
7. ANOVA – Analysis Of Variance
8. ANT – Adenine Nucleotide Translocator
9. AST – Aspartate Aminotransferase
10. BCA – Bicinchoninic Acid
11. Bfl – Bafilomycin
12. BSA – Bovine Serum Albumin
13. C/EBP – CCAAT Enhancer Binding Protein
14. cAMP – Cyclic Adenosine Monophosphate
15. CASP6 – Caspase 6
16. CAT – Catalase
17. CIC4 – Chloride Channel 4
18. c-PTIO – 2-(4-carboxyphenyl)-4,5-dihydro-4,4,5,5-tetramethyl-1H-imidazolyl-1-oxy-3-oxide
19. CsA – Cyclosporine A
20. Cu-DIPS – Copper(II)2(3,5-diisopropylsalicylate)4
21. CYP1A1 – Cytochrome P450 1A1

- 22. CYP2E1 – Cytochrome P450 2E1
- 23. CYP46 – Cytochrome P450, subfamily 46 (cholesterol 24-hydroxylase)
- 24. CypD – Cyclophilin D
- 25. DAG – Diacylglycerol
- 26. DHCR24 – 24-Dehydrocholesterol Reductase
- 27. DMEM – Dulbecco's Modified Eagle's Medium
- 28. DMSO – Dimethyl sulfoxide
- 29. DMU – Dimethyl Urea
- 30. ERK – Extracellular signal Regulated Kinase
- 31. EST – Expressed Sequence Tag
- 32. ETF1 – Eukaryotic Termination Factor 1
- 33. Etmx – Etomoxir
- 34. FB1 – Fumonisin B1
- 35. FBS – Fetal Bovine Serum
- 36. FCCP – p-trifluoromethoxy Carbonyl Cyanide Phenylhydrazone
- 37. FDA – Fisher's Discriminant Analysis
- 38. FFA – Free Fatty Acid
- 39. GA/PLS – Genetic Algorithm coupled Partial Least Squares
- 40. GAPDH – Glyceraldehyde phosphate dehydrogenase
- 41. GCS – Glutamyl Cysteine Synthase
- 42. GO – Gene Ontology
- 43. GOTM – Gene Ontology Tree Machine
- 44. GSH – Glutathione

- 45. HPLC – High Performance Liquid Chromatography
- 46. IBMX – 3-Isobutyl-1-Methylxanthine
- 47. IDF – Independent Document Frequency
- 48. IMGO – Integrative Mixture Model Gene Ontology
- 49. INPP5A – Inositol Polyphosphate Phosphatase 5 A
- 50. INPPL1 – Inositol Polyphosphate Phosphatase-like 1
- 51. IP3 – Inositol Triphosphate
- 52. JNK – c-Jun N-terminal Kinase
- 53. KEGG – Kyoto Encyclopedia of Genes and Genome
- 54. LCAT – Lecithin Cholesterol Acyl Transferase
- 55. LDH – Lactate Dehydrogenase
- 56. MAPK – Mitogen Activated Protein Kinases
- 57. MCD – Methionine Choline Deficient
- 58. MFA – Metabolic Flux Analysis
- 59. MnTBAP – Manganese(III) tetrakis(4-benzoic acid)porphyrin chloride
- 60. MPP – Mitochondrial Permeability Pore
- 61. MPT – Mitochondrial Permeability Transition
- 62. NAC – N-Acetyl L-cysteine
- 63. NaOH – Sodium Hydroxide
- 64. NASH – Non-Alcoholic Steatohepatitis
- 65. NDUFAB1 – NADH dehydrogenase (ubiquinone) 1, alpha/beta subcomplex, 1
- 66. NFIX – Nuclear Factor IX
- 67. PBS – Phosphate Buffered Saline

- 68. PCA – Principal Component Analysis
- 69. PDTC – Pyrrolidone dithiocarbamate
- 70. PKC – Protein Kinase C
- 71. PLS – Partial Least Squares
- 72. POBN –  $\alpha$ -(4-Pyridyl-1-Oxide)-N-tert-Butyl Nitron
- 73. PP2A – Protein Phosphatase 2A
- 74. PP2B – Protein Phosphatase 2B
- 75. PPAR- $\alpha$  – Peroxisome Proliferator Activated Receptor  $\alpha$
- 76. PTPN1 – Protein Tyrosine Phosphatase N1
- 77. ROS – Reactive Oxygen Species
- 78. RT-PCR – Reverse Transcriptase Polymerase Chain Reaction
- 79. SFA – Saturated Fatty Acid
- 80. SHIP2 – SH2-containing Inositol 5'-Phosphatase 2
- 81. SOD – Superoxide Dismutase
- 82. SREBP – Sterol Receptor Element Binding Protein
- 83. TBS-T – Tris buffered saline containing 0.1% Tween
- 84. TG – Triglyceride
- 85. tGSH – Total Glutathione
- 86. TNF- $\alpha$  – Tumor Necrosis Factor Alpha
- 87. UFA – Unsaturated Fatty Acid
- 88. VLDL – Very Low Density Lipoprotein
- 89. XIAP – X-linked Inhibitor of Apoptosis Protein

# **CHAPTER 1. INTRODUCTION**

## **1.1 Obesity and the effects of free fatty acids**

Obesity is on the rise and with it the incidences of obesity-associated disorders such as insulin resistance, type 2 diabetes, cardiovascular disorders and lipotoxicity. Not only adults, but even children are becoming obese at an increasing rate, and many obesity-related disorders also are developing in young patients (Chia and Boston, 2006). While it may be most prudent to target obesity itself which is the underlying cause of many metabolic disorders, this would mean significant changes in our lifestyles, something that will take many years, if not decades, to come to fruition. For now, treatment strategies have to be devised to effectively combat the scourge of disorders associated with obesity. This means understanding how obesity affects different organs of the body, and also how the organs interact to produce the disease phenotype.

Elevated circulating free fatty acid levels have emerged as a prime factor which mediates development of various disorders related to obesity (Felber and Golay, 2002, Scheen, 2000 and Boden 1997). The two sources of fatty acids in the body are diet (eating fat-rich food) (Astrup, 2005), and lipolysis (DeFronzo, 2004). Previous studies have indicated that both these sources contribute to the increased FFA-levels in obese people.

Prolonged exposure to elevated FFA levels causes many changes in the body. Numerous studies have been conducted to identify the effects of FFAs on different type of cells and



organelles. These studies have provided essential information on how FFAs regulate individual genes, enzymes or pathways, and have formed the basis to test various hypotheses. Most of these changes are due to the interactive effects of the various organs of the body. For example, increased exposure to fatty acids leads to accumulation of fat in the adipose tissue, leading to increase in the size of the tissue. This increase in the size of the tissue is not only due to an increase in the number of cells, but due to increase in the size of individual cells. The enlarged adipocytes release many factors (adipokines) such as leptin, interleukins and TNF-alpha, which affect the function of hepatocytes and muscle cells (Skurk et al., 2006). Similarly fatty acids can compete with glucose for oxidation and cause insulin resistance in muscle cells (Randle, 1964). This leads to a smaller rate of reduction of the levels of glucose and thus longer and greater release of insulin, as seen in the early stages of type 2 diabetes. This causes increased lipid synthesis and storage, which would increase adipose tissue size and increase adipokine secretion. Thus, there may be a vicious cycle of events that lead to the development of disorders at the whole body level. Exposure to elevated FFAs can also lead to multiple alterations in the function of hepatocytes, including cell death as discussed in section 1.2 below.

Exposure to fatty acids also alters cellular physiology by multiple means. Many fatty acid metabolites also act as signaling molecules, which not only control cellular physiology directly by altering the activity of many enzymes, but can also cause changes in the expression of many enzymes by activating transcription factors. Examples of such molecules include diacylglycerol (DAG) and ceramide. Elevated levels of DAG are

known to activate protein kinase C (PKC). PKCs are signaling kinases which alter many downstream processes. There are three types of PKCs: classical, novel and atypical. The classical and novel forms of PKCs are activated in response to elevated DAG levels, while the atypical forms respond to other lipid metabolites, such as ceramide. Activation of PKCs alters multiple processes such as growth, differentiation and even cell death (Musashi et al, 2000). Ceramide is another lipid which may affect signaling pathways and alter cellular physiology (Ruvolo, 2003). Among the signaling enzymes activated by ceramide is protein phosphatase 2A (PP2A). PP2A affects multiples cellular processes, including dephosphorylation of Bcl-2, an important protein involved in maintaining mitochondrial integrity and preventing cell death (apoptosis) (Chan and Yu, 2004). Fatty acids can also alter the functioning of cells by altering the enzyme make-up of the cells by regulating transcription of genes. Fatty acids, especially the unsaturated fatty acids, have been shown to be ligands for transcription factors such as peroxisome proliferator activated receptor alpha (PPAR- $\alpha$ ) and sterol receptor element binding protein (SREBP-1c), which have been shown to regulate multiple genes involved in lipid oxidation and synthesis (Jump et al, 2005).

## **1.2 Role of liver and the effects of FFAs on hepatic metabolism**

Liver is the central organ in the metabolism of fatty acids by the body. It is the organ that takes up the fat coming from the intestines as chylomicrons, and packages it into very low density lipoprotein (VLDL) which then goes into the bloodstream. Liver is among the most metabolically active organs, and produces other useful metabolites from fats, such as ketone bodies, cholesterol and hormones. Liver is also the organ that degrades

insulin, thereby controlling the level of this hormone. Given the central and important role played by this organ in fatty acid metabolism, it is a necessary first-step to identify the changes by the fatty acids on the liver itself. Hepatocytes are the primary cell type found in livers and are the primary contributors to FFA metabolism in the liver. Therefore, identifying the changes in the metabolism of the hepatocytes on exposure to elevated FFA levels would provide important information on the development of hepatic disorders observed in chronic obesity, and perhaps provide insight into the changes that occur in other organs as well.

Elevated FFAs significantly alter the function of hepatocytes. Fatty acids cause greater synthesis and secretion of cytokines by hepatocytes and other cells of liver (Feldstein et al., 2004). They inhibit insulin suppression of gluconeogenesis (formation of glucose by the breakdown of amino acids) and glycogenolysis (breakdown of glycogen to form glucose) in hepatocytes (Boden, 2004). They cause accumulation of lipids in the liver (steatosis). While steatosis is benign by itself, it sensitizes hepatocytes to oxidative injury (Farrell and Larter, 2006). In many individuals, chronic exposure to elevated FFAs leads to development of a hepatic disease called non-alcoholic steatohepatitis (NASH), which is characterized by extensive hepatocyte cell death. One study estimated that as much as 1-2% of the US population suffers from NASH. Even though the specific events leading to the development of NASH from steatosis are unclear, studies suggest that NASH develops by 'two hits' (Day and James, 1998). In the first hit, there is increased accumulation of lipids inside the cells which sensitizes the cells to lipid peroxidation and oxidative injury. In the second hit, an oxidative insult causes hepatocyte cell death,

causing alterations in hepatic function and increased levels of aspartate transaminase (AST) and alanine transaminase (ALT) in the serum. AST and ALT are (relatively) hepato-specific enzymes, whose levels increase on hepatic injury. While oxidative stress is known to play an important role in the development of NASH, the causes of increased oxidative stress are not clear. It is likely that FFAs themselves cause oxidative stress in hepatocytes as they do in other cell types, though it had not been shown previously. Similarly, the type of reactive oxygen species (ROS) produced on exposure to FFAs, as well as the differences in the types of FFAs in causing hepatotoxicity are not clear. It is now known that it is not just the amount of fat intake, but also its type, which determines the development of metabolic disorders. The differences in the types of fat arise due to their fatty acid composition. There are three major types of free fatty acids in the diet and plasma: saturated fatty acids (e.g. palmitate), monounsaturated fatty acid (oleate) and polyunsaturated fatty acid (e.g. linoleate). Many previous studies have indicated that the different types of fatty acids differ not only in their molecular structures, but also in their metabolic, genetic and physiological effects on the cells. However, the information on the systems level changes effected by them is lacking. Therefore, it is important to identify how different fatty acids affect cells at the level of physiological function, metabolism and gene expression, and how these effects could be related to the development of metabolic disorders.

While it may be best to study the responses of FFA exposure in primary human liver cells, their accessibility is relatively poor and the cost of experimentation very high. The other option is to use primary hepatocytes from animals (usually rodents) or human cell

lines. While primary rodent hepatocytes are a close mimic to in vivo hepatocytes in function, the experiments with these cells are limited to shorter durations because of their limited lifespan upon culturing. Furthermore, it is much easier to prepare stable transformed cells lines for further analyses than it is to manipulate primary cells. Human cell lines offer the advantages of retaining most of the major biological functions of hepatocytes, ease of long-term culture and possibility of creating stable transformed cells to study the long term effects of a target gene manipulation or the interactive effects of the target protein with other factors, for example, by creating HepG2 cell line overexpressing cytochrome P450 2E1 (CYP2E1), the role of this protein in ethanol cytotoxicity as well as arachidonic toxicity has been studied (Caro and Cederbaum, 2006 and Cederbaum, 2006). Considering these advantages, human hepatoma cell line HepG2/C3A was employed in the present study. HepG2 cells have been employed in many previous studies on fatty acid, lipid and lipoprotein metabolism. Studies have shown that the plasma concentrations of FFAs in obese and diabetic patients are about 0.7 mM. Therefore, this concentration of FFAs was employed in the study. Though most experiments were conducted at this concentration, some experiments on the physiological effects of saturated FFAs were also conducted at a lower concentration of 0.4 mM. No qualitative difference was observed upon reduction of the fatty acid concentration.

### **1.3 Systems biology approach to identify global changes in cellular make-up and function**

Cells can be considered as a network of three large interacting networks: metabolic, signaling and genetic, with significant cross-talk between the nodes (members) of these

networks. It is this highly interconnected nature of cellular networks that makes cells extremely resilient to various insults, and maintains cellular homeostasis. A change in the activity of a particular node usually causes a feedback response from the cells to maintain cellular homeostasis. These responses can be in the form of altered activity of the enzymes of the pathway, regulated through a change in the expression or allosteric control of the enzymes.

For comprehensive evaluation of cellular responses, global metabolic, genomic and proteomic responses should be measured. The development of high throughput techniques such as microarray analysis, as well as novel metabolite-detection techniques such as mass spectrometry etc. have made it possible to identify hundreds of fluxes or thousands of genes in relatively small times. The challenge is to (i) efficiently analyze the high-throughput information to identify altered cellular processes and (ii) integrate the multi-source information to generate comprehensive picture of cellular responses and identify the underlying genetic and metabolic changes which regulate desired processes. A lot of effort is being invested to meet these challenges, because the framework has potential to revolutionize the way medical investigations are done and to considerably reduce the time it takes to develop treatments against diseases.

#### **1.4 Aims of the current study**

The present study is an effort to understand the systems-level effects of different types of free fatty acids on the physiology, metabolism and gene-transcription of human hepatoma cells. The overall approach taken was to study the metabolic and genetic effects, using

high throughput techniques that provide system-level information on the effects of perturbations. Novel statistical models were employed to integrate the information generated and relate to the physiological function of interest. Not only was systems-level information on the metabolic and genetic effects of the different fatty acids generated, but also the interactions between the multiple levels were incorporated, thus providing a comprehensive snapshot of the perturbations caused by these treatments.

## **1.5 Organization of the thesis**

Because of the multi-level (physiological, metabolic, genetic and integrative) studies conducted in the current study, each chapter in this thesis is based on one of the aspects studied.

In chapter 2, the results and observations of the physiological responses of the cells to different FFAs are presented. It was observed that saturated FFA (palmitate) was the only toxic fatty acid among the different FFAs. Exposure to saturated FFA caused a significant increase in intracellular ROS levels, which played an important role in mediating the toxicity of this fatty acid and led to significant reduction in the mitochondrial potential of the cells, due to mitochondrial permeability transition (MPT). It was also identified that the MPT does not play a role in the toxicity of this FFA.

In chapter 3, the global metabolic changes caused by exposure to FFAs were studied using metabolic flux analysis (MFA). Exposure to FFAs led to accumulation of TG inside the cells. Exposure to palmitate caused lower TG accumulation, but greater ketone body

release and *de novo* ceramide synthesis by the cells as compared to the unsaturated FFAs. However, none of these alterations were associated with toxicity. On the other hand, increasing the TG accumulation was found to significantly reduce palmitate-toxicity. Exposure to palmitate also reduced the synthesis of glutathione by reducing the levels of cystine transporter and this alteration was found to play an important role in the toxicity of this fatty acid.

In chapter 4, the genomic changes caused by exposure to FFAs and TNF- $\alpha$  were studied. In addition, a framework is presented which can help identify genes that regulate multiple cellular processes. Such genes may serve as better targets to regulate the development of complex diseases. Application of the framework to current data identified that NADH dehydrogenase as well as MAPKs regulate both TG accumulation as well as cytotoxicity. These predictions were experimentally verified.

In chapter 5, a novel framework is presented to incorporate gene ontology information in the process to select genes pertinent to function(s) of interest, using mixture models to differentiate the sub-populations. Genes identified by this framework, which separated the toxic from non-toxic conditions, are presented and literature as well as experimental evidence is presented to discuss the role of the identified genes in lipotoxicity.

Finally, in chapter 6, the conclusions that can be made based on the current study, as well as certain predictions and the future directions are presented.



## **CHAPTER 2. IDENTIFICATION OF THE REACTIVE OXYGEN SPECIES CAUSING THE CYTOTOXICITY OF PALMITATE TO HEPATOMA CELLS AND THE RELATIONSHIP OF THE CYTOTOXICITY TO MITOCHONDRIAL PERMEABILITY TRANSITION**

### **2.1 Introduction**

Elevated plasma free fatty acid (FFA) concentrations are associated with the development of many hepatic disorders. FFAs increase the production of glucose (Lam Tony, Carpentier et al. 2003), the accumulation of triglycerides (Tanaka and Aoyama 2001), and inhibit insulin clearance by hepatocytes (Stroemblad and Bjoerntorp 1986). Chronically elevated fatty acid levels are associated with the development of non-alcoholic steatohepatitis (NASH), characterized by extensive hepatocyte cell death. Saturated FFAs cause cell death in a variety of cells including pancreatic beta-cells (El-Assaad, Buteau et al. 2003), cardiomyocytes (Kong and Rabkin 2000), and hepatocytes (Dashti, Feng et al. 2000; Ji, Zhang et al. 2005). According to the studies conducted in non-hepatic cells, such as beta-cells and myocytes, the potential mechanisms of cell death by these fatty acids involve increased ceramide production (Lu, Mu et al. 2003), reduced mitochondrial potential (Kong and Rabkin 2000) and increased production of reactive oxygen species (ROS) (Listenberger, Ory et al. 2001; Yamagishi, Okamoto et al. 2002). Studies in hepatocytes or hepatoma cells have suggested that lysosomal permeabilization (Wei, Wang et al. 2006), release of cathepsin B (Feldstein, Werneburg et al. 2004), and reduction of mitochondrial Bcl-2/Bax ratio (Ji, Zhang et al. 2005) play important roles in cell death caused by palmitate.

Different molecular species of ROS have been shown to mediate fatty acid toxicity in different types of cells, e.g. superoxide anion is known to mediate fatty acid toxicity in CHO cells (Listenberger, Ory et al. 2001), while nitric oxide mediates the cell death in pancreatic beta cell line INS-1 (Maestre, Jordan et al. 2003; Okuyama, Fujiwara et al. 2003). However, the type of ROS which mediate the palmitate-toxicity to hepatoma cells has not yet been elucidated. Herein, the results of our investigation towards identifying the ROS molecular species involved in the fatty acid-induced cytotoxicity of hepatoma cells are reported.

Membrane permeability transition (MPT) is considered an important step in cell death (Armstrong 2006). MPT leads to release of pro-apoptotic molecules such as cytochrome c, apoptosis inducing factor (AIF) and endonuclease G from the mitochondria (Bernardi, Broekemeier et al. 1994). Cell death in response to many stimuli can be abrogated by inhibiting MPT, e.g., inhibiting MPT has been shown to reduce ROS formation and cell death of hepatocytes in response to microcystin treatment (Ding, Shen et al. 2000) and the apoptosis of HepG2 cells in response to hypochlorous acid (Whiteman, Rose et al. 2005). Saturated fatty acids can cause MPT (Petronilli, Cola et al. 1993), which mediates the cell death by palmitate in cardiomyocytes (Kong and Rabkin 2000). However, it is not clear whether MPT plays a similar role in controlling fatty acid-induced toxicity of hepatocytes.

The objectives of this study were to investigate the mechanisms of fatty acid toxicity to hepatoma cells, identify the molecular species of ROS which mediate(s) the toxicity and study the inter-relationships between ROS production, MPT and cytotoxicity when these cells were exposed to FFAs at an elevated physiological concentration of 0.7 mM (Skowronski, Hollenbeck et al. 1991; Boden, Chen et al. 2001; Mensink, Blaak et al. 2001; Woerle, Popa et al. 2002). The results suggest that saturated fatty acids can cause lipotoxicity through increased production of hydrogen peroxide and  $\cdot\text{OH}$  radicals. Even though MPT was observed in the cells treated with the saturated fatty acid, the toxicity is not mediated through MPT.

## **2.2 Materials and Methods**

**2.2.1 Cell Culture.** 1 million HepG2/C3A cells (American Type Culture Collection, Manassas, VA) were seeded into each well of a 6-well plate. The cells were kept in 2 ml of the medium containing Dulbecco's modified Eagle's medium (DMEM, Invitrogen, Carlsbad, CA) supplemented with 10% fetal bovine serum (American Type Culture Collection) and 2% Penicillin-streptomycin (Invitrogen). Cells were incubated at 37°C and in 10% CO<sub>2</sub> atmosphere. After the cells reached confluency, the medium was replaced with 2 ml of the desired medium (Control, BSA, 0.7 mM FFA medium). Palmitate, oleate and linoleate were used as the representative fatty acids for the saturated, monounsaturated and polyunsaturated type of fatty acids. These fatty acids are the most abundant fatty acids of their class in the plasma, e.g. palmitate is the most abundant saturated fatty acid in the plasma. Plasma FFA levels in the obese and type 2 diabetic patients have been reported to be about 0.7 mM in many studies (Skowronski,

Hollenbeck et al. 1991; Boden, Chen et al. 2001; Mensink, Blaak et al. 2001; Woerle, Popa et al. 2002). Therefore, this concentration of FFAs was employed in the present study. Media were changed after every 24 h.

**2.2.2 Determination of cytotoxicity.** Cytotoxicity was measured by measuring the release of lactate dehydrogenase (LDH) into the medium using the cytotoxicity detection kit (Roche Applied Science, Indianapolis, IN). LDH is a cytosolic enzyme which is released when the membrane integrity of the cells has been compromised. In this assay, the NADH generated during the oxidation of lactate by LDH is utilized as a co-factor by the enzyme diaphorase to reduce tetrazolium salt (yellow) to formazan dye (red). To conduct the assay, the supernatant media was collected after desired exposure times (e.g. 24 and 48 h) and the LDH activity in the medium was determined (called LDH-medium). The cells were washed with phosphate buffered saline (PBS), and lysed with 1% triton-X-100 in PBS for 24 h at 37 °C. The lysate was collected, vortexed for 15 seconds and centrifuged at 5000 g for 3 minutes. LDH activity in the lysate was determined (called LDH-Triton). The LDH released into the medium was normalized to total LDH, as shown in the equation below

$$\%LDH_{release} = \frac{LDH(medium)}{LDH(medium) + LDH(triton)} \times 100$$

**2.2.3 Inhibitor experiments.** Fumonisin B1 (FB1) (Sigma-Aldrich, St. Louis, MO) and cyclosporine A (CsA) (Calbiochem, San Diego, CA) were employed for inhibiting ceramide synthase and MPT, respectively. 2 mM stock solution of FB1 was prepared in

PBS, and a 20mM stock solution of cyclosporine A was prepared in DMSO. The cells were treated with palmitate in the presence of 2-100  $\mu$ M FB1, and 0.5-5  $\mu$ M CsA.

**2.2.4. Measurement of ceramide.** The cells were treated with 0.7 mM palmitate in the presence or absence of 20  $\mu$ M FB1 (inhibitor of *de novo* ceramide synthesis). After the treatments, the cells were washed with PBS, trypsinized and pelleted down. Lipids were extracted by the method of Bligh and Dyer (Bligh and Dyer 1959). Briefly, the pellets were washed once with PBS, resuspended in 3 ml chloroform:methanol solution (1:2 v/v), and lyzed by sonication in this solution for 30 seconds. 0.8 ml water and 0.5 ml methanol were then added, and the solution was kept at room temperature for 15 minutes. Cell debris was pelleted by centrifugation at 5000 g for 5 min. The supernatant was decanted into a new tube and 1 ml each of chloroform and water was added. The solution was briefly vortexed and the phases were allowed to separate for 15 minutes. The tubes were then centrifuged at 3000 g for 5 minutes. The aqueous layer was removed, and 1 ml of the chloroform solution was transferred to a 1.5 ml microcentrifuge tube, and dried in a speedvac. The lipids were resuspended in 80  $\mu$ l chloroform. The levels of ceramide were then measured using liquid chromatography-tandem mass spectroscopy (LC-MS), according to a previously published method (Yamaguchi, Miyashita et al. 2004). Protein levels in the aqueous phase were measured using BCA assay. Ceramide results from LC-MS measurements were normalized to the total protein.

**2.2.5. Measurement of ROS.** Two different methods were employed to estimate relative ROS levels, as discussed below. In the first method, 6-carboxy-2',7'-

dichlorodihydrofluorescein diacetate, di(acetoxymethyl ester) (C-2938, Molecular Probes, Eugene, OR) dye was used to measure the increased oxidized status of the cells in response to palmitate treatment. Stock solution of the dye was prepared in DMSO, and diluted to 5  $\mu$ M in DMEM. Confluent cells were treated with palmitate for different time periods. Measurement of fluorescence was performed by flow cytometry according to a previously published protocol (Listenberger et al. 2001).

As a separate measurement, the hydrogen peroxide released into the medium was measured using a colorimetric hydrogen peroxide assay (Assay Designs, Ann Arbor, MI). This assay is based on the principle of reaction of coordinated iron with peroxide and xylenol orange in acidic solution to produce a purple-colored complex, whose color is proportional to the concentration of hydrogen peroxide in the sample. Confluent cells were exposed to either HepG2 medium or to palmitate for desired periods. Media were replaced every 24h. After the treatment periods, media were collected and the hydrogen peroxide levels in the media were analyzed immediately, according to the manufacturer's instructions. Blanks were generated by incubating the media without cells and subtracting the absorbance of the blanks from that of the samples. The estimated concentrations were multiplied by the volume of the culture to obtain the total amount, which were then normalized to the total protein levels. For estimation of the protein, the cells were washed with PBS and lysed with 1% triton-X-100 to estimate protein levels by the bicinchoninic acid (BCA) assay (Pierce Chemical, Rockford, IL). Hydrogen peroxide levels were then normalized to cellular protein levels.

**2.2.6 Radical Scavengers and spin trap.** 1, 3 Dimethyl urea (DMU) (MP Biomedical) and dimethyl sulfoxide (DMSO) (Sigma Aldrich) were employed to scavenge hydroxyl radicals. Solutions of these scavengers were prepared in the palmitate medium at 5-50 mM for DMU and 0.2-3% (v/v) for DMSO. The spin trap alpha-(4-pyridyl-1-oxide)-N-tert-butyl nitron (POBN, 20-100 mM) from Sigma Aldrich was dissolved in palmitate medium. Catalase (CAT, 3000 U/ml) was used to scavenge hydrogen peroxide. It was dissolved in the palmitate medium. Cu(II)<sub>2</sub>(3,5-diisopropylsalicylate)<sub>4</sub> (Cu-DIPS) and Mn(III) tetrakis(4-benzoic acid)porphyrin chloride (MnTBAP) are the cell permeable mimics of cytosolic (Cu-Zn) and mitochondrial (Mn) superoxide dismutase (SOD), respectively (Laurent, Nicco et al. 2004). These SOD-mimics were obtained from Sigma Aldrich, and utilized as scavengers for the superoxide anion. Stock solution of Cu-DIPS (5 mM) was prepared in DMSO and used in the concentration range 1-10 uM. Stock solution was prepared by dissolving 50 mM MnTBAP in 0.1 M NaOH, followed by addition of equal volume of 0.1 M HCl. MnTBAP was used in the concentration range 10-100 uM. Pyrrolidone dithiocarbamate (PDTC) and 4,5-dihydroxy-1,3-benzene-disulfonic acid (Tiron) were obtained from TCI chemicals, and employed as scavengers of superoxide anion (Listenberger, Ory et al. 2001). These scavengers were dissolved in the medium at concentrations of 0.25-10 mM and 2-40 mM, respectively. 2-(4-carboxyphenyl)-4,5-dihydro-4,4,5,5-tetramethyl-1H-imidazolyl-1-oxy-3-oxide (c-PTIO), procured from Axxora Chemicals, was used to scavenge nitric oxide (NO) (Dave, Farrance et al. 1997). 200 mM stock solution of carboxy-PTIO (cPTIO) was prepared in water and used at final concentration of 20-200 uM. Aminoguanidine hydrochloride (AG) and N-(3- (Aminomethyl)benzyl)acetamidine dihydrochloride (1400W), both from

Axxora Chemicals, were employed to inhibit nitric oxide synthesis (Dave, Farrance et al. 1997). AG was dissolved in PBS at a concentration of 1 M and used at 0.1-1 mM final concentration. A 100 mM stock solution of 1400 W was prepared in water, and used in the concentration range 50-500 uM.

**2.2.7 Dose-dependence studies.** For all the inhibitors and scavengers, dose-dependence studies were performed. That is, the cells were exposed to palmitate in the presence of various concentrations of these scavengers/ inhibitors and the LDH release was measured. The following treatment ranges were studied- FB1 (2-50 uM), catalase (500-3000 U/ml), DMU (2-50 mM), DMSO (0.5-2% v/v), CuDIPS (0.5-10 uM), MnTBAP (25-200 uM), Tiron (2-20 uM), PDTC (0.5-10 uM), cPTIO (25-200 uM), AG (0.1-1 mM), 1400W (50-500 uM), CsA (0.5-5 uM), POBN (20-100 mM), Rotenone (100-2000 nM), antimycin A (50-1000 nM). Results are presented for concentrations which were most effective in reducing LDH.

**2.2.8 Measurement of the mitochondrial potential.** Mitochondrial potential was measured using JC-1 dye (Calbiochem). Potential-sensitive uptake of this dye leads to its accumulation and aggregate formation in normal, active mitochondria. Aggregates of the dye (mitochondria) fluoresce red, while the dilute solution (cytoplasmic) fluoresces green. The ratio of red to green fluorescence was used to estimate the mitochondrial potential (Cossarizza, Ceccarelli et al. 1996). A 5 mM stock solution of the dye was prepared in DMSO. After treating the cells for desired times, the media were aspirated, and the cells were exposed to 5 uM JC-1 dye in DMEM. Cells were incubated in the dye-



containing medium for 30 min. Dye was aspirated and the cells washed twice with 1 ml PBS. 1 ml PBS was added to each well and the plates were bottom-read in a fluorescence reader (Molecular Probes, Eugene, OR) at excitation of 488 nm and emissions of 527 nm (green) and 590nm (red). p-trifluoromethoxy carbonyl cyanide phenyl hydrazone (FCCP) is an established mitochondrial uncoupler and abolishes the mitochondrial potential. The mitochondrial uncoupler FCCP (40  $\mu$ M) was used as a control for totally lost membrane potential.

**2.2.9 Statistical Analysis.** Treatments were analyzed with analysis of variance (ANOVA) followed by Bonferroni's post-hoc comparison to locate specific differences (Turner and Thayer 2001). Analyses were performed using S-plus software.

## **2.3 Results**

**2.3.1 Cytotoxicity of different types of fatty acids.** To evaluate the toxicity of various fatty acids, the HepG2 cells were exposed to 0.7 mM palmitate, oleate or linoleate- the three primary species of saturated, unsaturated and polyunsaturated fatty acids in the plasma, for two days. Media were changed after 24h of exposure, and the LDH release into the medium was measured. Among the fatty acids studied, only palmitate was found to be toxic to the cells and resulted in a significantly higher LDH release on both days (Figure 2.1a). The toxicity of palmitate was concentration dependent above 0.2 mM (Figure 2.1b). When exposed to free fatty acids, the cells metabolized about 0.2 mM of the different free fatty acids (not shown). This suggests that the amount of fatty acid present in excess to the metabolic capacity causes the toxicity, but this toxicity is specific

to saturated fatty acid, because the unsaturated fatty acids that were not fully metabolized were non-toxic.

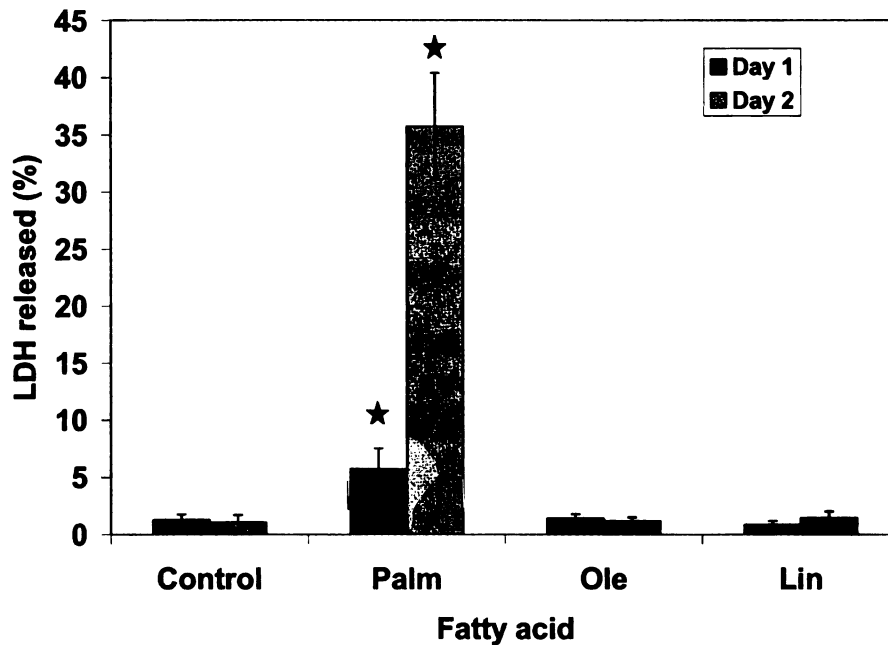


**Figure 2.1a Toxicity of different types of fatty acids.** Confluent HepG2 cells were exposed to different types of fatty acids (0.7mM, complexed to 4% w/v BSA) for 2 days, with medium-change everyday. LDH released on each day was measured and normalized to total LDH. Total LDH is defined as the sum of the LDH released and the intracellular LDH. The intracellular LDH values were obtained by lyzing the cells with 1% triton (see methods section). Data expressed as averages of nine samples  $\pm$  s.d. from three independent experiments. \*, significantly higher than control,  $p < 0.01$ .

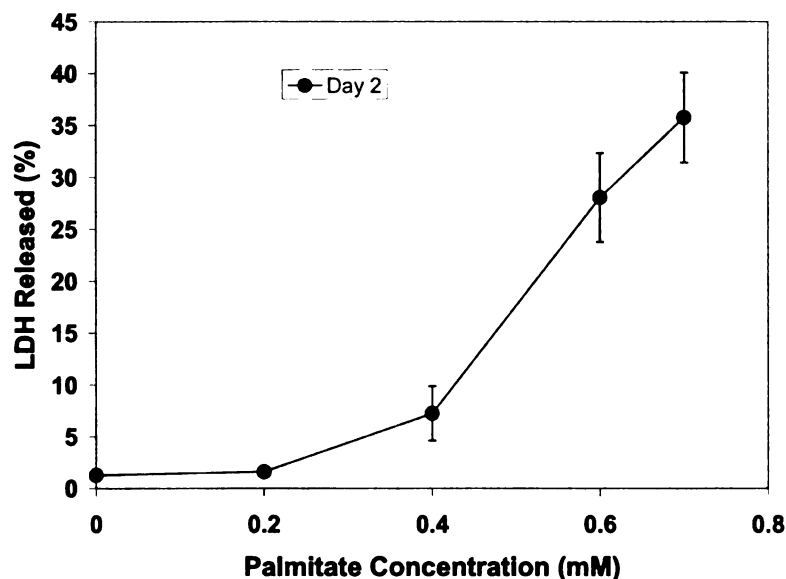


**Figure 2.1b Concentration-dependence of saturated fatty acid toxicity.** The LDH released after exposure to different concentrations of palmitate for two days was measured. Data expressed as averages of nine samples  $\pm$  s.d. from three independent experiments. \*, significantly higher than control,  $p < 0.01$ .

**2.3.2 Ceramide metabolism.** *De novo* ceramide synthesis has been shown to be a major factor in palmitate-induced toxicity in a variety of cell types (Lu, Mu et al. 2003). Among the primary mechanisms of ceramide-induced toxicity is increased ROS production (Gomez, Mendoza-Milla et al. 1996; France-Lanord, Brugg et al. 1997; Andrieu-Abadie, Gouaze et al. 2001). To investigate the role of *de novo* ceramide synthesis in the toxicity of palmitate to HepG2 cells, we studied the effect of inhibiting ceramide synthesis on the cytotoxicity. Fumonisin B1 (FB1) inhibits *de novo* ceramide synthesis by inhibiting ceramide synthase, a key enzyme of the pathway. The cells were treated with palmitate in the presence of 2-50  $\mu$ M FB1 (Van Der Westhuizen, Shephard et al. 1998). Similar concentrations of this inhibitor have been shown to inhibit *de novo* ceramide synthesis in HepG2 cells (Van, Van Der Wouden et al. 2004). The cells exposed to palmitate had high

levels of C-16 ceramide (Figure 2.2a) whereas the cells treated with 4% BSA (control) had negligible levels (not shown). Treatment with 20 uM FB1 reduced the ceramide levels significantly (42 and 72 % reductions on day 1 and day 2, respectively, Figure 2.2a). This suggested that the *de novo* ceramide pathway was responsible for the increased ceramide synthesis. However, the reduction in ceramide levels was not associated with a reduction in the toxicity (Figure 2.2b). Similarly, higher concentrations of the inhibitor (up to 50 uM) were unable to reduce the toxicity. FB1 is a specific inhibitor of ceramide synthase (Yu, Yoo et al. 2004; Basnakian, Ueda et al. 2005), the final enzyme of the *de novo* ceramide synthesis pathway. Therefore, the lack of reduction in the toxicity in response to FB1, in spite of a reduction in ceramide levels, suggests that the *de novo* synthesized ceramide does not play an important role in the toxicity. These results are in agreement with other studies on the toxicity of saturated fatty acids to hepatocytes (Feldstein, Werneburg et al. 2006; Wei, Wang et al. 2006). These studies indicate that saturated fatty acid may cause the toxicity to hepatocytes by mechanisms other than ceramide generation, such as lysosomal permeabilization (Feldstein, Werneburg et al. 2006), ER stress (Wei, Wang et al. 2006), reductions in the mitochondrial Bcl2/Bax ratio (Ji, Zhang et al. 2005) and activating JNK pathway (Malhi, Bronk et al. 2006).

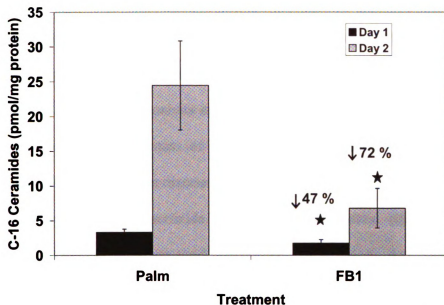


**Figure 2.2a Increased ceramide synthesis in response to palmitate and inhibition by Fumonisin B1 (FB1).** Cells were exposed for two days to 0.7 mM palmitate containing vehicle (PBS), or 20uM fumonisin B1 (FB1). The media were changed everyday. (a) Effect on C-16 ceramide levels. After treatments, the lipids were extracted. The levels of C-16 ceramide in the cells were measured using LC-MS, and normalized to the cellular protein. \*, significantly lower than palmitate,  $p < 0.01$ .

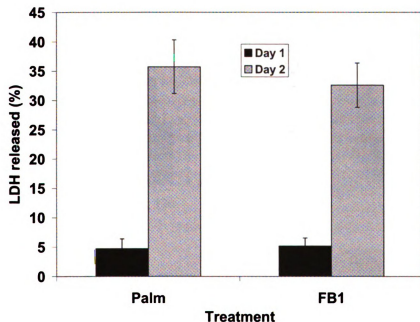


**Figure 2.2b Effect of inhibition of ceramide synthesis on the toxicity of palmitate.** The cells were treated with palmitate and FB1 for two days, and the LDH release was measured as described in materials and methods section. Data presented as mean  $\pm$  s.d. for nine samples from three independent experiments.

**2.3.3 Role of ROS in the cytotoxicity of palmitate.** ROS has been shown to be a major cause of palmitate-induced cytotoxicity in CHO and microvascular endothelial cells (Listenberger, Ory et al. 2001; Yamagishi, Okamoto et al. 2002). To investigate the role of ROS in palmitate-cytotoxicity in HepG2 cells, a two-pronged approach was employed - (a) the oxidized status of the cells was estimated using 6-carboxy-2',7'-dichlorodihydrofluorescein diacetate, di(acetoxymethyl ester) (AM-H2-DCFDA) dye and the release of hydrogen peroxide by the cells was measured, (b) the effects of species-specific ROS scavengers on the LDH release in response to palmitate were measured. Exposure to palmitate, but not to oleate or linoleate, led to a time-dependent increase in intracellular oxidized status (Figure 2.3a).

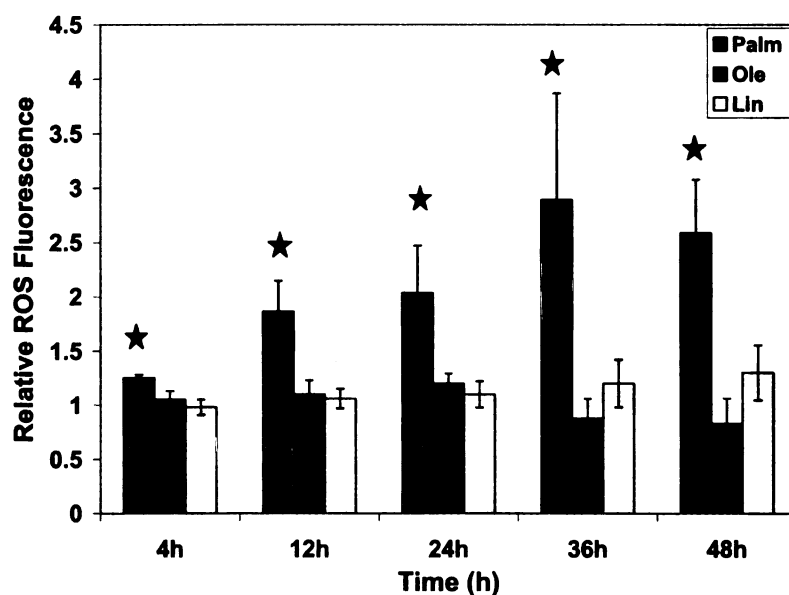


**Figure 2.3a Levels of reactive oxygen species (ROS) in the cells following exposure to palmitate.** Cells were exposed to 0.7 mM palmitate for different times. Medium was changed after 24h of exposure. Treatment with palmitate was followed by exposure to 5  $\mu$ M AM-DCFDA dye for 30 minutes at 37°C, and staining with 2  $\mu$ g/ml propidium iodide for 10 minutes. Fluorescence of viable (propidium iodide negative) cells was measured using flow-cytometry with excitation at 488 nm and emission at 530 nm. Relative fluorescence values  $\pm$  s.d. of six samples from two different experiments are presented. '\*' denotes significantly different, compared to control,  $p < 0.01$ .

A measure of ROS production by the cells is the release of hydrogen peroxide (Liu, Fiskum et al. 2002). The hydrogen peroxide released by the cells in response to palmitate was measured by a colorimetric assay as described in the methods section. Exposing cells to palmitate, led to a time-dependent increase in hydrogen peroxide release into the medium (Figure 2.3b). The profile of hydrogen peroxide release mirrored the observed toxicity, being lower on day 1 and increasing significantly on day 2, suggesting that hydrogen peroxide may be related to the observed toxicity.

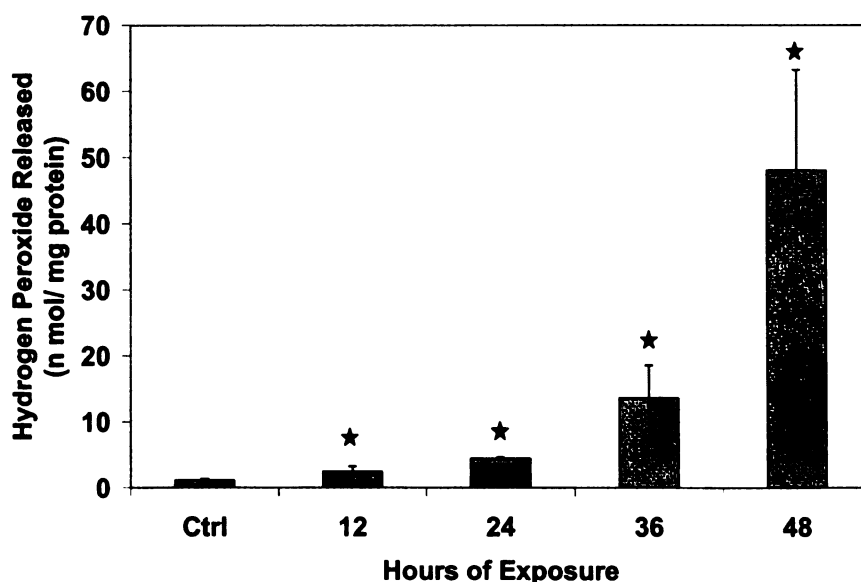


**Figure 2.3b Release of hydrogen peroxide into the medium following palmitate exposure.** Cells were treated with 0.7 mM palmitate for various times. The hydrogen peroxide released into the medium was measured and normalized to total cellular protein. Data presented as mean  $\pm$  s.d. for nine samples from three independent experiments. ‘\*’ denotes significantly different, compared to control,  $p < 0.01$ .

hydrogen peroxide can form  $\cdot\text{OH}$  radical, a much more reactive and damaging ROS species, in the presence of divalent cations such as  $\text{Fe}^{2+}$ . To evaluate the role of hydrogen peroxide and  $\cdot\text{OH}$  radical in palmitate toxicity, the cells were treated with palmitate in

the presence of catalase (3000U/ml) and \*OH radical scavengers 1, 3 dimethyl urea (DMU, 25mM) and dimethyl sulfoxide (DMSO, 1% v/v), and the spin trap alpha-(4-pyridyl-1-oxide)-N-tert-butyl nitron (POBN, 70 mM). All these scavengers reduced the cellular ROS levels (Figure 2.3c), as well as the palmitate-toxicity (Figure 2.3d) significantly. DMU and DMSO are two specific scavengers of hydroxyl radicals (Cederbaum, Dicker et al. 1977; Sandler and Andersson 1982; Bruck, Aeed et al. 1999; Zegura, Sedmak et al. 2003). Dimethyl thiourea (DMTU) is another commonly used \*OH scavenger, but was not employed in the current study because it had been shown to be toxic to rats (Beehler, Ely et al. 1994). The same study showed that DMU was not toxic, and therefore, DMU was used in the present study.

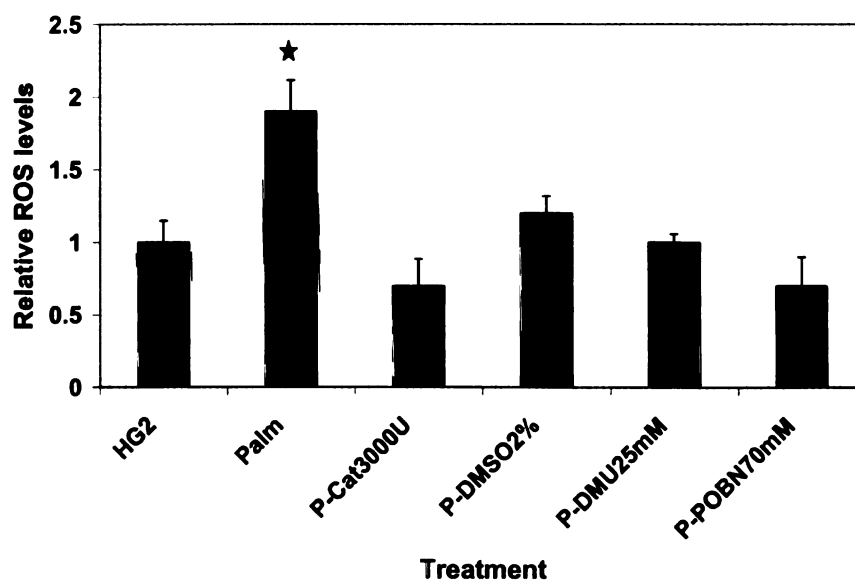


**Figure 2.3c Effects of scavengers of hydrogen peroxide and hydroxyl radical on the oxidized status of the cells.** The cells were treated with palmitate in the presence of 3000 U/ml catalase (scavenger for hydrogen peroxide), or scavengers of \*OH radical- dimethyl urea (25 m M), dimethyl sulfoxide (DMSO, 1% v/v), or the spin trap alpha-(4-pyridyl-1-oxide)-N-tert-butyl nitron (POBN, 70 mM) for 24h, followed by treatment with 5 uM AM-DCFDA for 30 min in DMEM. Fluorescence of the cells was measured using a microplate reader with excitation at 488 nm and emission at 530 nm. Relative fluorescence values +/- s.d. of six samples from two independent experiments are presented. “\*” denotes significantly higher, compared to control,  $p < 0.01$ .



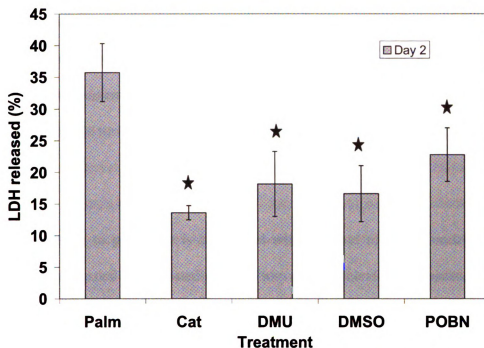


**Figure 2.3d Effects of scavengers of hydrogen peroxide and hydroxyl radical on palmitate-toxicity.** The cells were treated as in Figure 2.3(c) for 2 days. LDH released on day two is presented. Data presented as mean  $\pm$  s.d. for nine samples from three independent experiments. \*,\* denotes significantly lower, compared to palmitate,  $p < 0.01$ .

Studies with other cell types have also indicated that superoxide or NO may mediate the toxicity of palmitate (Listenberger, Ory et al. 2001; Maestre, Jordan et al. 2003; Okuyama, Fujiwara et al. 2003). To evaluate the role of superoxide anion in the toxicity, cells were either pretreated for 2h or co-treated with palmitate in the presence of cell-permeable SOD mimics CuDIPS (0.5-10  $\mu$ M) and MnTBAP (25-200  $\mu$ M), or the superoxide-specific scavengers 4,5-dihydroxy-1,3-benzene-disulfonic acid (Tiron, 2-20  $\mu$ M) and pyrrolidone dithiocarbamate (PDTC, 0.5-10  $\mu$ M). However, none of these treatments produced any significant reduction in the toxicity of palmitate, suggesting that the superoxide anion is not the primary toxicity causing species. To evaluate the role of NO in the toxicity, the effect of NO scavengers (cPTIO, 25-200  $\mu$ M and AG, 0.1-1 mM)

or iNOS inhibitor 1400W (50-500  $\mu$ M) on the palmitate toxicity was measured. Exposure to palmitate in the presence of these chemicals did not reduce the cytotoxicity, indicating that NO is not involved in the toxicity of palmitate. The efficacy of hydrogen peroxide and  $\cdot$ OH scavengers, but not of superoxide or nitric oxide scavengers or inhibitors, indicated that the former ROS are the likely mediators of the palmitate-toxicity in HepG2 cells.

#### **2.3.4 Exposure to palmitate is associated with the loss of mitochondrial potential.**

Cytotoxicity is usually associated with the loss of mitochondrial membrane potential. A significant reduction in the mitochondrial potential was observed when the cells were treated with palmitate, but not when they were treated with unsaturated fatty acids (Figure 2.4a). The potential after exposure to palmitate was higher than that observed on treating the cells with 40  $\mu$ M FCCP (positive control), suggesting a partial loss of potential upon palmitate-exposure. To test the involvement of ROS in the observed reduction of the mitochondrial potential in response to palmitate, the cells were exposed to 100  $\mu$ M hydrogen peroxide in the absence of palmitate. This treatment also significantly reduced the mitochondrial potential (Figure 2.4a), suggesting that the oxidative stress in response to palmitate may play a role in the loss of mitochondrial potential.

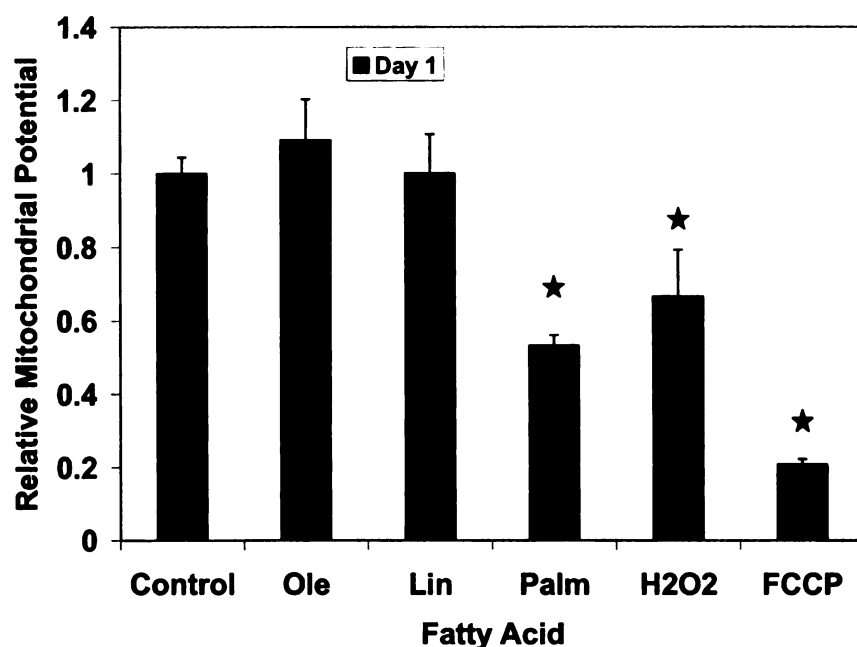


**Figure 2.4a Mitochondrial potential after exposure to fatty acids or hydrogen peroxide for 24 h.** Cells were exposed to 100  $\mu$ M hydrogen peroxide, to various free fatty acids (0.7 m M) or to 40  $\mu$ M FCCP for 24h. The cells were then incubated in 5  $\mu$ M JC-1 dye in serum-free medium for 30 min at 37°C, after which the cells were washed with PBS. The fluorescence was measured in a microplate fluorimeter, with excitation at 488 nm and emissions at 530 (green) and 590 nm (red). Data presented as mean  $\pm$  s.d. for nine samples from three independent experiments. \*, significantly different from control,  $p < 0.01$  relative to control.

MPT has been suggested as a cause of reduced mitochondrial potential and cell death in response to saturated fatty acid in beta cells (Kong and Rabkin 2000). To evaluate the involvement of MPT in the loss of mitochondrial potential and toxicity by the palmitate-treatment, MPT was inhibited by treating the cells with 0.5-5  $\mu$ M CsA in the presence of palmitate. This treatment restored the mitochondrial potential on both days (Figure 2.4b, data shown for 2  $\mu$ M). However, the improvement in the mitochondrial potential was not associated with a reduction in the toxicity (Figure 2.4c), indicating that the toxicity was not dependent on the loss of mitochondrial potential. Similarly, the other concentrations

of the inhibitor (0.5-5  $\mu$ M) were also unable to significantly reduce the toxicity (not shown).

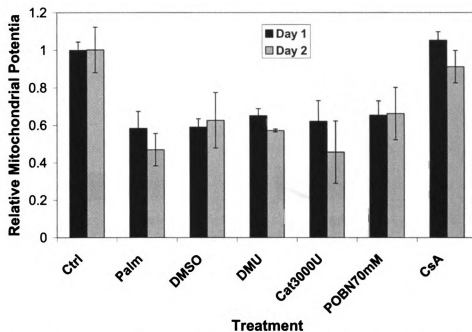


**Figure 2.4b Effect of hydroxyl radical scavengers and the MPT inhibitor on the mitochondrial potential.** Cells were treated with 0.7 mM palmitate in the presence of hydroxyl radical scavengers DMSO (1% v/v), DMU (25 mM), or MPT inhibitor CsA (2  $\mu$ M) for 24h and the mitochondrial potential was measured, as in 'a'. Data presented as mean  $\pm$  s.d. for nine samples from three independent experiments.

“\*” denotes significantly different from palmitate,  $p < 0.01$ .

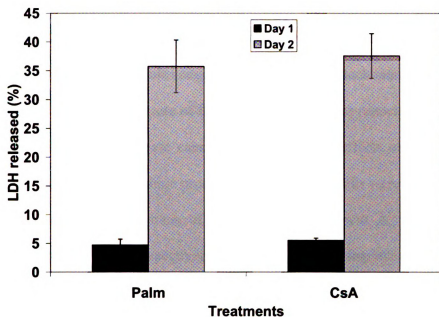


**Figure 2.4c Effect of MPT inhibitor cyclosporine A on the toxicity of palmitate.** Cells were treated for 2 days with palmitate in the presence of 2  $\mu$ M CsA. LDH release was measured and normalized to total LDH. Data shown is mean  $\pm$  s.d. for nine samples from three independent experiments.

In agreement with these observations, treating with palmitate in the presence of DMU, DMSO, catalase and POBN (all of which had reduced the LDH release significantly) did not affect the reduction in mitochondrial potential by palmitate (Figure 2.4b). Thus, the treatment with palmitate leads to MPT, but the toxicity of this fatty acid does not depend on MPT.

**2.3.5 Role of ROS in MPT: effect of mitochondrial complex inhibition.** ROS and MPT can have a two-way interaction, i.e., some studies have reported that MPT has been associated with increased production of ROS through mitochondrial uncoupling, while ROS can cause oxidation of the thiol-groups on cyclophilin D (Cyp-D) and adenine nucleotide translocator (ANT), causing MPT. Mitochondrial complexes I and III are

known to be the primary sites of ROS production (Chen, Vazquez et al. 2003; Nohl, Gille et al. 2005; Grivennikova and Vinogradov 2006). The observation of loss of mitochondrial potential also suggested alteration of mitochondrial structure and function. In order to evaluate the role of ROS production at these mitochondrial complexes on the MPT and the LDH release caused by palmitate, the effects of inhibiting mitochondrial complexes I and III on these processes were studied. Cells were pretreated for 30 minutes with various concentrations of rotenone and antimycin A, irreversible inhibitors of complex I and III, respectively. Inhibiting these complexes partially improved the mitochondrial potential (Figure 2.5a) on day 1 and reduced the LDH release (Figure 2.5b) on both days. The partial recovery on day 1 and no effect on day 2 suggested that mechanisms other than ROS generation at complexes I and III are playing roles in the MPT caused by palmitate. Furthermore, co-treatment of the cells with 100 nM rotenone (0.35 pmol/ mg protein) or 50 nM antimycin A (0.17 pmol/ mg protein), following the pretreatment of the cells with 500 nM rotenone (1.8 nmole/ mg protein) or 200 nM antimycin A (0.7 nmol/ mg protein), did not protect against the potential loss. These result show that the ROS production by complexes I and III mediates, partly, the early potential loss and the LDH release in response to palmitate-exposure, but mechanisms other than ROS production at these complexes are also involved in the MPT induced by palmitate. The effect of these inhibitors on the LDH release in the absence of palmitate was also evaluated. Pretreating the cells for 30 min with 500 nM rotenone (1.8 nmole/ mg protein) and 200 nM antimycin A (0.7 nmol/ mg protein), followed by treatment with control medium, caused a slight increase in toxicity. Nevertheless, even with 1  $\mu$ M rotenone and 500 nM antimycin A, the LDH release was less than 2% (not shown), much

less than that observed with palmitate and the inhibitors. This indicated that the remaining toxicity in the palmitate samples in the presence of these inhibitors is due to some mechanism other than ROS production at these sites (complexes) in response to palmitate.

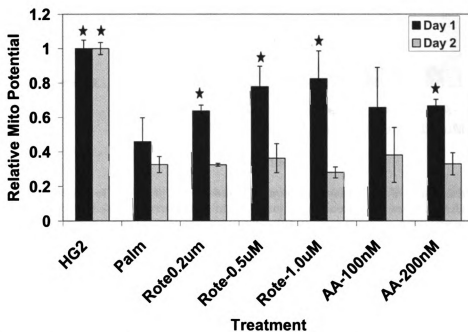


**Figure 2.5a Effects of inhibiting mitochondrial complexes I and III on mitochondrial potential loss.** Cells were pretreated with different concentrations of rotenone or antimycin A for 30 minutes, followed by the treatment with 0.7 mM palmitate. At the end of 24h exposure, the media were removed and cells treated with the same concentrations of rotenone and antimycin A for 30 min, followed by exposure to palmitate for another 24h. Mitochondrial potential was measured after the 24 and 48 h of exposure to palmitate, using JC-1 dye, as explained in the materials and methods. Data presented as mean  $\pm$  s.d. for nine samples from three independent experiments. ‘\*’ denotes significantly different, compared to palmitate,  $p < 0.01$ .

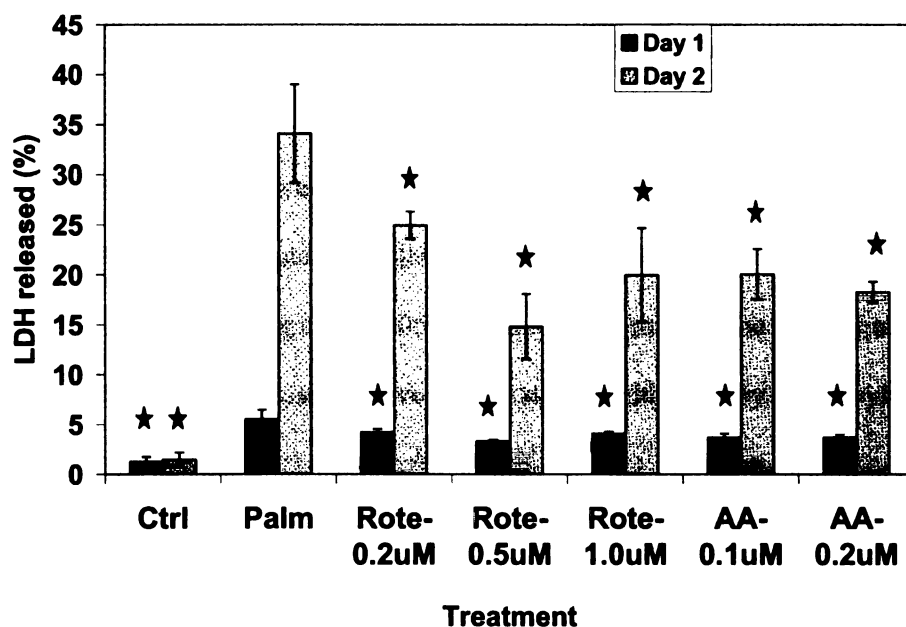


**Figure 2.5b Effects of inhibiting mitochondrial complexes I and III on the cytotoxicity of palmitate.** Cells were pretreated with different concentrations of rotenone (Rote) or antimycin A (AA) for 30 minutes, followed by treatment with 0.7 mM palmitate. After 24h of exposure, cells were treated again with the inhibitors for 30 min, and then exposed to palmitate for another 24h. LDH release after 24 and 48h were measured and normalized to the total LDH. ‘\*’ denotes significantly different, compared to palmitate,  $p < 0.01$ .

## 2.5 Discussion

Free fatty acids are known to play important roles in the development of many hepatic complications. Previous studies have shown that saturated fatty acids are important mediators of lipotoxicity. Studies with other cells have implicated *de novo* ceramide synthesis (Listenberger, Ory et al. 2001; Yamagishi, Okamoto et al. 2002) in the palmitate-induced cell death. Palmitate is a substrate of ceramide synthesis and has been shown to increase *de novo* synthesis of ceramide (Listenberger, Ory et al. 2001). The inhibitor experiments conducted in this study suggest that the palmitate-toxicity to hepatoma cells is not mediated by *de novo* ceramide synthesis. These results are in



agreement with another recent study (Wei, Wang et al. 2006), where the authors reported that the cell death caused by saturated fatty acids in murine hepatoma cells is independent of the *de novo* ceramide generation. It is likely that other mechanisms of cell death such as ER stress (Wei, Wang et al. 2006), lysosomal permeabilization (Feldstein, Werneburg et al. 2006), JNK activation (Malhi, Bronk et al. 2006) or reduction in mitochondrial Bcl2/Bax ratio (Ji, Zhang et al. 2005) play important roles in the toxicity of the saturated fatty acid to HepG2 cells, as observed in the studies with primary hepatocytes.

Another important mediator of cell death by saturated fatty acids is the increased production of ROS. Mitochondrial complexes I and III are the primary sites of ROS generation by the cells. Inhibiting these complexes reduced the cytotoxicity significantly, suggesting that these complexes are an important source of ROS in the palmitate-toxicity to hepatoma cells. The complex I and III inhibitors employed, rotenone and antimycin A, can themselves cause cell death through increased ROS production and MPT at higher concentrations or prolonged exposures (Niknahad, Khan et al. 1995; Isenberg and Klaunig 2000). Therefore, a dose-response study on the toxicity with these compounds in the presence of palmitate was conducted to identify the optimal treatment concentrations and times. In agreement with previous studies, an increase in the cytotoxicity was observed when the cells were treated at higher concentrations or longer durations. However, for the optimal treatment conditions shown (pretreatment for 30 min with 0.5  $\mu$ M rotenone or 0.2  $\mu$ M antimycin A), a maximum reduction in the cytotoxicity ( $55 \pm 10$  % decrease in LDH release for the rotenone pretreatment compared to palmitate treatment alone) was observed. The cytotoxicity was not completely prevented on

treating with mitochondrial complex inhibitors. This suggests that mechanisms other than ROS production in the mitochondria may also contribute to the toxicity of palmitate.

Treatment with palmitate can lead to increased generation of NO in iNOS dependent (Shimabukuro, Ohneda et al. 1997) and independent (Maestre, Jordan et al. 2003) ways. While increased NO generation has been suggested to play a role in palmitate toxicity to a beta-cell line INS-1 (Maestre, Jordan et al. 2003), studies in pancreatic islets have indicated no involvement of NO in response to elevated fatty acid exposure (Cnop, Hannaert et al. 2001). Conflicting roles of NO in mediating the cell death in hepatocytes have been reported. While NO can cause cell death by itself (D'Ambrosio, Gibson-D'Ambrosio et al. 2001), it has been shown to protect against TNF- $\alpha$ -induced cell death (Kim, de Vera et al. 1997; Kim, Kim et al. 2000). It is very likely that NO is non-toxic (and perhaps cytoprotective) at low concentrations, but becomes toxic beyond a certain threshold concentration, which depends on the cell-type. In the present study, either NO did not play a major role in the toxicity or the NO produced in response to palmitate does not reach toxic levels in these cells.

Hepatocytes are known to have high levels and activities of SOD. Therefore, the superoxide anions generated can be effectively neutralized to hydrogen peroxide. This may explain, in part, why the SOD mimics were not effective in reducing the cell death. The SOD mimics will not reduce the production of hydrogen peroxide - the cytotoxicity mediating species. Hydrogen peroxide is freely diffusible across membranes and thus may cause oxidative stress in neighboring cells as well. Extracellular neutralization of

hydrogen peroxide using a high molecular weight catalase reduced palmitate-toxicity significantly, indicating that hydrogen peroxide is the likely carrier of oxidative stress to nearby cells. An increased concentration of hydrogen peroxide was observed in the medium in response to palmitate-exposure, but not in the control medium. However, this increase is not due to an accumulation of hydrogen peroxide, as hydrogen peroxide is not expected to be stable for hours. While in the absence of cells, hydrogen peroxide is stable for at least 30 min (Dringen and Hamprecht 1997), the typical half-life in the presence of cells is a few minutes (Barnard and Matalon 1992; Dringen and Hamprecht 1997). Therefore, these values likely indicate an increase in cellular secretion rather than accumulation of hydrogen peroxide. Another variable which would control the net rate of release by the cells is the level of peroxide-metabolizing enzymes, such as catalase and glutathione peroxidase. Fatty acids have been shown to alter the expression of these enzymes. For example, a high fat diet rich in saturated fatty acid has been shown to reduce the activities of glutathione peroxidase (GPx) and catalase (CAT), while increasing the expression of SOD (Yuan, Kitts et al. 1998; Lu and Chiang 2001). Thus the saturated fat may lead to reduced catabolism of the generated hydrogen peroxide, thus increasing the net release.

One of the important mediators of hydrogen peroxide toxicity is the generation of  $\cdot\text{OH}$  in the presence of divalent cations by the Fenton and Haber-Weiss reactions.  $\cdot\text{OH}$  is an extremely reactive and damaging radical and can oxidize any lipid, protein or DNA molecule in its vicinity. Treating the cells with palmitate in the presence of  $\cdot\text{OH}$ -

scavengers significantly reduced the toxicity, indicating an involvement of this radical in the cytotoxicity of palmitate.

Mitochondria are the organelles centrally associated with many fundamental cellular processes, such as energy-generation. They are also the reservoirs of many apoptogenic factors, such as cytochrome c, apoptosis inducing factor and endonuclease G, etc. A loss of structural and functional integrity of these organelles can lead to cell death. Transport of chemicals and proteins to and from these organelles is strictly regulated. The concentration difference of solutes and the resulting potential gradient across mitochondrial inner membrane is crucial for mitochondrial structural and functional integrity. One of the key regulators of transport of low molecular weight solutes across the inner mitochondrial membrane is the mitochondrial permeability pore (MPP) complex. MPP is a protein complex found at the junctions of the inner and outer membranes, which controls the influx of small molecular weight compounds into the mitochondria. MPT refers to the opening of this pore, a process which brings in solutes of up to 1.5 kDa inside the mitochondria, resulting in the loss of mitochondrial potential, swelling of the mitochondria, a reduction in the ATP generation and production of ROS (Bernardi, Broekemeier et al. 1994). The swelling leads to the rupture of the outer membrane, releasing intermembrane apoptogenic factors such as cytochrome c, apoptosis inducing factor and endonuclease G (Weiss, Korge et al. 2003). MPT also causes loss of anti-oxidants such as glutathione from the mitochondria, making them even more susceptible to ROS-induced damage (Kroemer, Dallaporta et al. 1998). Two types of MPT have been reported- classical, which is inhibited by CsA, and non-classical, which

is not inhibited by CsA. According to *in vitro* studies, employing isolated mitochondria or liposomes, palmitate can cause non-classical MPT (NC-MPT) by forming channels in the mitochondrial membrane by complexing with  $\text{Ca}^{2+}$  (Agafonov, Gritsenko et al. 2003), or by interacting with and altering mitochondrial membrane permeability (Bernardi, Penzo et al. 2002). A complete prevention of mitochondrial potential loss upon treatment with CsA suggested that the loss of mitochondrial potential on exposure to palmitate is due to classical MPT. However, the inhibition of MPT had no effect on the cytotoxicity indicating that the cytotoxicity was not dependent on MPT. CsA may also inhibit protein phosphatase 2B (PP2B/ calcineurin). Inhibition of PP2B is also associated with a reduction in apoptosis (Su and Schneider 1997). Among the various organs, the liver isoform of PP2B is least active and is resistant to CsA inhibition (Wojtczak and Schonfeld 1993). Thus, it was presumed that the effects of CsA are not likely due to calcineurin inhibition.

Palmitate can also indirectly cause MPT by increasing the generation of ROS. ROS can oxidize the thiol groups on cyclophilin-D (CypD) and adenine nucleotide translocase (ANT) (Halestrap, Woodfield et al. 1997), two important proteins of MPP, causing MPT. Elevated ROS generation also leads to lipid peroxidation, which can also cause MPT (Gogvadze, Walter et al. 2003). Mitochondrial complexes I and III are the primary sites of ROS generation. Inhibiting these complexes reduced the loss of potential on day 1, albeit incompletely, but had no effect on the mitochondrial potential loss on the second day. These results suggest that (a) generation of ROS at complexes I and III plays an important role in the initial potential loss caused by these fatty acids, and (b) other

mechanisms are involved in the MPT by fatty acids. Fatty acids may cause MPT by many mechanisms other than mitochondrial ROS generation. It is likely that the production of hydrogen peroxide due to oxidation of fatty acids in peroxisomes may, over time, cause MPT. Fatty acids can also cause MPT independently of ROS. Fatty acids are mitochondrial uncouplers, and can reduce mitochondrial potential to below the 'gating potential' (mitochondrial potential below which MPT occurs), causing MPT (Schonfeld and Bohnensack 1997). They can also cause MPT by binding to and causing structural changes in the ANT (Wieckowski and Wojtczak 1998). Recently, it was demonstrated that fatty acids can cause endoplasmic reticulum (ER) stress (Wei, Wang et al. 2006). ER is an important reservoir of cellular  $\text{Ca}^{2+}$ . ER stress would increase cytosolic and mitochondrial  $\text{Ca}^{2+}$  levels (Berridge 2002; Tiwari, Kumar et al. 2006), which can cause MPT by itself, or increase the sensitivity of the MPT to oxidative stress (Halestrap, Connern et al. 1997). Palmitate can reduce ATP synthesis due to its uncoupling action (Kadenbach 2003), and reduce cardiolipin synthesis (Ostrander, Sparagna et al. 2001). Because MPT is sensitive to both ATP levels and mitochondrial membrane structure, these effects of palmitate would make the mitochondria more susceptible to MPT.

As both cytotoxicity and MPT were observed in the palmitate-treated cells, and were significantly reduced by the reduction in ROS generation, it might be tempting to speculate that the same ROS species is mediating both these effects. However, the inefficacy of the  $\cdot\text{OH}$  radical scavengers (which reduced the toxicity significantly) on MPT suggests that these radicals are not involved in causing the MPT in response to palmitate.

In summary, hydrogen peroxide and  $\cdot\text{OH}$  radical, but not *de novo* ceramide synthesis, are the primary mediators of the cytotoxicity of palmitate in hepatoma cells. ROS generation by the mitochondrial complexes I and III is responsible for mediating the toxicity as well as, in part, the early potential loss in response to palmitate. Thus, while MPT and cytotoxicity are related, in that the exposure to palmitate is associated with both MPT and cytotoxicity, the cytotoxicity is not mediated by MPT.

# **CHAPTER 3. APPLICATION OF METABOLIC FLUX ANALYSIS TO IDENTIFY ALTERED FLUXES ASSOCIATED WITH THE TOXICITY OF PALMITATE**

## **3.1 Introduction**

Hepatocytes play a central role in whole-body lipid metabolism and FFAs have been shown to play an important role in the development of such hepatic disorders as steatosis and non-alcoholic steatohepatitis (NASH) (Farrell and Larter, 2006). Steatosis refers to a condition where there is excess accumulation of lipids inside the cells, leading to altered cellular function. While benign by itself, steatosis primes the cells to injury by oxidative insults (Angulo and Lindor, 2002). NASH refers to a condition of severe inflammation and necrosis of the liver, and can be fatal. With the increased incidences of obesity, the reported cases of NASH are on the rise. It is suggested that about 30% of the population in the US suffers from steatosis (Browning et al., 2004). Of those, 20% of the patients develop NASH (McCullough, 2006). One of the important markers of NASH is extensive hepatocyte cell death and increased serum AST/ALT levels, an indicator of hepatocyte injury. FFAs have emerged as one of the primary factors in the development of NASH (Scheen and Luyckx, 2002). However, the mechanisms behind FFA toxicity remain unclear. Thus, it is important to elucidate the alterations in overall cellular metabolism in order to understand the development of this disease and devise effective treatments.

Previous studies have identified that the saturated FFAs are much more toxic to hepatocytes and hepatoma cells than the mono and poly-unsaturated FFAs (Srivastava and Chan, 2007, Malhi et al., 2006 and Wei et al., 2006). It has also been shown that



metabolism of these fatty acids is essential for their cytotoxic response (Shimabukuro et al., 1998). Therefore, we hypothesized that the differences in the metabolism of the saturated and unsaturated FFAs contribute to their differences in cytotoxicity. We studied the global changes in the metabolism of these cells in response to FFAs by utilizing Metabolic Flux Analysis (MFA). MFA has previously been applied to understand the hypermetabolism of hepatocytes following burn injury (Lee et al., 2003), to optimize hepatocyte functions for bio-artificial liver applications by identifying the changes in hepatocyte metabolism on exposure of plasma (Chan et al., 2003a) and the effects of supplementing the media with hormones and amino acids (Chan et al., 2003b). MFA has also been applied to identify the metabolic effects of hypoxia-inducible factor (HIF-1 $\alpha$ ), to identify if HIF-1 $\alpha$  can be a potential target in cancer treatment (Kim and Forbes, 2006).

In the current study, we measured various extracellular metabolic fluxes and applied MFA to identify the changes in the intracellular metabolism in response to the saturated and unsaturated FFAs for a period of three days. It was observed that the saturated FFA was oxidized to a greater extent and was channeled into TG to a lesser extent than the unsaturated FFA oleate. Studies with other cell types have identified that *de novo* ceramide synthesis in response to saturated FFA may play an important role in causing cell death. The flux through the *de novo* ceramide synthesis was indeed higher in the palmitate-treated cells, but inhibiting this pathway did not produce any change in the cytotoxicity. MFA also identified that the flux through the synthesis of glutathione (GSH) was significantly reduced in cells treated with palmitate but increased in cells treated with

oleate, which was experimentally verified. The levels of cysteine transporter xCT, but not that of glutamyl cysteine synthase (GCS), were reduced by palmitate. Supplementation of the cells with N-Acetyl L-cysteine (NAC), which increases the GSH synthesis by providing cysteine independently of the xCT activity, reduced the toxicity of palmitate. Thus, the metabolic alterations caused by saturated FFAs were identified by MFA and served as targets to regulate the FFA toxicity, which were experimentally validated.

## **3.2 Materials and Methods**

### **3.2.1 Materials**

Glucose, lactate and free glycerol kits were purchased from Sigma. Enzymatic triglyceride and beta-hydroxybutyrate assay kits were purchased from Stanbio Laboratories. Free Fatty Acid Half Micro kit was purchased from Roche Biochemicals. AccQTag amino acid analysis HPLC column, AccQTag solvent and the sample preparation reagents were purchased from Waters.

### **3.2.2 Measurements of Extracellular Fluxes**

Extracellular fluxes of various metabolites were measured by calculating the changes in the concentration of the metabolite in the medium after a specified duration of exposure (typically 24 h). The linearity of some fluxes over this interval was verified. The concentrations of glucose, lactate, FFA, glycerol and beta-hydroxybutyrate were measured by enzymatic kits based on manufacturers' instructions. The concentration of acetoacetate in the media was measured by an enzymatic fluorimetric assay (Olsen 1971). The accumulation of intracellular triglycerides was measured by lysing the cells with 1%

triton in PBS and measuring the concentration of triglycerides in the supernatant by enzymatic triglyceride assay kit from Stanbio, according to manufacturer's instructions. This method measures the amount of glycerol released due to the enzymatic hydrolysis of the TG. To correct for the free glycerol in the cells, the concentration of free glycerol in the cells were measured by free glycerol assay from Sigma, and subtracted from the glycerol values of the TG assay, to give actual triglyceride values. Concentrations of Asp, Glu, Gly, NH<sub>3</sub>, Arg, Thr, Ala, Pro, Tyr, Val, Met, Orn, Lys, Ile, Leu and Phe were measured by the AccQTag amino acid analysis method (Waters). The concentrations of Ser, Asn, Gln and His were measured by a modification of the AccQTag method. Cystine concentration in the media and supernatants was measured using HPLC according to a previously published protocol (Fiskerstrand et al, 1993). Briefly, the protein were precipitated using sulfosalicylic acid (final concentration 5% by weight), the cystine was reduced to cysteine using sodium borohydride and derivatized using monobromobimane (MBB). 20 ul of the samples were then injected onto a Hypersil-ODS silica column equilibrated with 30 mM ammonium nitrate and 40 mM ammonium formate buffer, pH 3.5. Cysteine was separated by a gradient of acetonitrile (0-10.5%) in 11 min. All the measured fluxes were normalized to total protein in the cell extract, measured with the bicinchoninic Acid (BCA) method (Pierce Chemicals).

### **3.2.3 Metabolic Flux Analysis**

MFA is essentially a mass-balance on various intracellular metabolites under the assumption of pseudo-steady state. Under this assumption, the differential equations representing the changes in the concentrations of the various metabolites may be

represented by the algebraic summation of the fluxes associated with a particular metabolite. Thus, various such balances for all the intracellular metabolites under consideration may be represented in matrix notation as

$$\mathbf{S} \cdot \mathbf{v} = \mathbf{0}$$

where,  $S$  is the stoichiometric matrix and  $v$  is the vector of metabolic fluxes. If  $m$  of the fluxes are measured, then it is possible to partition the matrix  $S$  into two submatrices  $S_m$  and  $S_u$  such that

$$\mathbf{S}_m \cdot \mathbf{v}_m + \mathbf{S}_u \cdot \mathbf{v}_u = \mathbf{0}$$

$$\text{Or, } \mathbf{v}_u = (\mathbf{S}_u \cdot \mathbf{S}_u')^{-1} \cdot \mathbf{S}_m \cdot \mathbf{v}_m$$

Thus, it is possible to obtain the vector of unknown fluxes  $v_u$  from knowledge of the stoichiometry and a list of measured fluxes  $v_m$ .

### **Assumptions**

The assumptions employed in the current study with respect to the MFA model are stated below:

- i. Pseudo-steady state was assumed. MFA requires that the intracellular metabolites be under the condition of pseudo-steady state, that is there is no significant accumulation of any metabolite. While the exposure to FFAs would change the concentrations of some of the intracellular metabolites, this change was assumed to be fairly small compared to the overall flux of the metabolite. Experiments were conducted to verify this assumption by measuring the profile of intracellular

metabolite levels and comparing them with the extracellular metabolic fluxes (See section 3 of the Results).

- ii. The fluxes of metabolites are linear over the 24 h period. Fluxes of the uptake or release of metabolites were assumed to be linear over the 24h period, such that the net change in the extracellular concentration of the metabolite after 24h duration represents the flux of that metabolite. To test this assumption, we measured the release of lactate over a 24 h period and found that the flux was linear for the 24 h period (See section 3 in Results).
- iii. The secretion of triglycerides is much lesser than its accumulation. It was assumed that the rate of secretion of triglycerides in the form of lipoproteins was much smaller than the intracellular accumulation of triglycerides. This assumption is valid based on studies with HepG2 cells which identified that these cells have active synthesis but impaired secretion of lipids (Gibbons et al., 1994). Additionally, we also measured the levels of extracellular triglycerides in response to various treatments and observed that the levels of extracellular TG were much lesser than that of the intracellular TG (not shown). It may be noted that intracellular TG was considered as an “external” flux, that is, it was assumed that the TG synthesized is rapidly sequestered into lipid droplets. This is valid because TG is very hydrophobic and forms lipid droplets inside cells (if not exported).
- iv. The metabolites are uniformly distributed inside the cell. This assumption implied that a single MFA model could be applied to perform metabolite balances and separate models were not needed for the various compartments. Many previous

studies have found that this is a fair assumption for mammalian cells (Chan et al, 2003 and Kim and Forbes, 2006).

- v. There is no formation of cysteine from methionine. HepG2 cells cannot synthesize cysteine from methionine due to the lack of S-adenosyl-methionine synthetase activity (Lu and Huang, 1994). Therefore, this equation was not included in the model.
- vi. Either fatty acid synthesis or its oxidation dominates: Formation of a stable system of equation requires that none of the equations be linear combinations of any other equation(s). Meeting this requirement meant that only one of the bidirectional pathways be considered. Therefore, it was assumed that, in FFA-treated cells, the exogenous FFA supply was much greater than the *de novo* fatty acid synthesis, and the latter may be neglected. Opposite assumption was made for the BSA control cells, i.e. fatty acid oxidation was neglected

Based on these assumptions, a MFA model consisting of 84 or 85 cellular metabolic reactions (for control and FFA-treated cells, respectively) involved in the metabolism of glucose, protein and lipids (including the synthesis of sphingo- and phospho- lipids) was developed (Table 3.1). The model consisted of 66 intracellular metabolites for control and palmitate-treated cells and 67 for oleate-treated cells (Table 3.2). In order to solve the system of equations, 28 metabolic fluxes were measured (Table 3.3). This yielded an over-determined system of equations which were solved by least-squares fit using the Moore-Penrose pseudo-inverse calculation.

**Table 3.1 List of the metabolic reactions included in the MFA model**

Flux #	Equation
<b>Glycolysis</b>	
1	G+ATP --> G-6-P
2	G-6-P -> F-6-P
3	F-6-P +ATP --> Glyceraldehyde-3-P + DHAP
4	DHAP --> Glyceraldehyde-3-P
5	Glyceraldehyde-3-P --> 3-PGA
6	3PGA --> PEP + NADH (+ 2ATP)
7	PEP --> Pyr
8	Pyruvate + NADH --> (Lactate)
9	Pyruvate --> Acetyl-CoA + NADH +CO2
<b>TCA cycle</b>	
10	Acetyl-CoA + OAA --> Citrate
11	Citrate --> a-KetoGlutarate + NADPH +CO2
12	a-Ketoglutarate --> Succinyl-CoA + NADH + CO2
13	Succinyl-CoA --> Fumarate + FADH2 + ATP
14	Fumarate --> OAA + NADH
<b>Pentose-phosphate pathway</b>	
15	G-6-P --> 12 NADPH + 6 CO2
16	CO2 out
<b>Ketone Body production</b>	
17	2 Acetyl-COA --> Acetoacetyl-CoA
18	Acetoacetyl-CoA --> Acetoacetate
19	Acac out
20	Acetoacetate + NADH --> (B-OH butyrate)
<b>Oxygen uptake and Oxidative Phosphorylation</b>	
21	O2 (In)
22	NADH + 0.5 O2 --> 2.5 ATP
23	FADH2 + 0.5 O2 --> 2 ATP
<b>FFA synthesis and oxidation</b>	
24	Glycerol + ATP --> Glycerol-3-P
25	Glycerol-3-P --> Glyceraldehyde-3-P + NADH
26*	FA-CoA --> 8(9) Acetyl-CoA + 14(16) NADH
26 <sup>a</sup>	8 Acetyl-CoA + 14 NADPH --> Palm-CoA
27	FA-CoA + DAG --> TG
77	2 FA-CoA + Glycerol-3-P --> Phosphatidate
78	Phosphatidate --> DAG
85*	FA-CoA (In)

**Table 3.1 continued**

**Amino acid metabolism**

- 28 Ser (In)
- 29 Ser  $\rightarrow$  NH<sub>3</sub> + Pyr
- 30 Gln In
- 31 His  $\rightarrow$  Glu + NH<sub>4</sub>
- 32 Asp (In)
- 33 Glu (In)
- 34 Gly (In)
- 35 Gly  $\rightarrow$  2 CO<sub>2</sub> + NH<sub>3</sub> + NADH + THF + ATP
- 36 NH<sub>4</sub> (In)
- 37 Arg In
- 38 Thr  $\rightarrow$  Pyr + CO<sub>2</sub> + NH<sub>4</sub> + 2 NADH + FADH<sub>2</sub>
- 39 Ala (In)
- 40 Glu + Pyr  $\rightarrow$  Ala + aKG
- 41 Pro In
- 42 Cys In
- 43 Tyr (In)
- 44 Tyr + aKG + 2 O<sub>2</sub>  $\rightarrow$  Glu + CO<sub>2</sub> + Acetoacetate + Fumarate
- 45 Val + aKG  $\rightarrow$  Glu + CO<sub>2</sub> + 2NADH + FADH<sub>2</sub> + Succ-CoA
- 46 Orn IN
- 47 Lys + 2 aKG + NADPH  $\rightarrow$  2Glu + Acetoacetyl-CoA + 2CO<sub>2</sub> + 4 NADH + FADH<sub>2</sub>
- 48 Ile + aKG  $\rightarrow$  Glu + Succ-CoA + Acetyl-CoA + NADH + FADH<sub>2</sub>
- 49 Leu + aKG  $\rightarrow$  Glu + Acetyl-CoA + Acetoacetate + CO<sub>2</sub> + NADH + FADH<sub>2</sub>
- 50 Phe + O<sub>2</sub>  $\rightarrow$  Tyr
- 51 Glu + Cys + Gly  $\rightarrow$  GSH
- 56 Gln  $\rightarrow$  Glu + NH<sub>4</sub>
- 58 Asp + NH<sub>4</sub>  $\rightarrow$  Asn
- 59 Thr  $\rightarrow$  Pyr + CO<sub>2</sub> + NH<sub>4</sub> + 2 NADH + FADH<sub>2</sub>
- 60 Val + aKG  $\rightarrow$  Glu + CO<sub>2</sub> + 2NADH + FADH<sub>2</sub> + Succ-CoA
- 61 Lys + 2 aKG + NADPH  $\rightarrow$  2Glu + Acetoacetyl-CoA + 2CO<sub>2</sub> + 4 NADH + FADH<sub>2</sub>
- 62 Ile + aKG  $\rightarrow$  Glu + Succ-CoA + Acetyl-CoA + NADH + FADH<sub>2</sub>
- 63 Leu + aKG  $\rightarrow$  Glu + HMG-CoA + NADH + FADH<sub>2</sub>
- 64 Phe + O<sub>2</sub>  $\rightarrow$  Tyr
- 84 Glu  $\rightarrow$  a-KG + NH<sub>3</sub> + NADPH

**Urea Cycle**

- 52 HCO<sub>3</sub><sup>-</sup> + NH<sub>4</sub> + Orn + 2 ATP  $\rightarrow$  Citrulline
- 53 Citrulline + Asp + ATP  $\rightarrow$  Fumarate + Arg
- 54 Arg  $\rightarrow$  Orn + Urea
- 55 Urea Out
- 57 Orn + a-KG + 0.5 NADPH + 0.5 NADH  $\rightarrow$  Pro

**Synthesis of Cholesterol and Cholesteryl ester**

- 67 Acetoacetyl-CoA + Acetyl-CoA  $\rightarrow$  HMG-CoA
- 68 HMG-CoA + 2 NADPH (+ 3ATP)  $\rightarrow$  IPP
- 69 2 IPP  $\rightarrow$  Geranyl-PP
- 70 Geranyl-PP + IPP  $\rightarrow$  Farnesyl-PP
- 71 2 Farnesyl-PP + 0.5 NADPH + 0.5 NADH  $\rightarrow$  Squalene
- 72 Squalene + O<sub>2</sub> + NADPH  $\rightarrow$  Lanosterol



**Table 3.1 continued**

- 73 Lanosterol + 10.5 NADPH + 4.5 NADH + 10 O<sub>2</sub> --> Chol + 3 CO<sub>2</sub>  
75 Chol + FA-CoA --> Cholesterol Ester

**Sphingolipid Metabolism**

- 65 Ser + 1 Palm-CoA + 1 FA-CoA + NADPH --> Ceramide + CO<sub>2</sub> + FADH<sub>2</sub>  
66 Ceramide + PhosphatidylCholine --> Sphingomyelin

**Phospholipid synthesis**

- 77 Phosphatidate --> CDP-DAG  
78 CDP-DAG + Ser --> PhosphatidylSerine  
79 PhosphatidylSerine --> PhosphatidylEthanolamine + CO<sub>2</sub>  
80 CDP-DAG + G-3-P --> PhosphatidylGlycerol  
81 2 PG --> Cardiolipin + Glycerol  
82 DAG + CDP-Choline --> PhosphatidylCholine  
83 DAG + CDP-Ethanolamine --> PhosphatidylEthanolamine
- 

\* Reactions 26 included only in FFA treatment models.

<sup>a</sup> Reaction 26a included only in model for control cells.

**Table 3.2 List of intracellular metabolites**

	Metabolite
1	glucose-6-P
2	fructose-6-P
3	glyceraldehyde-3-P
4	3-PGA
5	DHAP
6	Phosphoenolpyruvate
7	pyruvate
8	CO <sub>2</sub>
9	acetyl-CoA
10	oxaloacetate
11	citrate
12	$\alpha$ -ketoglutarate
13	succinyl-CoA
14	fumarate
15	acetoacetate
16	acetoacetyl-CoA
17	B-OH
18	O <sub>2</sub>
19	Glycerol-3-P
20	Palm-CoA
21	NADH
22	NADPH
23	FADH <sub>2</sub>
24	Ser
25	Cys
26	NH <sub>4</sub>
27	Glu
28	Gln
29	Val
30	Ile
31	Leu
32	Arg
33	Orn
34	Ala
35	Gly
36	Tyr
37	Thr
38	Lys
39	Phe
40	Pro
41	His
42	Asp
43	Urea
44	Citrulline
45	Ceramide
46	Sphingomyelin
47	HMG-CoA

<b>Table 3.2 continued</b>	
48	Isopentenyl-PP
49	Geranyl-PP
50	Farnesyl-PP
51	Squalene
52	Lanosterol
53	Cholesterol
54	Cholesterol Ester
55	Asn
56	Phosphatidate
57	DAG
58	CDP-DAG
59	PhosphatidylSerine
60	PhosphatidylEthanolamine
61	PhosphatidylGlycerol
62	Cardiolipin
63	CDP-Choline
64	PhosphatidylCholine
65	CDP-Ethanolamine

**Table 3.3 List of measured extracellular fluxes**

Flux #	Metabolite
1	Glucose
8	Lactate
19	AcAc
20	B-Ohbutyrate
21	O2 In
24	Glycerol
27	TG
28	Ser
30	Gln
31	His
32	Asp
33	Glu
34	Gly
36	NH3
37	Arg
38	Thr
39	Ala
41	Pro
42	Cys
43	Tyr
45	Val
46	Om
47	Lys
48	Ile
49	Leu
50	Phe
85	FFA (in)*

\* Flux 85 measured only for the FFA treatments

#### **3.2.4 Correlation analysis**

Correlation analysis was conducted to identify the relationship between the calculated metabolic fluxes and toxicity. Pearson's correlation coefficient was calculated between fluxes from the MFA and cytotoxicity.

### **3.2.5 Perturbation analyses**

To determine the effect of an extracellular flux on the intracellular flux of interest, perturbation studies were conducted *in silico*. The values of a particular extracellular flux were changed while keeping all other fluxes constant and the resulting intracellular fluxes were calculated by MFA.

### **3.2.6 Western Blotting**

The expression of the heavy subunit of glutamyl-cysteine synthase (GCS-H) and xCT (a subunit of system Xc- which transports cystine into the cell) were measured using western blotting. After desired treatments, the cells were washed twice with PBS and scraped off in 200 uL CellLytic M buffer (Sigma). The cells were sonicated in this buffer and centrifuged at 10,000 g for 5 minutes at 4 °C. The supernatants were mixed with sample loading buffer (5X from Cell Signaling Technologies) containing the reducing agent and heated at 95 °C for 10 min, followed by cooling on ice for 2 minutes and short centrifugation to collect the condensate. Equal amounts of protein (150 ug total) were loaded on a 10% Tris-HCl gel (Bio-Rad), as was 10 ul of the prestained protein ladder (Bio-Rad) and electrophoresed at 110 V for 95 min. Samples were then blotted onto nitrocellulose membrane at 110 V for 60 min, followed by blocking of the membrane in 5% fat-free milk solution in Tris buffered saline containing 0.1% Tween (TBS-T) for 1 h at RT. Samples were then incubated overnight in presence of the primary antibody for GCS-H or xCT (both from Abcam Inc. and used at a dilution of 1:1000) in the blocking buffer. After the incubations, the membranes were washed three times for 5 minutes each with TBS-T, followed by exposure to secondary antibody (1:2000 dilution in TBS-T of

goat anti-rat IgG from Pierce Biotechnology) for 1 h at RT. Blots were then washed thrice for 5 minutes each with TBS-T and developed using Supersignal West Femto substrate (Pierce Biotechnology) and imaged using a Bio-Rad imager. The chemiluminiscence was measured for 10 minutes. Following the imaging, the blots were washed thrice with TBS-T and exposed to anti-beta-actin antibody (1:2000 in TBS-T) overnight, then washed thrice and exposed to anti-mouse IgG for 1h in TBS-T (1:5000 dilution). Blots were washed again and imaged by measuring the chemiluminiscence for 1 min.

### **3.3 Results**

#### **3.3.1 Cytotoxicity of FFAs**

*In vivo* measurements of hepatotoxicity require measurements of activities of liver-specific enzymes, such as aspartate transaminase (AST) and alanine transaminase (ALT) in the serum. Many times, a ratio of the activities of ALT/AST is also calculated. Hepatotoxicity is usually associated with serum AST/ALT ratio of greater than 1. However, patients suffering from NASH may have AST/ALT ratio of less than 1 (Kojima et al., 2005). *In vitro*, with a single cell type, the cytotoxicity may be more easily and equally measured by calculating the % lactate dehydrogenase (LDH) activity released, as has been performed in many previous studies (Li et al, 2005 and Wang et al., 2002). Therefore, in the current study, the cytotoxicity of the FFAs was measured as % of lactate dehydrogenase (LDH) released. The saturated FFA, palmitate was found to be toxic and its toxicity increased significantly on the second day of exposure and remained elevated on the third day, while the unsaturated FFA was not toxic (Figure 3.1a). In addition,

exposure to palmitate led to a significant increase in caspase-3 activity (Figure 3.1b). Because the cytotoxicity of palmitate did not change much from day 2 to day 3, most of the experimental verifications were conducted until day 2. For some of the treatments, experiments were conducted until day 3 and it was found that the treatments effective on day 2 were almost equally effective on day 3.

### **3.3.2 Accumulation of TG**

The intracellular accumulation of TG by the cells was measured. The cells exposed to FFAs accumulated significant amount of TG, which were visible under the microscope as intracellular lipid droplets (not shown). Accumulation of lipids inside the liver cells is called steatosis and is considered the first step in the progression to NASH. The intracellular TG levels were quantified by enzymatic assay. Cells exposed to unsaturated FFAs accumulated greater amount of TG than saturated FFAs (Figure 3.2).

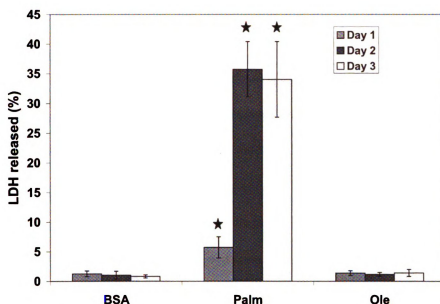


**Figure 3.1a Cytotoxicity of various treatments.** Confluent HepG2 cells were treated with 0.7 mM palmitate or oleate complexed to 4% BSA. Control cells were treated with just 4% BSA. Media were changed every 24h. The cytotoxicity was measured as % LDH released after each 24h exposure, as explained in the materials and methods. Data presented as average  $\pm$  s.d. of three independent experiments. \*, significantly higher than control,  $p < 0.01$ .

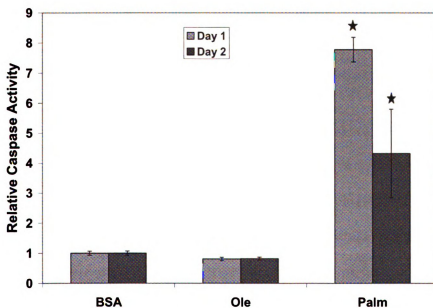


**Figure 3.1b Activation of caspase-3 by palmitate.** Confluent HepG2 cells were treated with 0.7 mM palmitate or oleate complexed to 4% BSA. Control cells were treated with just 4% BSA. Media were changed every 24h. Caspase-3 activity was measured after every 24 h of exposure. Data presented as average  $\pm$  s.d. of three independent experiments. \*, significantly higher than control,  $p < 0.01$ .



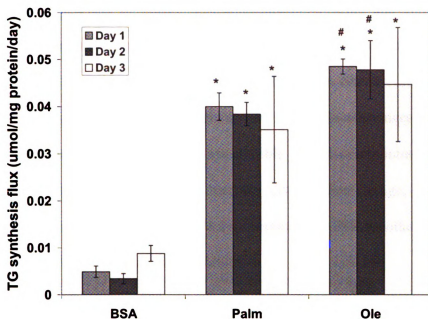


**Figure 3.2 Measured flux through the synthesis of triglycerides in response to FFAs.** Confluent HepG2 cells were treated with 0.7 mM palmitate or oleate complexed to 4% BSA. Control cells were treated with just 4% BSA. Media were changed every 24h. The cells were washed thrice with PBS after the desired time of treatment and lysed with 1% triton-X-100 in PBS. The fluxes of triglyceride synthesis were measured for each day. Data presented as mean  $\pm$  s.d. of  $n=9$  from 3 independent experiments. \*, significantly higher than control,  $p<0.01$ . #, significantly higher than palmitate treatment,  $p<0.01$ .

### 3.3.3 Verification of the pseudo-steady state and linearity of fluxes over 24 h

To verify that the pseudo-steady state (PSS) assumption is valid, the intracellular and extracellular concentrations of lactate were measured after 4, 8, 12 and 24h of exposure to different media. Lactate was chosen because it was the metabolite with the highest flux, and therefore, offered two advantages: (a) because of its high synthesis, it is likely to be the most concentrated metabolite, making it easier to detect with higher accuracy, and (b) because the changes in the levels of lactate were the highest of any metabolite, lactate may provide the most stringent test of the PSS assumption. As shown in Figures 3.3a, the intracellular concentrations of lactate increased with time in response to FFA exposure. Among the two FFAs, palmitate led to higher intracellular levels of lactate. The

extracellular levels of lactate also increased with time, and were not significantly different across the treatments (Figure 3.3b). The extracellular release was approximately linear over the 24h period across different treatments. Similar intra- and extra- cellular profiles were observed on day 2 (not shown). The ratio of changes in the intracellular to extracellular lactate levels are shown in Table 3.2. Since the intracellular changes were about a thousand fold smaller than the extracellular change, it indicates that the accumulation of lactate is negligible and therefore, the PSS hypothesis is valid.

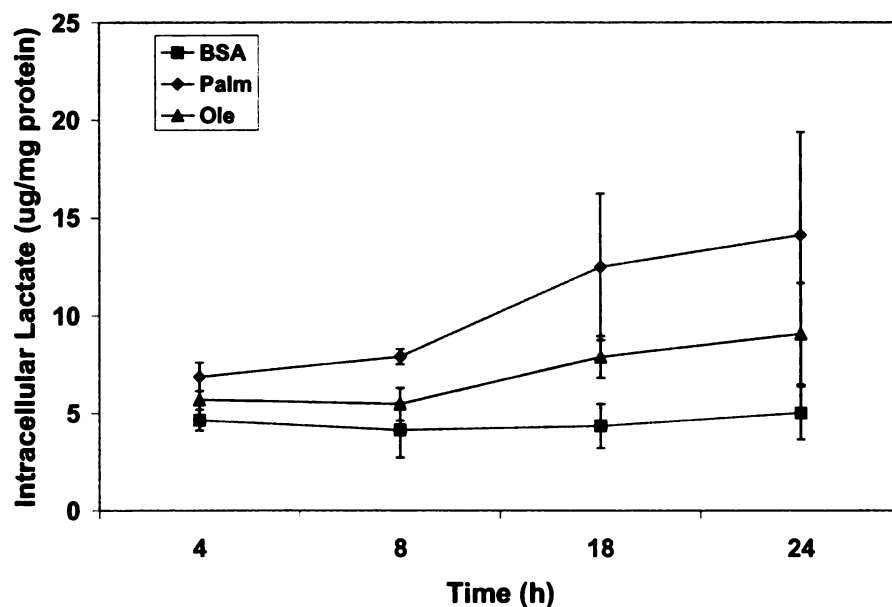


**Figure 3.3a Profile of intracellular lactate levels in response to various treatments.** The cells were treated with 0.7 mM palmitate and oleate complexed to FFAs for various times as indicated, following which the media were collected, cells were trypsinized, washed with thrice with PBS and lyzed in perchloric acid. The lactate levels in the cell-extracts were measured by enzymatic assays. Data presented as mean  $\pm$  s.d. of  $n=9$  from 3 independent experiments.

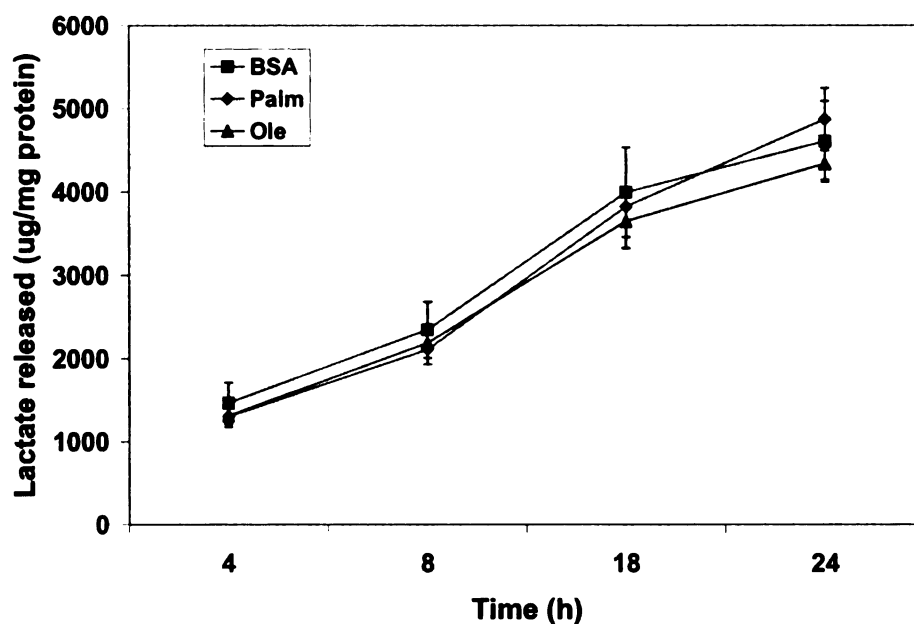


**Figure 3.3b Profile of extracellular lactate levels in response to various treatments.** The cells were treated with 0.7 mM palmitate and oleate complexed to FFAs for various times as indicated, following which the media were collected. The lactate levels in the media were measured by enzymatic assays. Data presented as mean  $\pm$  s.d. of  $n=9$  from 3 independent experiments.

**Table 3.4 Ratio of change in the intracellular to extracellular lactate levels.** The maximum changes in the levels of intra and extra-cellular fluxes for lactate were calculated and their ratios calculated.

	Intra	Extra	Ratio (Intra/Extra)
<b>BSA</b>	0.88	4603.2	<b>1.91 e-4</b>
<b>Palm</b>	7.24	4869.2	<b>1.49 e-3</b>
<b>Ole</b>	3.60	4333.8	<b>8.31 e-4</b>

### 3.3.4 MFA analysis

The results of the MFA analysis for days 1, 2 and 3 are displayed in Figures 3.4, 3.5 and 3.6, respectively (Figures available at the end of the chapter). The figures show the major fluxes, for a complete list of the fluxes, see appendix 1-3. Exposure to FFAs led to an increase in intracellular TG accumulation (measured flux) and therefore, the reactions leading to TG formation, such as phosphatidate and diacylglycerol synthesis, were also

increased. Exposure to palmitate led to reduced uptake of glycerol and increased release of ketone bodies as compared with oleate or BSA. No changes in glucose metabolism were observed in response to the various treatments. Cells exposed to palmitate also had altered amino acid metabolism. They had, in general, reduced His, Gly, Arg, Cys, Tyr and Val uptake, but had greater uptake of Ser, Thr, Ile, Leu and Phe than controls (BSA-treated cells). Among these, Phe, Val, Tyr, Thr, Ile, His, Arg and Leu are essential amino acids while Gly and Cys are required for glutathione synthesis. Palmitate-treated cells also secreted less Ala as compared to controls. Most of these differences in amino acid uptake/ release were also observed in palmitate-treated cells when compared to oleate-treated cells. However, both the palmitate and oleate exposure reduced Arg uptake as compared to the controls. Some of the fluxes altered by exposure to palmitate were chosen for further analysis, based on their strong correlation to the toxicity or known involvement in toxicity, as discussed below. The results of the experiments to evaluate the roles played by these metabolites in the palmitate cytotoxicity are also presented.

#### **3.3.4.1 Correlation analysis**

In order to gain insights into the fluxes which might contribute to the cytotoxicity, correlation analysis of the calculated fluxes to cytotoxicity was conducted. Table 3.5 lists the results of the correlation analysis in decreasing order of the correlation coefficients. It was observed that reactions involved in ketone body production (fluxes 18-20) had the highest positive correlation coefficient to the cytotoxicity. Similarly, *de novo* ceramide synthesis also had high positive correlation coefficient to toxicity. These results suggested a relation between cytotoxicity and these fluxes, which was experimentally

investigated (see section below). Ala release (flux 39) as well as serine uptake (flux 28) also had high positive correlation coefficients.

Uptake of cysteine (flux 42) had the greatest negative coefficient, followed by uptake and metabolism of lysine and valine. These results suggested that supplementation of cysteine could reduce cytotoxicity, which was experimentally validated (see section below). Lysine and valine are essential fatty acids. Exposure to palmitate reduced the uptake of these. Essential fatty acids have been shown to affect cell growth (Gardner and Lane, 1993). Certain studies have also shown protective effects against cell death by supplementing with these amino acids (Hong-Ping and Bao-Shan, 1999).

**Table 3.5 Ranked list of Pearson's correlation coefficient of the metabolic fluxes with cytotoxicity**

<b>Flux #</b>	<b>Equation</b>	<b>Corr. Coeff</b>
18	Acetoacetyl-CoA → Acetoacetate	0.98
20	Acetoacetate + NADH → (B-OH butyrate)	0.97
19	Acac out	0.96
65	Ser + 2 Palm-CoA + NADPH → CO <sub>2</sub> + Ceramide + FADH <sub>2</sub>	0.87
66	Ceramide + PhosphatidylCholine → Sphingomyelin	0.82
39	Ala (In)	0.80
17	2 Acetyl-CoA → Acetoacetyl-CoA	0.80
38	Thr (In)	0.70
84	Glu + 2 NADPH → Pro	0.65
28	Ser (In)	0.65
56	Gln → Glu + NH <sub>4</sub>	0.57
82	DAG + CDP-Choline → PhosphatidylCholine	0.55
36	NH <sub>4</sub> (In)	0.53
26	Palm-CoA → 8 Acetyl-CoA + 14 NADH	0.50
15	G-6-P → 12 NADPH + 6 CO <sub>2</sub>	0.49
64	Phe + O <sub>2</sub> → Tyr	0.41
30	Gln In	0.39
59	Thr → Pyr + CO <sub>2</sub> + NH <sub>4</sub> + 2 NADH + FADH <sub>2</sub>	0.36
62	Ile + aKG → Glu + Succ-CoA + Acetyl-CoA + NADH + FADH <sub>2</sub>	0.32
63	Leu + aKG → Glu + HMG-CoA + NADH + FADH <sub>2</sub>	0.31
49	Leu (In)	0.28
50	Phe (In)	0.25
77	Phosphatidate → CDP-DAG	0.25
52	HCO <sub>3</sub> <sup>-</sup> + NH <sub>4</sub> + Om + 2 ATP → Citrulline	0.21
78	CDP-DAG + Ser → PhosphatidylSerine	0.20
79	PhosphatidylSerine → PhosphatidylEthanolamine + CO <sub>2</sub>	0.19
53	Citrulline + Asp + ATP → Fumarate + Arg	0.16
48	Ile (IN)	0.11
81	2 PG → Cardiolipin + Glycerol	0.07
80	CDP-DAG + G-3-P → PhosphatidylGlycerol	0.07
9	Pyruvate → Acetyl-CoA + NADH + CO <sub>2</sub>	0.04
73	Lanosterol + 10.5 NADPH + 4.5 NADH + 10 O <sub>2</sub> → Chol + 3 CO <sub>2</sub>	0.03
72	Squalene + O <sub>2</sub> + NADPH → Lanosterol	0.03
71	2 Farnesyl-PP + 0.5 NADPH + 0.5 NADH → Squalene	0.03
70	Geranyl-PP + IPP → Farnesyl-PP	0.03
68	HMG-CoA + 2 NADPH (+ 3ATP) → IPP	0.03
69	2 IPP → Geranyl-PP	0.03
75	2 Palm-CoA + Glycerol-3-P → Phosphatidate	-0.02
74	Cholesterol Ester → Chol + FA-CoA	-0.04
67	Acetoacetyl-CoA + Acetyl-CoA → HMG-CoA	-0.05
33	Glu (In)	-0.13
83	DAG + CDP-Ethanolamine → PhosphatidylEthanolamine	-0.15
27	Palm-CoA + DAG → TG	-0.16
29	Ser → NH <sub>3</sub> + Pyr	-0.18
76	Phosphatidate → DAG	-0.19

	<b>Table 3.5 continued</b>	
22	NADH + 0.5 O <sub>2</sub> → 2.5 ATP	-0.22
16	CO <sub>2</sub> out	-0.24
44	Tyr + aKG + 2 O <sub>2</sub> → Glu + CO <sub>2</sub> + Acetoacetate + Fumarate	-0.28
41	Pro In	-0.36
21	O <sub>2</sub> (In)	-0.40
54	Arg → Orn + Urea	-0.45
55	Urea Out	-0.45
1	G+ATP → G-6-P	-0.49
8	Pyruvate + NADH → (Lactate)	-0.50
58	Asp + NH <sub>4</sub> → Asn	-0.50
25	Glycerol-3-P → Glyceraldehyde-3-P + NADH	-0.50
57	Orn + a-KG + 0.5 NADPH + 0.5 NADH → Pro	-0.52
34	Gly (In)	-0.54
37	Arg In	-0.54
51	Glu + Cys + Gly → GSH	-0.54
11	Citrate → a-KetoGlutarate + NADPH + CO <sub>2</sub>	-0.55
12	a-Ketoglutarate → Succinyl-CoA + NADH + CO <sub>2</sub>	-0.55
35	Glycine → 2 CO <sub>2</sub> + NADH + NH <sub>3</sub>	-0.56
10	Acetyl-CoA + OAA → Citrate	-0.57
46	Orn IN	-0.57
4	DHAP → Glyceraldehyde-3-P	-0.57
3	F-6-P + ATP → Glyceraldehyde-3-P + DHAP	-0.58
2	G-6-P → F-6-P	-0.58
14	Fumarate → OAA + NADH	-0.58
13	Succinyl-CoA → Fumarate + FADH <sub>2</sub> + ATP	-0.60
7	PEP → Pyr	-0.61
6	3PGA → PEP + NADH (+ 2ATP)	-0.61
5	Glyceraldehyde-3-P → 3-PGA	-0.61
23	FADH <sub>2</sub> + 0.5 O <sub>2</sub> → 2 ATP	-0.64
43	Tyr (In)	-0.66
32	Asp (In)	-0.68
61	Lys + 2 aKG + NADPH → 2Glu + Acetoacetyl-CoA + 2CO <sub>2</sub> + 4 NADH + FADH <sub>2</sub>	-0.70
24	Glycerol + ATP → Glycerol-3-P	-0.73
31	His → Glu + NH <sub>4</sub>	-0.75
60	Val + aKG → Glu + CO <sub>2</sub> + 2NADH + FADH <sub>2</sub> + Succ-CoA	-0.81
40	Glu + Pyr → Ala + aKG	-0.83
45	Val (In)	-0.86
47	Lys (In)	-0.89
42	Cys In	-0.91

### 3.3.4.2 Fatty acid oxidation

Exposure to palmitate led to a greater release of ketone bodies than the controls or oleate (Figure 3.7a). The profile of beta-oxidation resembled that of the cytotoxicity, suggesting

a relationship between the two. In fact, the fluxes of ketone body production had the highest Pearson's correlation coefficient to the cytotoxicity (see Table 3.5). In order to test a causative role of increased oxidation on cytotoxicity, we tested the effect of inhibitors of beta-oxidation on cytotoxicity. Etomoxir (Etmx) and 2-mercaptoacetate (2-MA) were employed to inhibit mitochondrial oxidation. Etomoxir has been shown to completely inhibit beta-oxidation of palmitate in HepG2 cells (Minnich, 2001). Multiple concentrations of these inhibitors (20, 50 and 100  $\mu$ M were tested for their ability to reduce the cytotoxicity. However, inhibiting FFA oxidation did not reduce the cytotoxicity (Figure 3.7b). This indicated that the increased beta-oxidation of palmitate, despite its strong correlation, was not responsible for the cytotoxicity of the FFA.

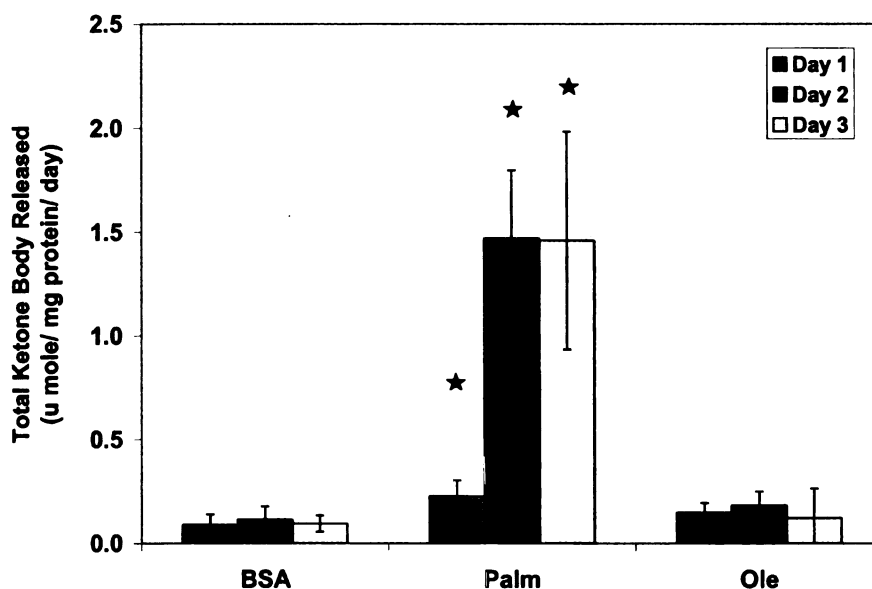


**Figure 3.7a Measured flux of release of total ketone bodies (acetoacetate + beta-hydroxybutyrate) by the cells.** Confluent HepG2 cells were treated with 0.7 mM palmitate or oleate complexed to 4% BSA. Media were replaced daily. The fluxes of acetoacetate and beta-hydroxybutyrate release were measured for each day. Data presented as mean  $\pm$  s.d. of  $n=9$  from 3 independent experiments. \*, significantly higher than control,  $p<0.01$ .



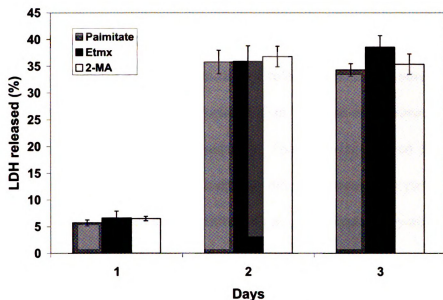


**Figure 3.7b** Effect of inhibition of fatty acid beta-oxidation on the toxicity of saturated FFA. Cells were treated with 0.7 mM palmitate in the presence of 100  $\mu$ M etomoxir (Etmx) or 100  $\mu$ M 2-mercaptoacetate (2-MA) for 3 days. Media were changed daily and the cytotoxicity was measured as LDH release. Data presented as mean  $\pm$  s.d. of n=9 from three independent experiments.

### 3.3.4.3 *De novo* ceramide synthesis

Because *de novo* ceramide synthesis has been suggested as an important player in the cytotoxicity of saturated FFAs, the fluxes of *de novo* ceramide synthesis were calculated in the various treatments. Cells treated with saturated FFA had increased flux through *de novo* ceramide synthesis (Figure 3.8 a), as well as higher intracellular levels of ceramide (Figure 3.8 b). To identify the limiting metabolite in ceramide synthesis, perturbation analysis of serine and palmitate levels (the two metabolites required for *de novo* synthesis of ceramide) on ceramide synthesis was performed. This analysis revealed that ceramide synthesis in palmitate-treated cells was more responsive to changes in the uptake of serine than palmitate (Figure 3.8 c). This suggests serine as a potential regulator of ceramide synthesis in palmitate-treated cells. Exposure to palmitate also led to higher uptake of serine. Thus, it is likely that the increased synthesis of *de novo* ceramide is due

to increased availability of both substrates in palmitate-treated cells. Correlation analysis identified that *de novo* ceramide synthesis also had high positive correlation to the cytotoxicity (Table 3.5). In order to test the role of increased *de novo* ceramide synthesis on the cytotoxicity, we tested the effect of an inhibitor of *de novo* ceramide synthesis, fumonisin B1 (FB1), on the cytotoxicity. The inhibitor reduced the accumulation of ceramide significantly (Figure 3.8 d), but did not reduce the cytotoxicity of the FFA (Figure 3.8 e). These results suggested that *de novo* ceramide synthesis does not play a significant role in the palmitate-induced toxicity of HepG2 cells.

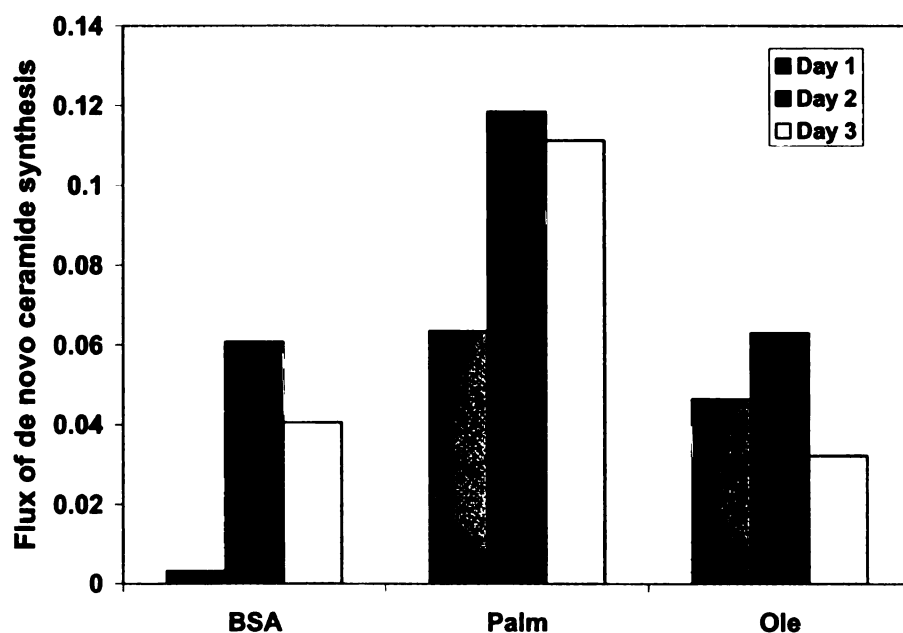


**Figure 3.8a** Calculated flux through ceramide synthesis. The flux through *de novo* ceramide synthesis as predicted by MFA is presented.

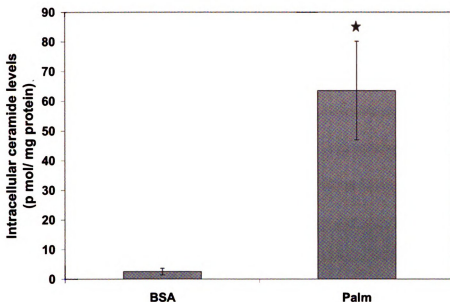


**Figure 3.8b Intracellular C-16 ceramide levels in response to palmitate.** The cells were treated with 0.7 mM palmitate for 48 h. Intracellular ceramide levels were measured using LC/MS. Data presented as mean  $\pm$  s.d. of n=6 from two independent experiments.

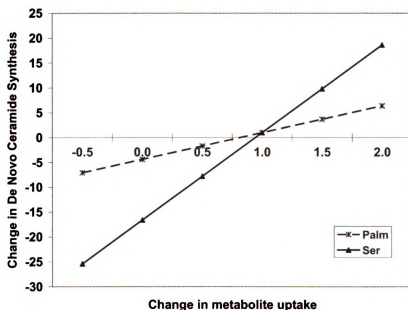


**Figure 3.8c Results of *in silico* perturbation studies for the effect of serine or palmitate on the flux of *de novo* ceramide synthesis.** The fluxes of uptake of palmitate or serine were altered while keeping all the other measurements same and the changes in the fluxes of *de novo* ceramide synthesis were calculated. Data presented as relative change in the flux of *de novo* ceramide synthesis with respect to relative change in the flux of metabolite.

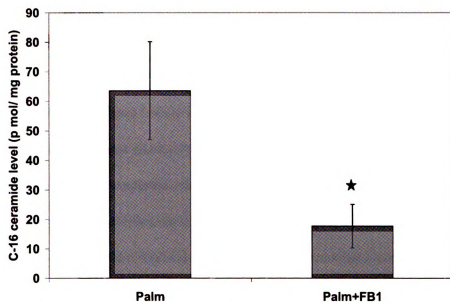


**Figure 3.8d Effect of inhibition of ceramide synthesis on the levels of C-16 ceramide in the cells.** Cells were cultured for 48 h in 0.7 mM palmitate in the presence or absence of 20  $\mu$ M Fumonisin B1 (FB1). The intracellular lipids were extracted and the levels of C-16 ceramide measured by LC-MS. Data presented as mean  $\pm$  s.d. of n = 6 from 2 independent experiments. \*, significantly smaller than palmitate.

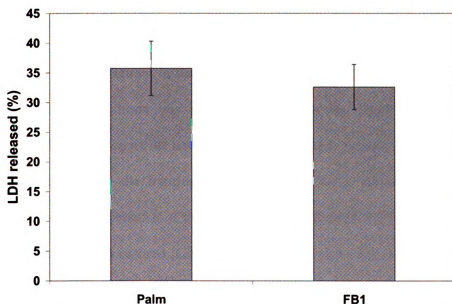


**Figure 3.8e Effect of inhibition of ceramide synthesis on the cytotoxicity of palmitate.** Cells were treated with palmitate in presence of 20  $\mu$ M FB1 and the cytotoxicity after 48 h of treatment was measured. Data presented as mean  $\pm$  s.d. of n=9 from 3 independent experiments.

#### 3.3.4.4 Glutathione synthesis

Oxidative stress is considered an important factor in the development of NASH. We have previously identified an important role of oxidative stress in the toxicity of palmitate (Srivastava and Chan, 2007). GSH is the primary anti-oxidant molecule of the cell and protects cells against oxidative insults. Among the different FFAs, palmitate treatment was consistently associated with reduced flux through GSH synthesis, while oleate had higher flux (Figure 3.9a). In order to test the predicted reduction in the GSH synthesis, the total GSH (GSH + GSSG) levels in the cells were measured. The total GSH (tGSH) levels were measured because tGSH levels are resistant to oxidative stress (Glosli et al., 2002) and thus, will not be affected by the oxidative stress caused by palmitate. Exposure to palmitate was associated with reduced levels of tGSH, while exposure to oleate had increased tGSH levels (Figure 3.9b). A reduction in the synthesis of GSH would render the cells more susceptible to oxidative stress. To understand the mechanism of reduction in GSH synthesis, *in silico* perturbation studies of the constituent amino acids in GSH synthesis was performed in the palmitate-treated cells. The perturbation study identified that the GSH synthesis was limited primarily by the supply of cysteine. It was also observed that exposure to palmitate led to reduced cysteine uptake (Figures 3.5-3.7), suggesting it may be the limiting amino acid. To further identify what limits the GSH synthesis, the expressions of the rate-limiting enzyme of GSH synthesis and the cystine transporter were measured. Glutamyl-cysteine synthase (GCS) is the first and the rate-limiting enzyme of GSH synthesis and catalyzes the synthesis of glutamate and cysteine. Another important regulator of GSH synthesis is the availability of cysteine, the primary source of which is cystine in the medium. Cystine is taken up through a transporter, the

system Xc- (Anderson and Meister, 1987), which is composed of two proteins- xCT and 4F2hc/CD98. Western blot analyses revealed that the expression of GCS was increased (Figure 3.9d), but that of xCT was decreased (Figure 3.9e) significantly in palmitate-treated cells. Both these proteins were altered in a time-dependent manner, i.e., the change was greater on day 2 than on day 1. These results identified that the reduced cystine uptake in the palmitate-treated cells was due to reduced levels of the transporter and not of GCS. These studies, in conjunction with the perturbation and correlation studies, indicated that increasing cysteine supply would increase GSH synthesis and thus, may reduce cytotoxicity, while supplementing glycine would not significantly affect GSH levels or cytotoxicity. To test these predictions, we measured the cytotoxicity of palmitate in the presence of N-Acetyl L-cysteine (NAC) and glycine. NAC supplementation has been shown to increase the cellular GSH levels in HepG2 cells (Gruetter et al., 1985). Uptake of NAC is independent of the levels of system Xc- (Sato, 2005). The supplementation of NAC significantly reduced the cytotoxicity of the FFA (Figure 3.9f), while supplementation of glycine had no effect (not shown). Thus, the predictions of MFA and perturbation studies were experimentally verified.

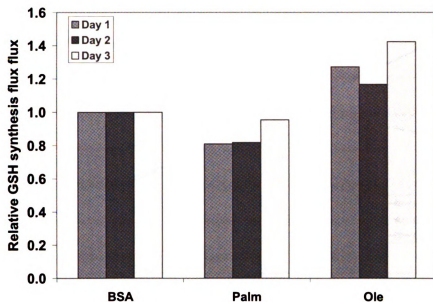


**Figure 3.9a** Calculated relative fluxes of GSH synthesis, as predicted by MFA.

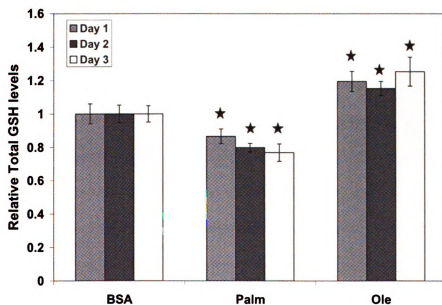


**Figure 3.9b** Measured relative levels of total intracellular GSH. Cells were treated with palmitate or oleate for 3 days. At the end of each day, cells were harvested and the total GSH (tGSH) in the cells were measured colorimetrically. The data was corrected to the cellular protein levels, measured using BCA assay. Data presented as mean  $\pm$  s.d. of three independent experiments.

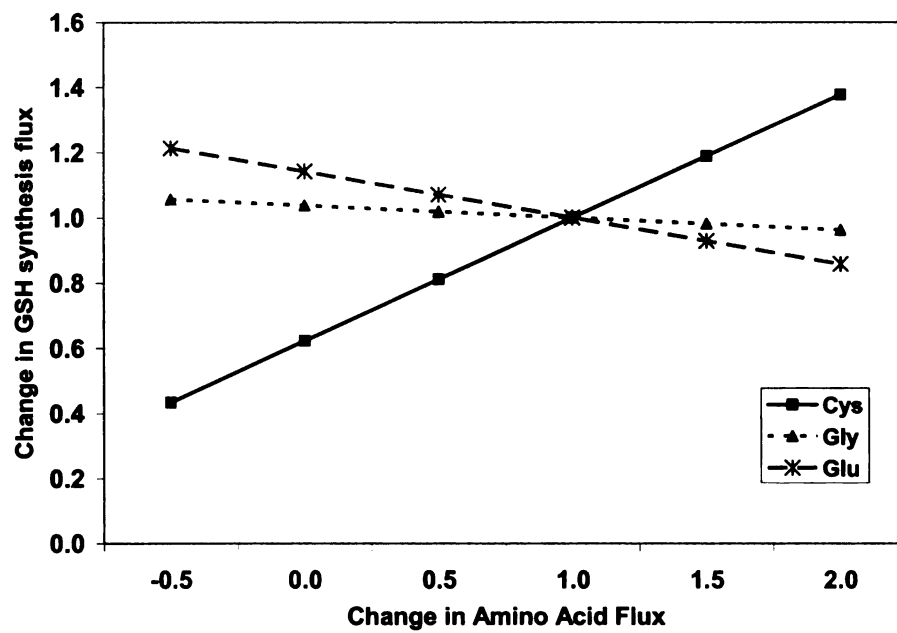
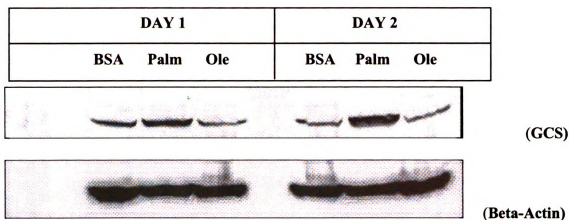


**Figure 3.9c Results of *in silico* perturbation studies on the effect of increasing uptake of amino acids on GSH synthesis.** The fluxes of Glutamate, Glycine or Cysteine were varied and the effect on the flux of GSH synthesis was calculated by the MFA model.





#### Quantification of western blot intensities

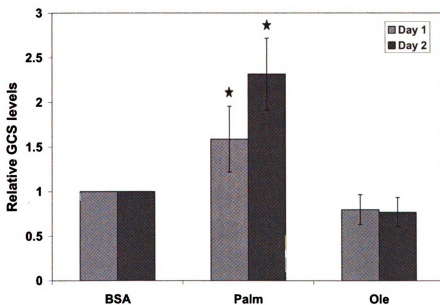
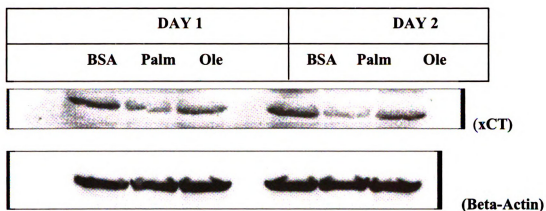


**Figure 3.9d Effect of the treatments on the expression of gamma-glutamyl cysteine synthetase (GCS) heavy subunit.** Cells were exposed to BSA, palmitate or oleate for 24 and 48 h, following which cells were lysed and the expression of GCS were measured using Western Blot. The details of the Western Blot analyses are provided in the methods section. Beta-actin was employed as the loading control. The intensities of different blots were analyzed using available software. The relative intensities of three different blots are presented as mean  $\pm$  s.d.



### Quantification of western blot intensities

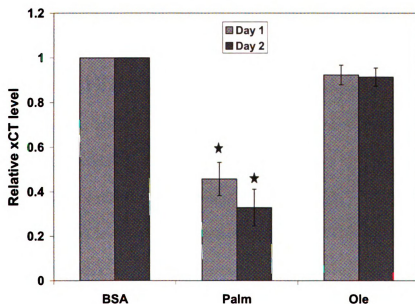


**Figure 3.9e** Effect of the treatments on the expression of xCT (a subunit of cystine transporter). Cells were exposed to BSA, palmitate or oleate for 24 and 48 h, following which cells were lysed and the expression of xCT were measured using Western Blot. The details of the Western Blot analyses are provided in the methods section. Beta-actin was employed as the loading control. The intensities of different blots were analyzed using available software. The relative intensities of three different blots are presented as mean  $\pm$  s.d.

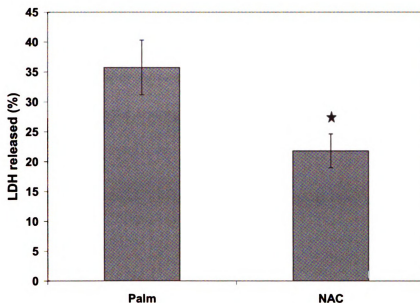


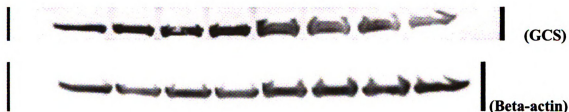
**Figure 3.9f Effect of NAC supplementation on the cytotoxicity of palmitate.** The cells were treated with 0.7 mM palmitate in the presence or absence of 1 mM NAC for two days and the LDH released after 48h of treatments were measured. Data presented as mean  $\pm$  s.d. of  $n=9$  from 3 independent experiments. \*, significantly higher than control,  $p<0.01$ .

### 3.3.4.5 Effect of NAC supplementation on the levels of GCS

Many previous studies have suggested that oxidative stress or cysteine limitation increases the levels of GCS (Lu, 1999), and our study shows that exposure to palmitate produces both oxidative stress and cysteine limitation. Therefore, it is likely that the increase in GCS levels in palmitate-treated cells was due to reduced cysteine availability and/ or oxidative stress. NAC supplementation increases the intracellular cysteine (Anderson, 1987) and GSH levels (Gruetter et al., 1985) and reduces oxidative stress (Quanungo et al., 2004). Acute (24 h) NAC supplementation increased the expression of GCS in both palmitate and control media (Figures 3.10 a and b), but a synergistic increase in GCS levels was observed in the palmitate-treated cells (Figure 3.10a). However, chronic exposure to NAC reduced the levels of GCS (day 2) in the palmitate-

containing medium, while no significant changes were observed in the control medium. This suggests that chronic exposure to palmitate increases GCS levels by reducing cysteine levels and/ or by causing oxidative stress. The increase in GCS levels by NAC supplementation in the control medium are in agreement with that of Lee et al. (2006). In addition, we also identify an increase in the levels of GCS in the presence of palmitate and NAC.

	DAY 1				DAY 2			
NAC (mM)	0	1	5	10	0	1	5	10



#### Quantification of western blot intensities

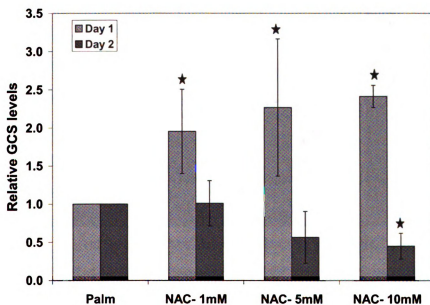
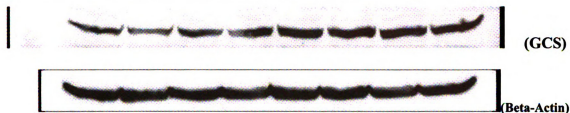


**Figure 3.10a** Effect of NAC supplementation on GCS levels in palmitate-treated cells. Cells were treated with palmitate in the presence of increasing amounts of NAC (0, 1, 5 and 10 mM) for 48 h in the presence of 0.7 mM palmitate. Media were changed every 24 h. At the end of desired exposure times, the expression of GCS was measured using western blots.

DAY 1					DAY 2			
NAC (mM)	0	1	5	10	0	1	5	10



#### Quantification of western blot intensities

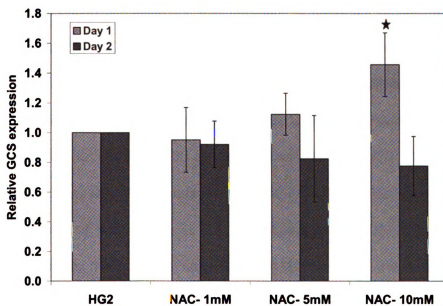


**Figure 3.10b** Effect of NAC supplementation on GCS levels in control medium. Cells were treated with increasing amounts of NAC (0, 1, 5 and 10 mM) for 48 h in control medium. Media were changed every 24 h. At the end of desired exposure times, the expression of GCS was measured using western blots.

### **3.4 Discussion**

While it is known that altered metabolism and generation of ROS play important roles in the development of hepatic lipotoxicity, the underlying global metabolic responses are not clearly known. MFA of human hepatoma cells in response to various FFAs identified changes in the intracellular fluxes in response to the different FFAs and helped to differentiate between the potential mechanisms involved in the cytotoxicity of the saturated FFAs as compared to the unsaturated FFAs. Additionally, MFA also identified those external fluxes which regulate the internal fluxes of interest, thus suggesting possible supplementation methods to combat lipotoxicity.

We have previously identified that exposure to palmitate causes significant oxidative stress and this oxidative stress plays an important role in the toxicity of this fatty acid. GSH is the primary anti-oxidant thiol. In this paper we find that palmitate also reduces the synthesis of GSH by reducing cysteine uptake. The underlying mechanism was identified to be reduced levels in the cysteine transporter xCT. These results indicate a multi-pronged effect of palmitate on the cellular redox homeostasis which leads to the cytotoxicity of this fatty acid. The underlying mechanism in the reduction of xCT expression by palmitate is unknown, but may provide important insights into the oxidative stress caused by exposure to this FFA. It was also identified that the GSH synthesis was not limited by the levels of GCS, the first and rate-limiting enzyme of GSH synthesis. In fact, the expression of GCS was found to be increased in the palmitate-treated cells, in a time-dependent fashion. However, the observation that NAC supplementation did not reduce the acute increase in GCS expression in response to

palmitate suggests that the acute increase by palmitate was not mediated by oxidative stress or cysteine limitation, but perhaps through the activation of certain transcription factors involved in regulating GCS expression, e.g. Nrf2 (Wild, 1999). In fact, activation of Nrf2 has been shown to protect HepG2 cells against the toxicity of CYP2E1 and arachidonic acid (Gong and Cederbaum, 2006). The reduction in GCS levels in palmitate-treated cells by chronic (48 h) treatment of NAC suggests that the chronic increase in GCS by palmitate (which is much greater than the acute increase in response to palmitate) was, indeed, mediated through a reduction in cysteine supply and / or oxidative stress.

Another important result is the lack of involvement of *de novo* ceramide synthesis in the toxicity of palmitate. While the *de novo* ceramide synthesis and ceramide accumulation were increased in the palmitate-treated cells, inhibiting this pathway did not reduce the FFA toxicity. In fact, studies by other groups have also indicated that saturated FFA-toxicity to hepatocytes is independent of *de novo* ceramide synthesis (Wei et al., 2006 and Feldstein et al., 2006). In our study, the ceramide accumulation was in picomoles/mg protein, while the flux of synthesis and metabolism of ceramide were in nanomoles/ mg protein. This indicates that these cells in particular, and probably hepatocytes in general, can effectively metabolize ceramide so that the accumulations do not reach cytotoxic levels.

Our results demonstrate the applicability of MFA in identifying the altered metabolic processes under simulated conditions of metabolic disorders. The results show



differential metabolism of the saturated vs. unsaturated FFAs, which results in the toxic effect of the former and suggest potential treatments to reduce the FFA toxicity. MFA identifies more than one cellular process to be altered. This information help narrow down targets for further study, as was illustrated here. Though the treatments did not reduce the cytotoxicity to basal levels, it is likely that there is some non-specific cytotoxicity of the FFA due to its hydrophobic effects. Among the different FFAs, palmitate has the highest hydrophobicity. Therefore, palmitate may cause the disruption of the plasma membrane (Oliver and Opie, 1994) leading to the cytotoxicity.

The MFA study indicated the complex metabolic alterations induced by FFAs were caused in part by changes in the levels of proteins (e.g. xCT), leading to altered physiological response (cytotoxicity). Exposure to FFAs would also alter various other cellular processes which may not cause a significant change in metabolism, but still initiate cell death, for example, the activities of certain signaling pathways may be regulated by palmitoylation (Resh, 2006) as well as affect the transcription of genes involved in multiple cellular processes (Swagell et al., 2005). Though, these processes were not investigated in this study, a more complete understanding of the development of lipotoxicity requires generation and integration of such multi-source information. Application of novel high throughput techniques coupled with advanced modeling would help in achieving this goal. Such analysis would provide important insights into the underlying changes, as well as novel information into the inter-relationships among the changes, thus providing more effective alternatives to regulate the deleterious effects of FFAs.

**Figure 3.4 Results of MFA analysis, depicting major intracellular fluxes on day 1**

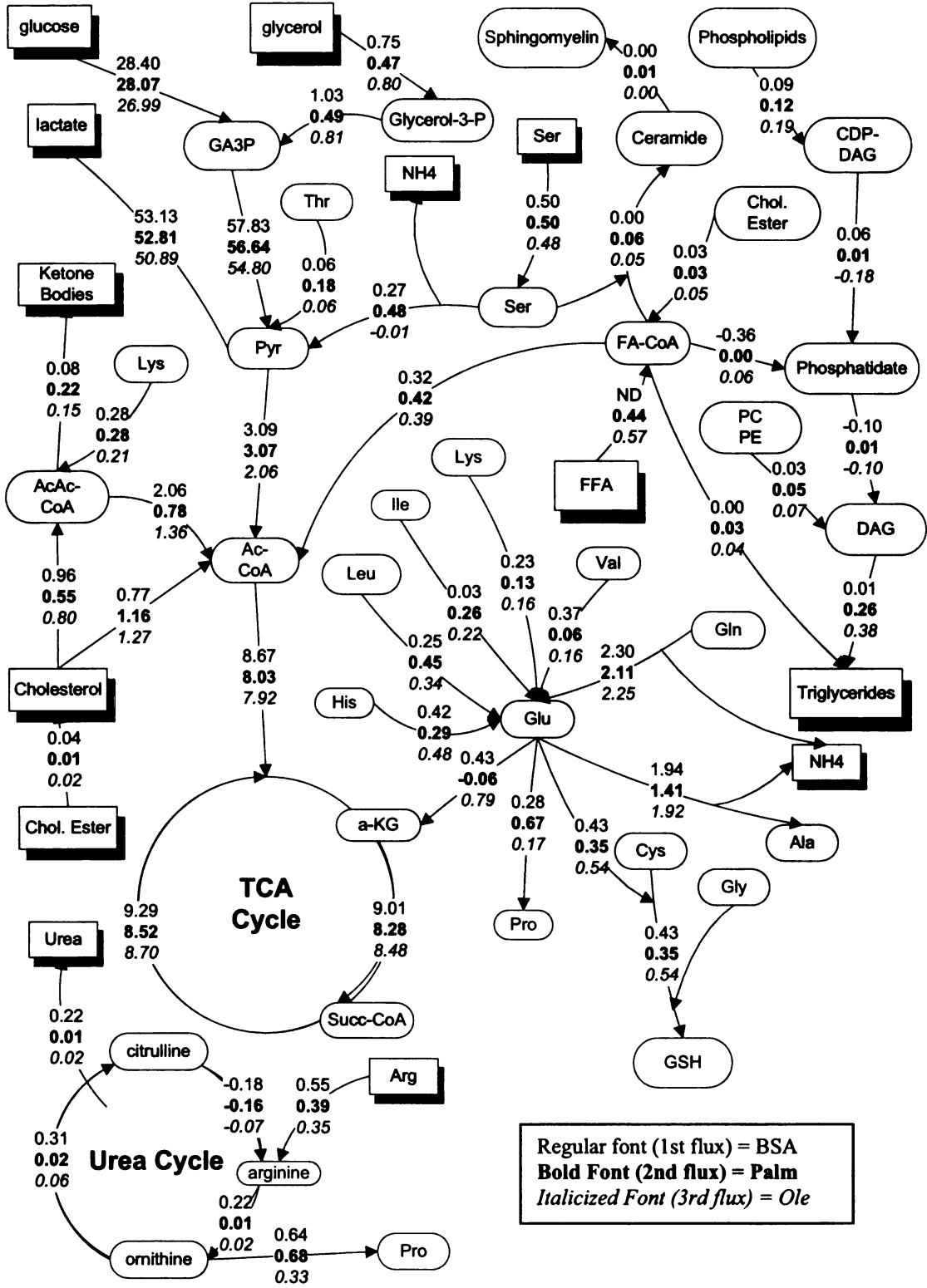


**Figure 3.5 Results of MFA analysis, depicting major intracellular fluxes on day 2**

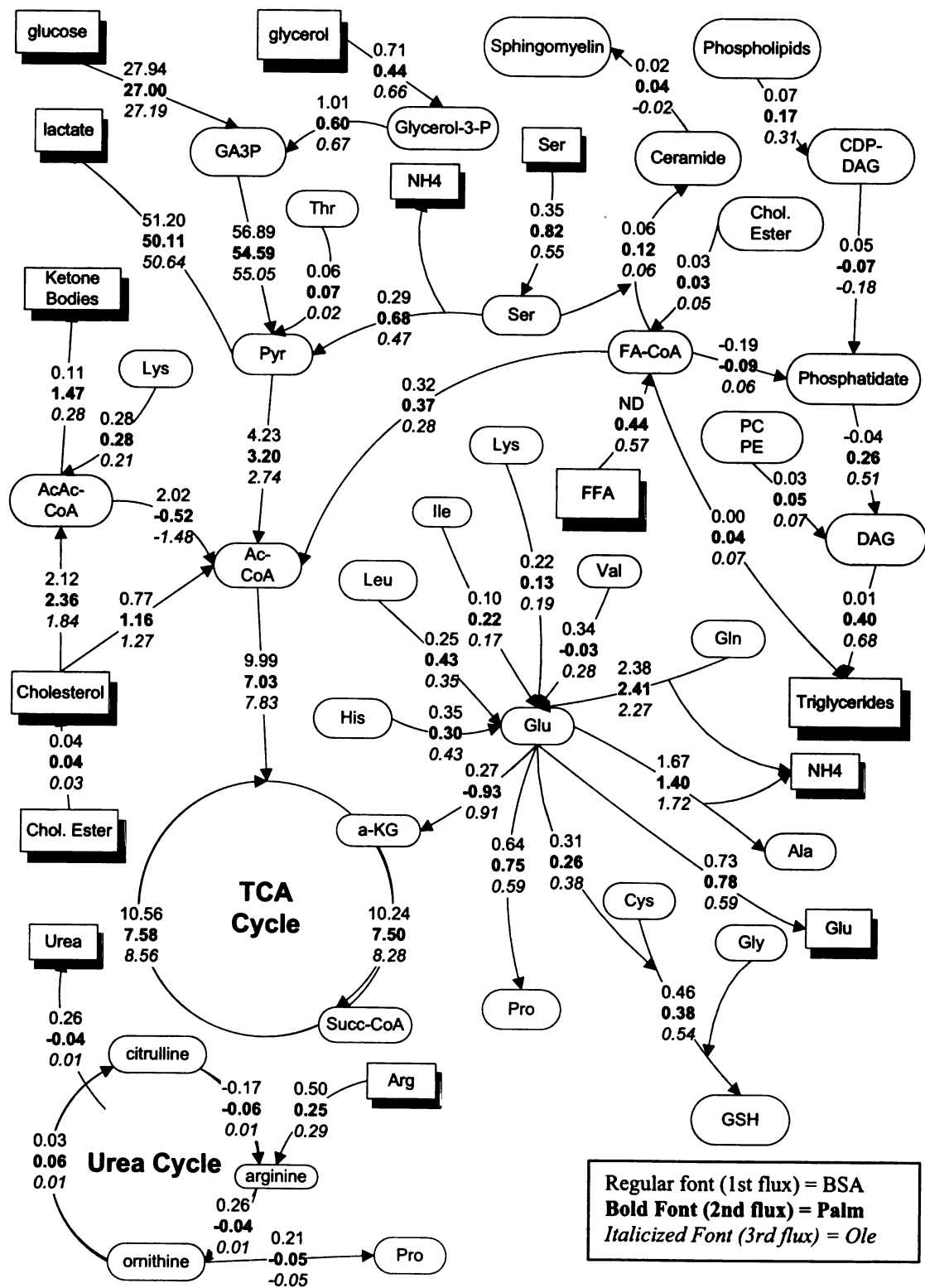
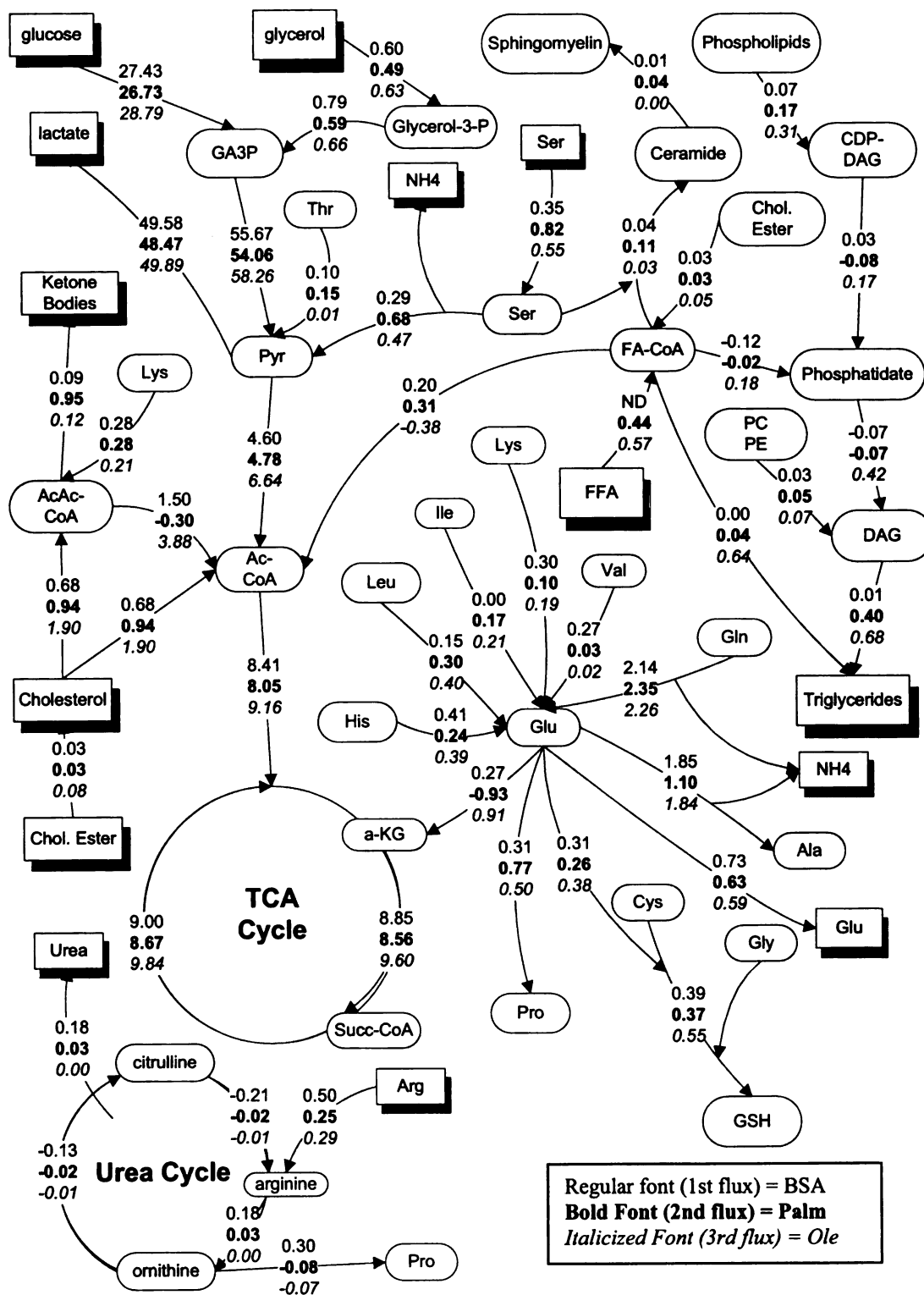


**Figure 3.6 Results of MFA analysis, depicting major intracellular fluxes on day 3**



## **CHAPTER 4. IDENTIFICATION OF GENES THAT REGULATE MULTIPLE CELLULAR PROCESSES/RESPONSES IN THE CONTEXT OF LIPOTOXICITY TO HEPATOMA CELLS**

### **4.1 Introduction**

Many human diseases result from alterations in multiple cellular processes. Therefore, targeting an individual process or response may not be sufficient to combat the progression of such diseases. For efficient treatment of such diseases, it is imperative to identify those cellular targets which control multiple functions of interest. For example, prolonged exposure of cells to elevated levels of FFAs can alter multiple cellular processes such as reactive oxygen species (ROS) production (Srivastava and Chan, 2007 and Listenberger et al., 2001), mitochondrial (Ji et al. 2005), endoplasmic reticulum (Wei et al., 2006 and Wang et al., 2006) and lysosomal dysfunction (Feldstein et al., 2006) and activation of a variety of signaling pathways such as protein kinase C (PKC) (Newsholme et al., 2007) and caspases (Fernanda et al., 2006). The resultant effect of these disturbances is lipotoxicity, that is, cell death due to exposure to elevated lipid levels.

Many recent studies have identified that saturated FFAs cause greater lipotoxicity than unsaturated FFAs. It has been suggested that channeling the saturated fatty acids to TG reduces their cytotoxicity (Listenberger et al, 2003). Therefore, genes that regulate TG synthesis from saturated FFAs may be useful targets to combat the lipotoxic action of saturated FAs. We hypothesized that those genes which affect lipid synthesis as well as lipotoxicity may serve as better targets than those regulating TG synthesis alone. To test this hypothesis, we studied the cytotoxicity and the accumulation of TG in human

hepatoma cells (HepG2) in response to various types of FFAs and concentrations of TNF- $\alpha$ . The global gene expressions were obtained by cDNA microarray analyses. A modified genetic algorithm coupled partial least squares (GA/PLS) analysis (Li and Chan, 2004) was applied to identify the genes that regulate toxicity and lipid accumulation, which were selected as potential targets for further functional analysis and experimental testing.

As a proof of concept, we applied the GA/PLS framework to identify the genes associated with TG accumulation. Many genes with known roles in lipid metabolism (e.g. stearoyl-CoA desaturase (SCD) and inositol polyphosphate phosphatase-like 1 (INPPL1)) were identified by GA/PLS analysis for TG accumulation, attesting to the applicability of this approach. Then, the dual-response GA/PLS analysis was applied to identify the genes that regulate both TG accumulation and cytotoxicity. In addition to genes with known roles in the regulation of lipid metabolism and cell physiology, this analysis identified NADH dehydrogenases and MAPKs as important regulators of both lipid accumulation and cell death. While NADH dehydrogenases and MAPKs have been shown to play roles in cell death caused by other insults, this analysis suggested that they regulate not only cell death in response to fatty acid exposure, but also affect lipid accumulation. The predicted roles of NADH dehydrogenases and MAPKs were verified experimentally by employing inhibitors specific to them. Inhibiting NADH dehydrogenase and JNK significantly reduced the cytotoxicity and increased the intracellular TG accumulation, while inhibiting ERK reduced the toxicity without affecting the lipid accumulation.

This study demonstrates the applicability of the dual-response GA/PLS analysis to identify genes which affect diverse cellular processes, and incorporating more

information provides better targets to control cellular responses. It must be pointed out that although the method was applied to identify genes involved in regulating two responses in the current study, the method is capable of handling more than two responses for multi-factorial diseases.

## **4.2 Materials and Methods**

### **4.2.1 Cytotoxicity measurement**

The cytotoxicity of the treatments was measured as the fraction of lactate dehydrogenase (LDH) released into the medium as described in chapter 2. For the experiments with inhibition of NADH dehydrogenases, the cells were pre-treated with 0.2-1.0  $\mu\text{M}$  rotenone for 30 min, followed by exposure to 0.7 mM palmitate for 24h without any inhibitor. The LDH released after the 24h exposure was measured and normalized to the triton-lyzed values, as described above.

For experiments with the MAPK-inhibitors, stock solutions of these inhibitors, were prepared in DMSO and diluted to desired concentrations in palmitate medium. Cells were treated with the palmitate medium containing the desired concentrations of the MAPK inhibitors. Under no condition was the concentration of the resulting DMSO greater than 0.2% v/v. At these concentrations, DMSO does not affect the cytotoxicity of the FFA.

### **4.2.2 Measurement of intracellular TG levels**

The cells were pretreated for 30 minutes with 0-1  $\mu\text{M}$  rotenone, and then exposed to 0.7 mM palmitate or oleate. In the experiments with MAPK inhibitors, cells were treated

with the desired concentrations of the inhibitor dissolved in the FFA medium. After exposure to the FFAs, the cells were washed thrice with PBS and lysed with 1% triton in PBS. The lysates were centrifuged at 10000 g for 2 min, and the concentration of TG in the supernatant was measured by an enzymatic assay kit from Stanbio, according to manufacturer's instructions. This method measures the amount of glycerol released by the enzymatic hydrolysis of the TG. To correct for the free glycerol in the cells, the concentration of free glycerol in the cells were measured by free glycerol assay from Sigma, and subtracted from the glycerol values of the TG assay, to give actual TG values. These values were normalized to total protein in the extract, measured with the bicinchoninic acid (BCA) method (Pierce Chemicals).

#### **4.2.3 Measurement of caspase-3 activity**

Caspase-3 activity was measured using a commercially available colorimetric assay (Biovision) according to manufacturer's instructions. The cells were treated with the control medium or 0.7 mM palmitate for 24 h, washed once with PBS and lysed using the available lysis buffer. The activity in the lysate was measured and normalized to the total protein, measured by bicinchoninic acid (BCA) assay (Pierce Chemicals).

#### **4.2.4 Microarray analyses**

Cells were cultured in 10 cm tissue culture plates until confluence and then exposed to different treatments for 24h. RNA was isolated with the Trizol reagent. The expression profiles of about 19500 genes were obtained with the cDNA microarrays. The microarray analyses were conducted at the Van Andel Institute, Grand Rapids, MI. The protocols are



available online at (<http://microarray.vai.org/protocols/>). There were two biological replicates for each condition and each replicate was measured with the Cy3 and Cy5 dyes (i.e. there were two technical replicates for each biological replicate).

#### **4.2.5 RT-PCR**

Total RNA was extracted from cells with an RNeasy mini kit (Qiagen) and depleted of contaminating DNA with RNase-free DNase (Qiagen). Equal amounts of total RNA (1 µg) were reverse-transcribed using an iScript cDNA synthesis kit (Bio-RAD). The first-strand cDNA was used as a template. The primers used for quantitative RT-PCR analyses of human SCD (5'-TGAGAACTGGTGATGTTCCA-3' and 5'-CCACAGCATATCGCAAGAAA-3') and human GAPDH (5'-AACTTTGGTATCGTGGAAGGA-3' and 5'-CAGTAGAGGCAGGGATGATGT-3') were synthesized by Operon Biotechnologies, Inc.. RT-PCR was performed in 25-µl reactions using 1/10 of the cDNA obtained from the reverse transcription, 0.2 µM each primer, 1 X SYBR green supermix from Bio-RAD, and an annealing temperature of 60 °C for 40 cycles. Each sample was assayed in three independent RT reactions and triplicate reactions each and normalized to GAPDH expression. Negative controls included the absence of enzyme in the RT reaction and absence of template during PCR. The cycle threshold (CT) values corresponding to the PCR cycle number at which fluorescence emission in real time reaches a threshold above the base-line emission were determined using MyIQ<sup>TM</sup> Real-Time PCR Detection System.

#### 4.2.6 GA/PLS analysis

Metabolic functions are regulated in part by the enzymes catalyzing the reactions, which in turn are determined partly by their gene expression levels. Therefore, we hypothesized that the metabolic functions can be predicted from the expression level of a subset of genes that are associated with the metabolic function. We approximated the relation between the metabolic function and expression level of this subset of genes with a log-linear model:

$$\frac{Met(treatment)}{Met(control)} = \prod_{i=1}^n \left( \frac{Gene(treatment)_i}{Gene(control)_i} \right)^{C(i)} \quad (2)$$

where  $Met(treatment)$  and  $Met(control)$  are the metabolic function for the treated and control cultures, respectively;  $Gene(treatment)_i$  and  $Gene(control)_i$  are the expression level of gene  $i$  for the treated and control cultures, respectively.

Denoting  $Y$  as

$$\log_2 \left( \frac{Met(treatment)}{Met(control)} \right), \text{ and}$$

$X_i$  as

$$\log_2 \left( \frac{Gene(treatment)_i}{Gene(control)_i} \right)$$

The equation (2) is transformed to:

$$Y = \sum_{i=1}^n C(i) X_i \quad (3)$$

Since DNA microarray data are typically measured with respect to a reference level, we applied a log-linear model, which works well when the data are presented as relative levels. Furthermore, a log-linear model allowed some of the nonlinear relationships between metabolic function and gene expression to be captured. Log-linear models have been applied to approximate nonlinear processes in biochemical systems [Ni 1996a, Ni 1996b]. In this study the coefficients  $C(i)$  in equation (3) were determined by PLS analysis and the genes,  $Gene_i$ , were selected by GA/PLS as described in reference [Li and Chan, 2004]. Briefly, multiple subsets of genes that provide a good prediction of the metabolic functions with equation (3) were selected and the frequency of each gene that appeared in these subsets was counted. Those genes with high frequencies were deemed as important genes to the metabolic function. In equation (3)  $Y$  is a matrix of multiple metabolites, therefore the genes that were important to multiple metabolites ( $Y$ ) were selected with the modified GA/PLS. Multiple metabolites in  $Y$  were assumed to be independent of each other. The genes were selected so that the overall prediction accuracy for all the metabolites, e.g.  $[Y1, Y2]$  was maximized, therefore, genes of modest importance to  $Y1$  and  $Y2$  in single metabolite analysis might be identified to be of high importance to  $[Y1, Y2]$  in multiple metabolite analysis. Because the GA/PLS method does not guarantee a global minimum, the method was run multiple times and the frequency with which each gene was selected was counted. A total of 14 runs were performed. The genes that were selected with a frequency of 8 or greater were selected as important. The greater frequency of selection indicated a greater significance of that gene in regulating the function.

### 4.3 Results

#### 4.3.1 Lipid accumulation and cytotoxicity

Cells exposed to FFAs accumulated TG, which was quantified using an enzymatic assay. The intracellular accumulation of TG was higher in the cells exposed to unsaturated FFAs- oleate and linoleate, as compared to those exposed to saturated FFA- palmitate (Figure 4.1). No significant effect of TNF- $\alpha$  treatment on TG accumulation was observed (not shown), in agreement with others (Bruce and Dyck, 2004).

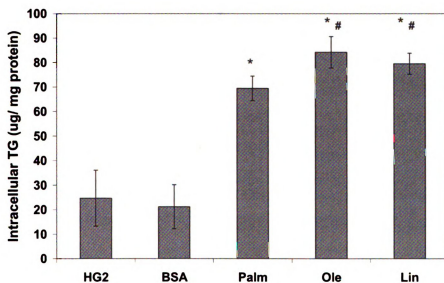


**Figure 4.1 Intracellular accumulation of TG in response to various FFAs and TNF- $\alpha$ .** The cells were exposed to various FFA and TNF- $\alpha$  for 24 h, after which they were washed with PBS and lysed in 1% triton-X-100 in PBS. The levels of TG in the lysates were analyzed using an enzymatic assay and normalized to the protein levels. Results presented as mean  $\pm$  s.d of n=9 from 3 independent experiments.

**\***, significantly higher than control ( $p < 0.01$ ).

The cytotoxicity was measured after 24h of treatment as the fraction of the total LDH activity released. The saturated fatty acid, palmitate, was found to be toxic to these cells

and TNF- $\alpha$  exacerbated this toxicity, while the unsaturated fatty acids with or without TNF- $\alpha$  co-supplementation did not have a toxic effect (Table 4.1).

Medium	TNF (ng/ml)	LDH Released (%)	
		Mean	SD
HG2	0	1.12	0.68
HG2	20	1.64	1.06
HG2	100	1.58	0.69
BSA	0	1.52	0.85
BSA	20	2.23	1.42
BSA	100	1.95	0.92
Palm	0	4.67 *	1.22
Palm	20	8.87 *	2.3
Palm	100	9.82 *	2.13
Oleate	0	1.34	0.8
Oleate	20	1.35	0.48
Oleate	100	1.43	0.35
Linoleate	0	1.23	0.46
Linoleate	20	1.82	0.39
Linoleate	100	1.25	0.1

**Table 4.1. The cytotoxicity of various treatments.** Cells were treated for 24 h with 0.7 mM FFA in the presence or absence of 20 or 100 ng/ml TNF- $\alpha$ . LDH released was measured and normalized to total LDH.

Data presented as mean  $\pm$  s.d. of  $n = 9$  from three independent experiments. \*, significantly higher than control,  $p < 0.01$ .

#### 4.3.2 Microarray analyses

To identify the genomic response of the cells to the treatments, cDNA microarray analyses were performed. Two-way ANOVA followed by removal of ESTs identified that 830 genes were affected at a significance level of  $p < 0.01$  by either FFAs, or TNF- $\alpha$  or their interaction. Further analyses were conducted using these differentially affected genes to identify pathways and processes related to lipid accumulation and cytotoxicity. Since FFAs were the primary effectors of both lipid accumulation and cytotoxicity while

TNF- $\alpha$  had no significant effect on either the lipid accumulation or the toxicity by itself, the genes affected only by FFAs are discussed below.

#### **4.3.3 Identification of pathways important in lipid accumulation and cytotoxicity**

In order to identify the genes associated with intracellular TG accumulation, cytotoxicity or both, we conducted single and dual-response GA/PLS analysis. The pathways enriched in the selected genes were identified by Gene Ontology (GO)-based analyses using the Gene Ontology Tree Machine (GOTM) (Zhang et al., 2004) and FatiGO<sup>+</sup> (Al Shahrour et al., 2005) online tools. While the GOTM used all the genes for the analysis and identified the significantly enriched processes by employing the hypergeometric test, FatiGO<sup>+</sup> provided information on the KEGG pathways as well as the transcription factors whose target genes were enriched in the list. Since the two analyses provided complementary information, both were employed.

##### **4.3.3.1 Genes relevant to TG accumulation**

The GA/PLS analysis identified 88 genes among the 830 differentially expressed genes as relevant to TG accumulation. Genes with the highest frequencies are listed in Table 4.2.

**Table 4.2. Top genes identified for TG accumulation.** GA/PLS analysis was conducted to identify genes related to intracellular TG accumulation. The genes with highest frequencies are presented.

Accession Number	Gene Name	Freq
AA457700	(gC) stearyl-CoA desaturase (delta-9-desaturase) (SCD)	12
AA279072	(gK) inositol polyphosphate phosphatase-like 1 (INPPL1)	11
T81764	(gC) cell division cycle 27 (CDC27)	11
AA464195	(gC) protein phosphatase 1, regulatory (inhibitor) subunit 12C (PPP1R12C)	11
H16833	(gN) steroid-5-alpha-reductase, alpha polypeptide 1 (3-oxo-5 alpha-steroid delta 4-dehydrogenase alpha 1) (SRD5A1)	11
R33650	(gM) inner mitochondrial membrane peptidase 2 like (IMMP2L)	11

Many genes with known roles in the regulation of lipid metabolism were identified. For example, SCD was identified as the most important gene in regulating TG accumulation. SCD catalyzes the unsaturation of stearyl-CoA, the higher derivative of palmitate, to yield oleoyl-CoA. The activity of SCD has been shown to regulate hepatic TG synthesis in response to a lipogenic diet rich in saturated FFAs (Miyazaki et al., 2001). SCD increases TG synthesis by increasing the amounts of unsaturated FFA, a preferred substrate for monoacylglycerol acyltransferase (MGAT), the enzyme which catalyzes the synthesis of diacylglycerol (DAG) (Coleman and Lee, 2004). The microarray analyses indicated that exposure to palmitate reduced the transcript levels of SCD, which was also verified by RT-PCR (Figure 4.2a). Other FFAs also reduced the expression of SCD (Table 4.3). However, the protein levels of SCD were significantly reduced only in the palmitate-treated cells (Figure 4.2b). Reduced transcript levels, but no change in protein levels in the unsaturated FFAs, suggests that these FFAs also reduced the rate of degradation of SCD so that the net protein levels did not change significantly. Reduced SCD levels in palmitate would hamper the channeling of this FFA by reducing the amounts of unsaturated FFA, the preferred substrate for MGAT and thus, TG synthesis. Reduced channeling of palmitate to TG may exacerbate the toxicity of this fatty acid.

Increasing the levels of SCD has been shown to reduce the cytotoxicity of palmitate by increasing TG synthesis (Listenberger et al., 2003).

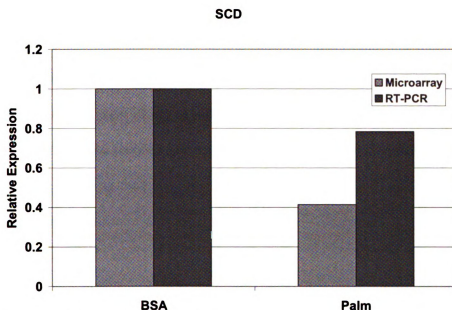


**Figure 4.2a** Effect of palmitate on the transcript levels of SCD, measured by microarray and RT-PCR. Cells were exposed to 0.7 mM palmitate for 24 h, controls were exposed to 4% BSA only. The transcript levels of SCD were measured by RT-PCR. RT-PCR conducted by Xuerui Yang.

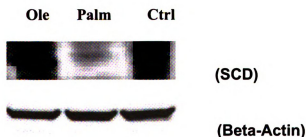


**Figure 4.2b** Effect of palmitate and oleate on the protein levels of stearoyl-CoA desaturase (SCD). Cells were exposed to 0.7 mM palmitate for 24 h, controls were exposed to 4% BSA only. The protein levels of SCD were measured by western blotting. Experiment conducted by Zheng Li and Xuerui Yang.

Another important regulator of TG synthesis identified by the GA/PLS analysis was INPPL1. The product of INPPL1 is the phosphatase SH2-containing inositol 5'-



phosphatase 2 (SHIP2), which is known to inhibit insulin signaling by hydrolyzing the inositol triphosphate (IP3). SHIP2 is considered an important target in controlling obesity, type 2 diabetes and insulin resistance (Sasaoka et al., 2006). It has been shown that INPPL1-null mice are highly resistant to dietary obesity (Sleeman et al., 2005) and liver-specific expression of a dominant-negative SHIP2 improves glucose metabolism and insulin resistance in the db/db mice (Fukui et al., 2005). Palmitate upregulated the expression level of INPPL1 (Table 4.3) and thus is expected to cause a greater inhibition of insulin signaling than the other FFAs. Indeed, insulin resistance in muscle cells has been shown to correlate with intracellular levels of saturated FFAs (Manco et al., 2000).

FatiGO<sup>+</sup> analysis of the selected genes indicated that the KEGG pathways of insulin signaling, MAPK signaling, phosphatidylinositol metabolism and apoptosis (Table 4.4) were related to TG accumulation. The importance of insulin signaling in lipid metabolism and the role of inositol metabolism in regulating insulin signaling were discussed above. The analysis also suggested an important role of MAPK in TG accumulation, which was verified experimentally, see section below. The identification of the apoptosis pathway suggested a relation between TG accumulation and cell death. It is well known that excessive intracellular lipid accumulation alters cellular physiology and is considered the first step of lipotoxicity (Weinberg, 2006). However, despite greater TG accumulation, the unsaturated FFAs were not toxic. Efficient TG synthesis in response to these fatty acids prevented their acute toxicity. However, chronic exposure to elevated levels of the unsaturated FFAs is cytotoxic (Dymkowska et al, 2006).

GOTM analysis of the 88 genes selected for TG accumulation vs. the initial list of 830 differentially expressed genes identified that the genes in the GO category of ‘regulation of cell growth’ were significantly enriched (Table 4.5), suggesting a relationship between intracellular lipid accumulation and cell growth, which has been previously reported (Tietge et al., 2001).

#### **4.3.3.2 Genes relevant to cytotoxicity**

Of the initial 830 genes, GA/PLS identified 115 as important for LDH release. Table 4.6 lists the genes with the highest frequencies, see additional file 2 for the complete list. Among the genes with highest frequencies to LDH release were those involved in ROS generation and scavenging, e.g., cytochrome P450 subfamily 1 (CYP1A1) and glutamate cysteine ligase (GCL), respectively. Our previous study had identified an important role of ROS generation in palmitate toxicity (Srivastava and Chan, 2007). In addition, genes involved in the regulation of cell death such as caspase 6 (CASP6) and eukaryotic translation termination factor 1 (ETF1) were also identified (not shown).

**Table 4.6 Top genes identified for cytotoxicity (LDH release) by GA/PLS analysis.** GA/PLS analysis was conducted to identify genes related to cytotoxicity. The genes with highest frequencies are presented.

Accession Number	Gene Name	Freq
AA418907	(gC) cytochrome P450, subfamily I (aromatic compound-inducible), polypeptide 1 (CYP1A1)	12
AA679907	(gC) isocitrate dehydrogenase 2 (NADP+), mitochondrial (IDH2), nuclear gene encoding mitochondrial protein	12
AA877618	(gC) fatty acid amide hydrolase (FAAH)	12
R32848	(gC) S100 calcium binding protein P (S100P)	12
H93482	(g) glutamate-cysteine ligase, catalytic subunit	11
AA406269	(g) nuclear factor I/X (CCAAT-binding transcription factor) (NFI-X)	11
H09819	(gC) phosphomevalonate kinase (PMVK)	11
N95011	(gC) pleckstrin homology domain containing, family A (phosphoinositide binding specific) member 1 (PLEKHA1)	11

FatiGO<sup>+</sup> analysis of the genes selected by GA/PLS to be important in regulating LDH release identified that the KEGG pathways of MAPK signaling, oxidative phosphorylation and insulin signaling had the highest number of genes, suggesting that alterations in these pathways were significantly associated with LDH release. The cellular components categories of ‘membrane’ and ‘mitochondrion’ had the highest number of members (20 and 11, respectively, out of the 63 genes used by FatiGO<sup>+</sup>), suggesting an important role of membrane integrity and mitochondria in the release of LDH (see additional file 2). LDH is a cytosolic enzyme that is released when the cellular membrane integrity is compromised. We also observed a significant reduction in the mitochondrial potential (Figure 4.3a) in the palmitate-treated cells. Loss of mitochondrial integrity would lead to the release of cytochrome c, causing caspase activation. In support of this, increased caspase-3 activation was observed in the cells treated with palmitate (Figure 4.3b). Thus, these experimental observations corroborated with the genes identified to be involved in regulating mitochondrial structure and function.

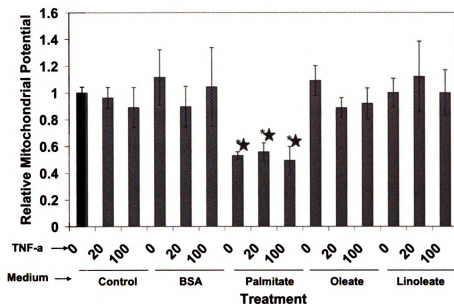


**Figure 4.3a Effect of various treatments on the mitochondrial potential.** Cells were treated with 0.7 mM of the indicated FFAs in the absence or presence of indicated concentrations of TNF- $\alpha$  (in ng/ml). After 24 h of treatments, the mitochondrial potential was measured using JC-1 dye, and represented as relative ratio of red to green fluorescence. Data presented as mean  $\pm$  s.d. of  $n = 9$  from 3 independent experiments.

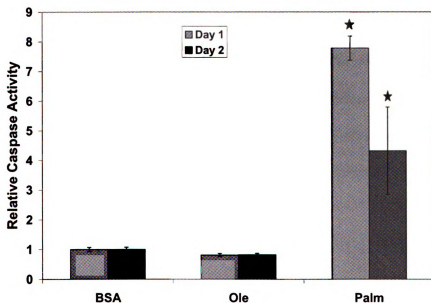


**Figure 4.3b Activation of caspase-3 by palmitate treatment.** Cells were treated with 0.7 mM of the indicated FFAs. After 24 h of treatments, cells were lysed and the caspase-3 activity was measured using a fluorimetric assay. Data presented as mean  $\pm$  s.d. of  $n = 9$  from 3 independent experiments.

The GOTM analysis indicated that genes belonging to the category ‘Tumor necrosis factor receptor binding’ were significantly enriched in the selected list of genes. This suggests that a number of genes selected for the LDH-release were affected by TNF- $\alpha$ . Indeed, the LDH release was affected by palmitate and the interaction of palmitate and TNF- $\alpha$  (Table 4.1). The genes altered in the selected list were altered by FFAs or TNF- $\alpha$  alone, or by their interaction. To identify the genes affected by the FFAs only, two-way ANOVA was performed. Genes related to lipid metabolism, such as lecithin cholesterol acyl transferase (LCAT), 24-dehydrocholesterol reductase (DHCR24) (Table 4.3) were affected by FFAs. DHCR24 is involved in cholesterol biosynthesis, while LCAT is involved in the esterification of the cholesterol. Exposure to palmitate reduced the expression of LCAT while increased that of DHCR24 (Table 4.3). These results suggest an increased synthesis, but reduced esterification of cholesterol in the palmitate cultures. Cholesterol is transported from liver in the form of cholesterol esters. Reduced esterification of cholesterol would reduce secretion of lipoproteins. In agreement with this, diets rich in saturated FFAs have been shown to have reduced lipoprotein secretion as compared to monounsaturated or polyunsaturated FFAs (Cheema and Agellon, 1999). The effect of palmitate on these genes also suggests increased accumulation of cholesterol in the cells, which itself may cause cytotoxicity (Jiminez-Lopez et al., 2006).

#### **4.3.3.3 Dual-response GA/PLS to identify genes relevant to both TG accumulation and cytotoxicity**

In order to find better targets to regulate the toxicity of saturated FFAs, it is important to identify genes that affect lipid accumulation as well as toxicity. To identify such genes

which affect both responses, the dual-response GA/PLS (LDH + TG) was applied. This analysis identified 92 genes which may regulate both TG accumulation and cytotoxicity (see Table 4.7 for the genes with the highest frequencies).

**Table 4.7 Top genes selected for TG+LDH by dual response GA/PLS.** Modified GA/PLS analysis was performed to identify the genes which regulate both TG accumulation and LDH release. Genes with the highest frequencies are presented.

Accession Number	Name	Freq
AA447569	(gN) NADH dehydrogenase (ubiquinone) 1, alpha/beta subcomplex, 1, 8kDa (NDUFAB1)	12
R50953	(gC) mitogen-activated protein kinase kinase kinase kinase 2 (MAP4K2)	12
H23978	(gW) general transcription factor IIB (GTF2B)	12
T58773	(gN) inositol polyphosphate-5-phosphatase, 40kDa (INPP5A)	11
AA464580	(gC) acetyl-Coenzyme A carboxylase alpha	11
AA431988	(gC) fatty acid amide hydrolase (FAAH)	11
AA463931	(gC) inositol 1,3,4-triphosphate 5/6 kinase (ITPK1)	11
N22904	(gC) 3-phosphoinositide dependent protein kinase-1 (PDPK1)	11
AA025112	(gC) BCL2/adenovirus E1B 19kDa interacting protein 3-like	11
AA019459	(gC) protein tyrosine kinase 9 (PTK9)	11
AA064638	(gl) ubiquitin specific protease 7 (herpes virus-associated) (USP7)	11

NADH dehydrogenase (ubiquinone) 1, alpha/beta subcomplex, 1, 8kDa (NDUFAB1) and mitogen-activated protein kinase kinase kinase kinase 2 (MAP4K2) were identified to have the highest frequency among all the genes in the group. In fact, NADH dehydrogenases formed the most prominent group of genes in the list, with 7 different NADH dehydrogenases selected. In accordance with this, the GOTM analysis also identified that the GO category of 'oxidoreductase activity, acting on NADH or NADPH, quinone or similar compound as acceptor' was significantly enriched ( $p < 0.01$ ) in the selected list. These results indicated an important role of NADH dehydrogenases in regulating both cytotoxicity and TG accumulation.

Another gene that had the highest frequency was the mitogen-activated protein kinase kinase kinase 2 (MAP4K2). The FatiGO<sup>+</sup> analysis of the selected genes identified that the maximum number of genes belonged to the KEGG pathway of MAPK signaling (Table 4.4). In fact, all three GA/PLS analyses identified the KEGG pathway of MAPK and insulin signaling to be among the most important in regulating lipid accumulation and cell death. MAPKs are known to regulate diverse cellular processes. For example, JNK (Simbula et al. 2006, Lee and Bae 2006) and p38 (Kim et al 2006) play important roles in mediating the cytotoxicity of various stimuli. JNK has also been shown to regulate TG accumulation in liver (Schattenberg et al., 2006). It is well-known that insulin signaling increases FFA esterification and reduces cytotoxic stresses, in part, by activating the cytoprotective protein kinase B (PKB) (Mitsui et al., 2001). PKB phosphorylates and inactivates apoptotic proteins such as procaspase-9 and BAD (Bcl-2/Bcl-X<sub>L</sub> antagonist causing cell death), while activating anti-apoptotic proteins such as X-linked inhibitor of apoptosis protein (XIAP) (Dickson and Rhodes 2004). Thus, reduced insulin signaling would reduce lipid accumulation and increase cytotoxicity. Among the different FFAs, exposure to palmitate altered many genes involved in insulin signaling. Thus, it is likely that palmitate affected insulin signaling to a greater extent than the other FFAs (Chavez et al., 2003).

#### **4.3.4 Experimental validation of the identified gene-groups**

##### **4.3.4.1 NADH dehydrogenases**

The dual-response analysis identified that NADH dehydrogenase regulate both TG accumulation and cytotoxicity. Therefore, the roles of this enzyme in these processes

were investigated. NADH dehydrogenases form the mitochondrial complex I, which is involved not only in the synthesis of ATP, but is also an important site of ROS generation. ROS generation has been shown to be one of the important mechanisms of palmitate-toxicity (Srivastava and Chan, 2007). Though a role of ROS generation at complex I has been suggested in the cell death caused by sulforaphane (Singh et al, 2005), transforming growth factor (Herrera et al., 2004) and deoxycholate (Payne et al., 2005), a similar role of complex I in lipotoxicity or triglyceride accumulation has not been indicated. We tested the effects of inhibiting NADH dehydrogenases on the cytotoxicity and lipid accumulation in response to palmitate. Inhibiting these enzymes with rotenone reduced the cytotoxicity of palmitate significantly (as shown in Figure 2.5b and reproduced in Table 4.8 to facilitate its comparison with TG). In addition to its effect on cytotoxicity, NADH dehydrogenase also increased the accumulation of triglycerides in response to palmitate (Table 4.8). Inhibiting NADH dehydrogenase also increased slightly the lipid accumulation in response to oleate (not shown). These results suggest that the NADH dehydrogenases may indeed regulate both lipid accumulation and cytotoxicity in response to palmitate.

**Table 4.8 Effect of inhibition of NADH dehydrogenase on the cytotoxicity and TG accumulation in response to palmitate.** Cells were pretreated with the indicated concentrations of rotenone for 30 minutes and then exposed to 0.7 mM palmitate for 24 h. The cells were then treated again for 30 minutes with rotenone and put again in 0.7 mM palmitate. The cytotoxicity as well as TG accumulation after 24 and 48 h was measured. Data presented as mean  $\pm$  s.d. of  $n = 9$  from 3 independent experiments. \*, significantly less than the no inhibitor condition,  $p < 0.01$ . #, significantly more than the no inhibitor condition,  $p < 0.01$ .

Concentration	LDH release (DAY 1)	LDH release (DAY 2)	TG (Day 1) ug/mg protein	TG (Day 2) ug/mg protein
None	4.5 $\pm$ 0.3	35.7 $\pm$ 3.4	69.4 $\pm$ 16.1	173.8 $\pm$ 16.7
250 nM	3.4 $\pm$ 0.3 *	24.9 $\pm$ 1.4 *	63.3 $\pm$ 14.2	191.1 $\pm$ 12.1
500 nM	2.7 $\pm$ 0.2 *	14.8 $\pm$ 3.2 *	74.3 $\pm$ 12.0	197.8 $\pm$ 11.3
1000 nM	3.4 $\pm$ 0.2 *	20.0 $\pm$ 4.6 *	104.6 $\pm$ 7.8 #	204.9 $\pm$ 8.5 #



#### **4.3.4.2 MAP kinases**

All three cases (TG, LDH and TG+LDH) identified genes belonging to the KEGG pathway of MAPK signaling. MAPKs play an important role in cellular signaling pathways and effect diverse processes. There are three primary branches of the MAPK signaling network, viz., the c-Jun N-terminal kinase (JNK), the extracellular signal regulated kinase (ERK) and the p38 kinase. The roles of the different branches of MAPK signaling network were evaluated by studying the effect of inhibitors specific to each. Inhibiting ERK and JNK reduced the toxicity of palmitate significantly (Figure 4.4a), while p38 had no effect. Inhibiting JNK, but not ERK or p38, also increased the lipid accumulation in response to palmitate (Figure 4.4b). Thus, important roles of MAPKs in regulating the lipotoxicity as well as lipid accumulation, as predicted by the integrative GA/PLS, were corroborated experimentally. Among the different MAPK pathways, only JNK has been shown to play an important role in the development of NASH (Schattenberg et al., 2006). This study found that mice with deletion of JNK gene were resistant to development of NASH when fed methionine-choline deficient (MCD) diet. Very low steatosis was observed in these animals and that could partly suggest lower steatohepatitis. Our results are similar to theirs only in terms of cell death, but different from their lipid accumulation results. However, no previous study has shown important role of ERK in lipotoxicity, as shown in the current study.

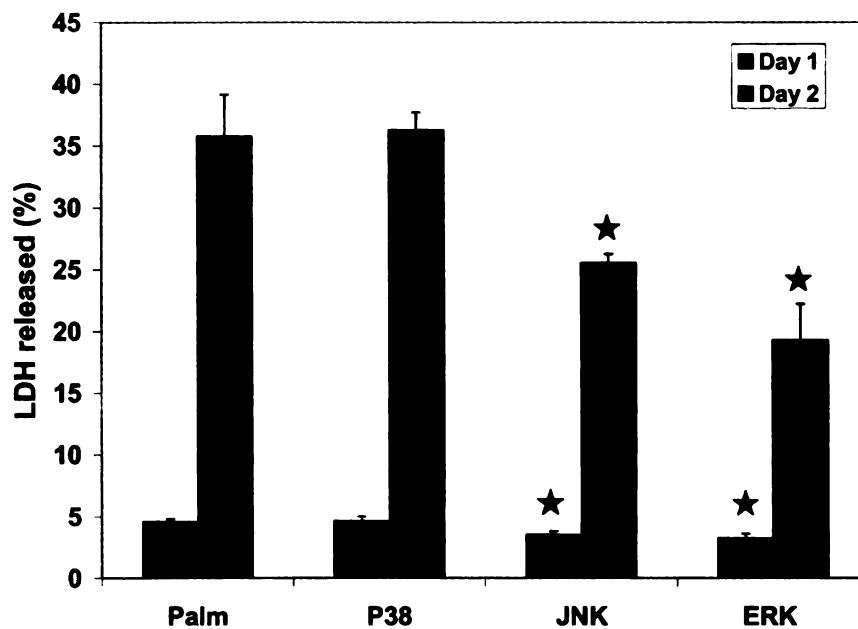


**Figure 4.4a Effect of inhibition of various MAPKs on the cytotoxicity of palmitate.** Cells were treated for 48 hours with palmitate in the presence of 2  $\mu$ M SB203580 (to inhibit p38 pathway), 75  $\mu$ M SP-600125 (to inhibit JNK pathway) or 50  $\mu$ M U-0126 (to inhibit ERK pathway). Media were changed daily. The LDH released into the medium after 24 and 48 h of treatments was measured and normalized to total LDH. \*, significantly lower than palmitate ( $p < 0.01$ ).

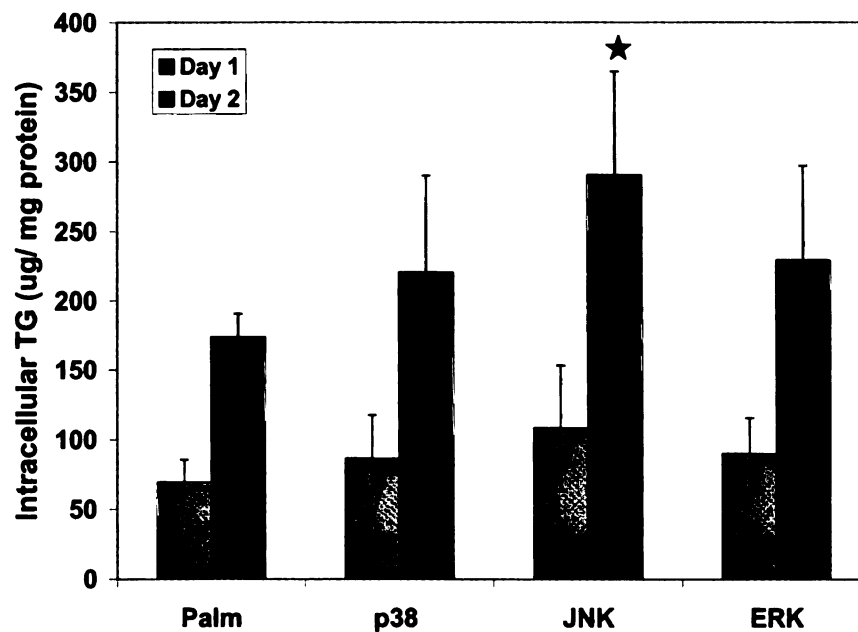


**Figure 4.4b Effect of inhibition of various MAPKs on the TG accumulation in response to palmitate.** Intracellular levels of TG in the cell lysates were measured after desired time of exposure. Data presented as mean  $\pm$  s.d. of 3 independent experiments. \*, significantly higher than palmitate ( $p < 0.01$ ).

#### **4.3.5 Genes affected by exposure to palmitate**

Exposure to palmitate significantly increased the expression of INPP5A, PTPN1, INPPL1, NFIX, DHCR24, SSI-3 and CASP6 (Table 4.3). CASP6 is a caspase which can activate caspase-3, the effector caspase which lyses and activates downstream proteins causing apoptosis. It is likely that increased activity of CASP6 plays a role in the caspase-3 activity observed in palmitate-treated cells. The effect of palmitate on the expression of INPP5A, PTPN1, INPPL1 and NFIX was different than the effect of the other FFAs on these genes. These genes have been shown to play important roles in a variety of physiological processes. The product of INPP5A is a type I inositol 1,4,5-trisphosphate (InsP3) 5-phosphatase, which antagonizes insulin-signaling by hydrolyzing Ins(1,4,5)P3. The hydrolysis of IP3 mobilizes intracellular calcium and acts as a second messenger mediating the cells response to various stimuli. Exposure to palmitate has been shown to cause increases in intracellular  $\text{Ca}^{++}$  (Remizov et al. 2003). Hydrolysis of IP3 would also counteract the insulin signal transduction. Thus increased levels of INPP5A would cause multiple deleterious effects on cellular function. PTPN1 codes for protein tyrosine phosphatase PTP-1B. PTP-1B has also been shown to counter insulin signal transduction by dephosphorylating phosphotyrosine residues in the insulin signaling molecules, and has been suggested as a risk factor for the development of type 2 diabetes (Kennedy and Ramachandran 2000, Wagman and Nuss 2001). PTPN1 and INPPL1 were increased only in the cells treated with palmitate, indicating that the saturated fatty acids may be important mediators of insulin resistance. Indeed, insulin resistance in skeletal muscles is known to correlate directly with the saturated FFA levels (Manco et al., 2000). Our results suggest that a similar relationship between saturated FFA and insulin resistance

may exist in hepatocytes as well. Thus, the genes affected by palmitate suggest a greater inhibition of insulin signaling in the palmitate-treated cells as compared to the other FFAs.

#### **4.4 Discussion**

Hepatocytes are central to whole-body lipid metabolism. Exposure of hepatocytes to elevated FFAs and TNF- $\alpha$  is associated with altered lipid metabolism and cell death (lipotoxicity). However, our study has identified that saturated FFA are the primary effectors of hepatic lipotoxicity and that the effect of TNF- $\alpha$  are secondary to the saturated FFAs. FFA and TNF- $\alpha$  exert their physiological and metabolic effects, in part, by altering the expression of many enzymes of lipid metabolism and signal transduction. No previous study had investigated the genomic effects of combined exposure to these factors on hepatocytes or hepatoma cells. In addition to identifying the genomic effects of these treatments, we identified the genes and processes involved in simultaneous regulation of both lipid accumulation and FFA-toxicity. These analyses identified novel targets to combat lipotoxicity at multiple levels, some of which were experimentally validated. A comparison of the genes selected for the (TG+LDH) case with those selected for TG or LDH individually showed that most (53 out of 92) of the genes selected by the dual-response analysis were novel to this list. Among the genes selected only in the dual-response analysis were many NADH dehydrogenases genes, such as NADH dehydrogenase (ubiquinone) 1, alpha/beta subcomplex, 1, 8kDa (NDUFAB1), NADH dehydrogenase (ubiquinone) 1 beta subcomplex, 1, 7kDa (NDUFB1), NADH dehydrogenase (ubiquinone) 1 alpha subcomplex, 7, 14.5kDa (NDUFA7), NADH

dehydrogenase (ubiquinone) flavoprotein 2, 24kDa (NDUFV2), NADH dehydrogenase (ubiquinone) flavoprotein 1, 51kDa (NDUFV1). In fact, out of the 6 NADH dehydrogenase genes that were identified by the dual-response analysis, only 1 (NADH dehydrogenase (ubiquinone) 1 beta subcomplex, 4, 15kDa) was found for TG analysis, and none was found in the LDH analysis. As our experiments showed (in this chapter and in chapter 2), NADH dehydrogenases played an important role in regulating TG accumulation as well as toxicity. No previous study has shown the role of NADH dehydrogenases in regulating both lipotoxicity and lipid accumulation. Because NADH dehydrogenases are known to be involved in oxidative phosphorylation and the generation of energy as well as ROS (Starkov and Fiskum 2003), their role in mediating lipotoxicity may not be very surprising. However, the GA/PLS analysis and the experiments identified that these enzymes also play an important role in regulating TG synthesis. One of the potential ways by which inhibiting NADH dehydrogenases could increase TG accumulation may be through the reduction of ATP levels. ATP has been shown to inhibit the incorporation of FFAs into TGs (Hansen et al., 1984 a and b). Inhibition of NADH dehydrogenases would reduce ATP levels, thus, could increase TG accumulation. The MAPKs, JNK and ERK, were found to play important roles in the cytotoxicity of FFA. Inhibiting JNK also increased lipid accumulation, while ERK had no effect on lipid accumulation. Thus, inhibiting JNK may have reduced the cytotoxicity, in part, through increased TG synthesis. However, even though we agree with the conclusion of others on the importance of JNK in obesity (Karin and Gallagher 2005), insulin resistance (Hirosumi et al., 2002), type 2 diabetes (Bennett et al., 2003,) and steatohepatitis (Schattenberg et al., 2006), our results suggest an increase in lipid

accumulation in response to JNK inhibition, which is contrary to a decrease of obesity and intrahepatic lipid accumulation in the JNK-knockout mice observed in these studies. Although the reasons behind the differences in observation are not clear, it is likely that the differences are due to the different models (rodents in all these studies vs. cell culture in ours) or the treatments (MCD diet in the study of Schattenberg et al. vs. elevated FFA levels in ours). In this context, it is important to identify the mechanisms by which JNK affect lipid metabolism *in vivo* as well as on different cell types, before proceeding with therapeutic applications of these inhibitors. Among the potential ways JNK regulates lipid metabolism is by inhibiting insulin signaling through phosphorylation of insulin receptor at serine residues (Hirosumi et al. 2002) and by regulating the activity of SREBP (Chang et al. 2005). It is also likely that the difference in observation on inhibition of JNK between this study and others is because of very low levels of insulin (coming only from the serum in the medium) in our study vs. higher (*in vivo* system) in the others. In designing treatment strategies for lipotoxicity, it would be useful to identify targets that reduce cell death without affecting lipid accumulation, because excessive lipid accumulation can itself alter cellular physiology and make cells prone to lipid peroxidation (Weinberg 2006). Our study identified ERK as another potential target to reduce the cytotoxicity without affecting lipid accumulation. While a role for ERK has been shown in various alterations caused by FFAs, such as the pro-inflammatory effects of FFAs (Hennig et al., 2006), TNF- $\alpha$  expression (Jove et al., 2006), NF- $\kappa$ B expression (Ajuwon and Spurlock, 2005), apoptosis by conjugated linoleic acid (Miglietta et al., 2006) and 15d-PGJ2 (Hashimoto et al., 2006), ERK's role in palmitate induced lipotoxicity has not been previously shown. The significant reduction in palmitate-

toxicity by inhibiting ERK without affecting lipid accumulation identified it as a potentially important target for lipotoxicity.

Finally, the dual-response GA/PLS methodology was able to integrate the metabolic, physiologic and genetic information to identify genes relevant to multiple metabolic functions. While we have applied this analysis to only two responses of interest, the analysis is amenable to multiple quantitative responses. To incorporate larger number of metabolites, latent variables can be extracted from the metabolite data with methods such as principal component analysis (PCA), partial least squares (PLS) (Griffin 2005) and Fisher Discriminant Analysis (FDA) [Chan 2003]. PCA and PLS can extract latent variables that account for most of the variance in the data while FDA extracts latent variables that have the largest discriminating capability. The number of latent variables can be determined based upon the variance captured by the latent variables. For example, if we want to capture 90% of the variance in the raw data, we will include enough latent variables to extract 90% (or more) of the variance. For complex diseases which affect multiple cellular processes, such analysis could be a useful tool to identify targets which can simultaneously regulate multiple processes. It is likely that the incorporation of multiple measurements would provide better targets to regulate cellular responses and the development of complex diseases.

**Table 4.3 Effect of various treatments on the expression of selected genes based on the microarray data.** NC indicates that no significant change.  
2. \*, gene affected differently in palmitate cultures, as compared with the other FFAs. 3. †, gene affected similarly by all FFAs.

Accession #	Names	Palmitate	Oleate	Linoleate
<b>Genes selected for TG</b>				
AA457700	(gC) stearoyl-CoA desaturase (delta-9-desaturase) (SCD) †	Decrease	Decrease	Decrease
AA279072	(gK) inositol polyphosphate phosphatase-like 1 (INPPL1) *	Increase	Decrease	Decrease
AA464580	(gC) acetyl-Coenzyme A carboxylase alpha	NC	Decrease	Decrease
AA007687	(gC) serine palmitoyltransferase, long chain base subunit 2	NC	Increase	Increase
T58773	(gN) inositol polyphosphate-5-phosphatase, 40kDa (INPP5A)	Increase	NC	NC
AA490208	(gM) glutathione S-transferase theta 2 (GSTT2) †	Decrease	Decrease	Decrease
<b>Genes selected for LDH</b>				
AA406269	(g) nuclear factor I/X (CCAAT-binding transcription factor) (NFIX) *	Increase	Decrease	NC
R06458	(g) lecithin-cholesterol acyltransferase (LCAT)	Decrease	Decrease	NC
AA446463	(gC) 24-dehydrocholesterol reductase (DHCR24)	Increase	NC	Increase
W72329	(gC) lymphotoxin alpha (TNF superfamily, member 1) (LTA) †	Decrease	Decrease	Decrease
AA001219	(gC) suppressor of cytokine signaling 3 (SSI-3) †	Increase	Increase	Increase
AA456664	(gM) eukaryotic translation termination factor 1 (ETF1) *	NC	Decrease	Decrease
W45688	(gN) caspase 6, apoptosis-related cysteine protease (CASP6), transcript variant beta	Increase	NC	Increase
<b>Genes selected for (TG+LDH)</b>				
R50953	(gC) mitogen-activated protein kinase kinase kinase 2 (MAP4K2)	NC	NC	Increase
AA001614	<b>Table 4.3 continued</b>	Decrease	Decrease	Decrease



AA441895	(gC) insulin receptor † (gC) glutathione-S-transferase like; glutathione transferase omega (GSTTLP28) †	Decrease	Decrease	Decrease
W68281	(gF) mitogen-activated protein kinase-activated protein kinase 3 (MAPKAPK3) *	NC	Decrease	Decrease
R06605	(gC) protein tyrosine phosphatase, non-receptor type 1 (PTPN1) *	Increase	NC	Decrease
AA019459	(gC) protein tyrosine kinase 9 (PTK9) †	Decrease	Decrease	Decrease

**Table 4.4 KEGG pathway represented by the genes identified for TG, LDH and (TG + LDH)**

TG			LDH		(TG + LDH)		
Name of the pathway	# of genes	% of total genes	Name of the pathway	# of genes	% of total genes	Name of the pathway	# of genes
Insulin signaling pathway	6	13.33	MAPK signaling pathway	5	7.94	Insulin signaling pathway	7
MAPK signaling pathway	5	11.11	Oxidative phosphorylation	4	6.35	MAPK signaling pathway	6
Phosphatidylinositol signaling system	4	8.89	Insulin signaling pathway	3	4.76	Oxidative phosphorylation	4
Inositol phosphate metabolism	3	6.67				Calcium signaling pathway	4
Apoptosis	3	6.67				Wnt signaling pathway	3
						Adherens junction	3
							6.25
							6.25



# **CHAPTER 5. INTEGRATING THE ONTOLOGY INFORMATION AND EXPRESSION DATA TO IDENTIFY GENES THAT REGULATE METABOLIC AND PHENOTYPIC FUNCTIONS**

## **5.1 Introduction**

The development of microarray technology has made it possible to procure information on the genomic responses of the cells to virtually any condition. The challenge now is to efficiently identify the genes that regulate the desired metabolic/ phenotypic response of the cells to identify better targets to regulate cellular responses. A substantial amount of effort has been invested to develop techniques that efficiently analyze gene expression data. However, current methods to integrate gene-phenotype or gene-metabolite information do not actively incorporate the functional information of genes. We hypothesized that active incorporation of functional information of the genes would help identify better targets to regulate cellular responses.

Many techniques have been developed to identify the genes which can identify the subpopulations and discriminate between categories, e.g. cancerous vs. non-cancerous tissue from a set of microarray samples. The simpler 'filtering' techniques include the Wilcoxon's ranksum test (Troyanskaya et al., 2002), Fisher Discriminant Analysis (FDA) (Hwang et al, 2003), partial least squares (Tan et al., 2004), GA- (Liu et al., 2005) and principal components- (Tan et al, 2005) based classification and clustering (Guo et al., 2006 and Chen et al., 2006) etc. The filtering techniques separate the subgroups by maximizing the ratio of between-group to within-group variance. Genes are ranked

according to their correlations to a phenotype and the genes with the highest ranks are considered discriminatory. However, these techniques suffer from various drawbacks, e.g., they require the features (genes) to be independent and uncorrelated, which microarray data is obviously not. Techniques which combine multiple filter methods include genetic algorithm coupled partial least squares (GA/PLS) (Li and Chan, 2003). Therefore, sophisticated ‘wrapper’ techniques have been developed, which employ a trained learning machine to identify a subset of genes and evaluate the relevance of the genes in the subset to a phenotype. Examples of wrapper techniques include support vector machines (SVM) (Brown et al., 2000). The wrapper methods are considered better than the filter methods because they can incorporate the inter-correlation of genes and can also determine the optimal number of variables. However, these methods are conceptually difficult and often require significant computational power. A third set of techniques are also being developed which combine the wrapper and the filter techniques (e.g. the kernel Fisher discriminant analysis, KFDA) (Cho and Lee et al., 2004) or multi-layer perceptrons (Wang et al., 2006). The typical procedure is to identify the discriminating genes and then apply gene ontology (GO) to identify selected/discriminating GO processes. However, these techniques rely primarily on the microarray data for information generation and the GO analysis is essentially passive. While conceptually straight-forward, these purely data-based models have two major shortcomings. One, they strongly depend on the quality of the microarray data and can miss genes with altered expressions if the data is noisy. The microarray data is inherently noisy, increasing the probability of false-negatives. Two, data-based models do not incorporate the vast amount of information already available on the function of the genes.

Usually, the functional information of the genes is employed only in the post-processing of the selected genes. In order to circumvent these issues, alternative analysis methods are being developed in which prior information on the genes are being incorporated (Pan, 2005, Morrison et al., 2005, Le Philip et al., 2004). Many of these studies support the hypothesis that incorporation of prior knowledge either improves the classification efficiency or identify more relevant biological processes.

In the knowledge-based processes the association of a pre-defined gene ontology (GO) category to a phenotype is statistically evaluated, identifying the discriminating cellular processes. One such approach is gene set enrichment analysis (GSEA) (Subramanian et al., 2005, Beisvag et al, 2006 and Draghici et al., 2003). Even though such GO-based techniques identify the gene sets having significant association with a phenotype, they usually identify a subset of a GO category as potential contributors. Individual genes which may be significantly altered and have important association with the phenotype may not be selected if the gene-group they belong to is not enriched. Even among the subsets that are identified as important, the identification of a few (one or two) targets can be very subjective. Another major drawback of these approaches is the tedious manual preparation of predefined data sets for the analysis. While data sets are available for Affymetrix chip for some species, for other platforms, such as the custom cDNA microarrays, one would need to manually define the gene sets, which can delay procurement of downstream information or introduce errors. Therefore, such techniques are useful when the expressions of many genes of an important, causative pathway change. For other conditions where there is change of only a few, rate-controlling genes

of the pathway, such approaches may not be as informative. Therefore, methods that combine both gene expression as well as the domain knowledge are needed.

Here, we present a new method which integrates the functional information of the genes with their expression data (X) to identify the genes that regulate a specified quantifiable cellular response (Y). One of the major advantages of this method is the rapid assimilation and the ease of update of the functional information of the genes. Another advantage is the parallel identification of genes relevant to multiple cellular responses making it a more efficient high-throughput analysis. The ability of this method to handle potentially thousands of genes makes it possible to utilize less stringent pre-processing constraints, reducing the risk of false negatives. The method also incorporates the variance of the microarray data to better identify average expressions. Even with good quality controls, microarray data are typically noisy and have large variances. Traditionally, averages of the log-ratios are utilized in the analysis. However, because of large variance and small number of replicates used to calculate the averages, the average expression values may not be accurate representation of the true expressions. Therefore, in the current study, the gene expression data were approximated by a multivariate Gaussian distribution and the regression weights were estimated by minimizing the regression error that was averaged over the Gaussian distribution. The regression mixture models employed in the analysis offer the ability to accurately capture processes with multiple sub-populations, for example, the clinical data obtained for different age-groups or gender, or in vitro experiments where cells are exposed to multiple treatments, etc. The main idea behind the regression mixture model is to first cluster the experimental

conditions into a desired number of groups, and build a different regression model for each group of conditions that relates the gene expression data (X) to the cell response (Y). The clustering of experimental conditions is based on their regression weights, for example, two experimental conditions will be grouped into the same clusters if they share similar regression weights. However, the regression weights of each experimental condition also depend on the clustering results because a regression model can be built only for a group of experimental conditions. Hence, the technical challenge of regression mixture model lies in resolving this dilemma. In this paper, the Expectation Maximization (EM) algorithm was applied to effectively resolve this problem.

As a model application, we applied the framework to identify the genes that differentiate the toxicity of the saturated FFA (SFA), palmitate, and  $\text{TNF-}\alpha$ , from the non-toxicity of the unsaturated FFAs (UFAs). A mixture model with 2 sub-groups was able to separate the toxic conditions from the non-toxic ones. Incorporation of prior knowledge improved the separation achieved by the mixture models. The analysis identified important genes that separated the cytotoxic and non-toxic responses. The roles of these proteins in regulating the cytotoxicity of the SFA are discussed. Thus, incorporation of prior knowledge helped to identify targets that regulate the phenotypes of interest.

## 5.2 Materials and Methods

### 5.2.1 Bayesian Regression Model

Let  $X = (\mathbf{x}_1, \mathbf{x}_2, \dots, \mathbf{x}_m)$  denote the gene expression data of  $m$  different experimental conditions, where  $\mathbf{x}_k = (x_1, x_2, \dots, x_n)$  represents the expression data of  $n$  genes under the  $k$ th condition. Let  $\mathbf{y} = (y_1, y_2, \dots, y_m)$  denote the cellular responses for the  $m$  different conditions. By assuming that the conditional probability  $\Pr(\mathbf{y} | X, \mathbf{w})$  follows the Gaussian distribution  $N(X^T \mathbf{w}, \sigma^2 I)$ , the regression error could be computed as

$$err(\mathbf{w}) = \sum_{i=1}^m (y_i - \mathbf{x}_i^T \mathbf{w})^2 = \|\mathbf{y} - X^T \mathbf{w}\|_2^2 \quad (1)$$

where,  $\mathbf{w} = (w_1, w_2, \dots, w_n)$  are the regression weight assigned to the  $n$  genes. The optimal solution for  $\mathbf{w}$  that minimizes the above regression error is

$$\mathbf{w} = (XX^T)^{-1} X\mathbf{y} \quad (2)$$

Now, consider multiple replicates of the gene expression data under each experimental condition. Let  $\mathbf{x}_k^1, \mathbf{x}_k^2, \dots, \mathbf{x}_k^r$  denote the  $r$  replicates of the gene expression data under the  $k$ th condition. We can approximate the distribution of gene expression data under the  $k$ th condition, i.e.,  $\Pr(\mathbf{x}_k)$ , by a Gaussian distribution  $N(\bar{\mathbf{x}}_k, S_k)$  where  $\bar{\mathbf{x}}_k$  and  $S_k$  are calculated as follows:



$$\bar{\mathbf{x}}_k = \frac{\sum_{i=1}^r \mathbf{x}_k^i}{r}, S_k = \sum_{i=1}^r (\mathbf{x}_k^i - \bar{\mathbf{x}}_k)(\mathbf{x}_k^i - \bar{\mathbf{x}}_k)^T \quad (3)$$

Then, instead of regressing the cellular response to the averaged gene expression data  $\bar{\mathbf{x}}_k$ , the Bayesian regression model will search for the regression weights  $\mathbf{w}$  that minimizes the following *expected* regression error:

$$\langle err(\mathbf{w}) \rangle = \sum_{i=1}^m \int (y_i - \mathbf{x}_i^T \mathbf{w})^2 \Pr(\mathbf{x}_i) d\mathbf{x}_i = \|\mathbf{y} - \bar{X}^T \mathbf{w}\|_2^2 + \mathbf{w}^T \left( \sum_{i=1}^m S_k \right) \mathbf{w} \quad (4)$$

where,  $\bar{X} = (\bar{\mathbf{x}}_1, \bar{\mathbf{x}}_2, \dots, \bar{\mathbf{x}}_m)$ . The optimal solution for Bayesian regression model is

$$\mathbf{w} = (\bar{X}\bar{X}^T + S)^{-1} \bar{X}\mathbf{y} \quad (5)$$

where,  $S = \sum_{i=1}^m S_k$ . Comparing the above expression for  $\mathbf{w}$  to the expression in (2), we see that the primary difference between the two expressions is that (5) incorporates covariance matrix  $S$  into its denominator. The introduction of  $S$  will assign smaller regression weights to the genes whose expression data exhibit large variance compared to the genes with small variance.

### 5.2.2 Mixture Model

In the regression mixture model, we don't assume that all the experimental conditions share the same regression weights  $\mathbf{w}$ . Instead, we assume that there are underlying  $K$  ( $K < m$ ) different sets of regression weights, and each experimental condition will

choose the most suitable set of regression weights. More precisely, the conditional probability  $\Pr(\mathbf{y} | X, \mathbf{w})$  is modeled as

$$\log \Pr(\mathbf{y} | X) = \sum_{i=1}^m \log \Pr(y_i | \mathbf{x}_i) = \sum_{i=1}^m \log \left( \sum_{k=1}^K p_k N(\mathbf{x}_i^T \mathbf{w}_k, \sigma^2) \right) \quad (6)$$

In order to incorporate the variance in the gene expression data, similar to the Bayesian regression model, we compute the expected of  $\log \Pr(\mathbf{y} | X)$  that is averaged over the distribution of the gene expression data  $X$ . More specifically, we have the expected  $\log \Pr(\mathbf{y} | X)$  computed as

$$\langle \log \Pr(\mathbf{y} | X) \rangle = \sum_{i=1}^m \int \log \left( \sum_{k=1}^K q_k N(\mathbf{x}_i^T \mathbf{w}_k, \sigma^2) \right) \Pr(\mathbf{x}_i) d\mathbf{x}_i \quad (7)$$

Where  $q_k$  is the prior of choosing the  $k$ th regression model. To facilitate the computation, we follow the idea of variational method by introducing a variational distribution  $\phi_{i,k} = \Pr(k | y_i, \mathbf{x}_i)$ ,  $i = 1, \dots, m$ ,  $k = 1, \dots, K$  and approximating the above log-likelihood expression as follows

$$\langle \log \Pr(\mathbf{y} | X) \rangle \geq$$

$$\sum_{i=1}^m \sum_{k=1}^K \phi_{i,k} \left( \log q_k - \frac{1}{2} \log(2\pi\sigma^2) - \frac{1}{2\sigma^2} \int (y_i - \mathbf{x}_i^T \mathbf{w}_k)^2 \Pr(\mathbf{x}_i) d\mathbf{x}_i \right) \quad (8)$$

$$= \sum_{i=1}^m \sum_{k=1}^K \phi_{i,k} \left( \log q_k - \frac{1}{2} \log(2\pi\sigma^2) - \frac{(y_i - \bar{\mathbf{x}}_i^T \mathbf{w}_k)^2 + \mathbf{w}_k^T S_i \mathbf{w}_k}{2\sigma^2} \right)$$

Thus, we have the following equations for computing  $\phi_{i,k}$ ,  $q_k$ ,  $\mathbf{w}_k$ , and  $\sigma^2$

$$\begin{aligned} \phi_{i,k} &\propto q_k \exp \left( - \frac{(y_i - \bar{\mathbf{x}}_i^T \mathbf{w}_k)^2 + \mathbf{w}_k^T S_i \mathbf{w}_k}{2\sigma^2} \right) \\ q_k &= \frac{1}{m} \sum_{i=1}^m \phi_{i,k} \\ \mathbf{w}_k &= \left( \sum_{i=1}^m \phi_{i,k} [\bar{\mathbf{x}}_i \bar{\mathbf{x}}_i^T + S_i] \right)^{-1} \left( \sum_{i=1}^m \phi_{i,k} y_i \bar{\mathbf{x}}_i \right) \\ \sigma^2 &= \sum_{i=1}^m \sum_{k=1}^K \phi_{i,k} \left[ (y_i - \bar{\mathbf{x}}_i^T \mathbf{w}_k)^2 + \mathbf{w}_k^T S_i \mathbf{w}_k \right] \end{aligned} \quad (9)$$

We further improve the robustness of the model by the introduction of prior for the regression weights  $\Pr(\mathbf{w}_k)$  as a Gaussian distribution  $N(\mathbf{0}, \lambda^{-1})$ . Then, instead of just maximizing the log-likelihood, we will maximize the logarithm of the posterior probability, i.e.,

$$\log \Pr(W | X, \mathbf{y}) = \log \Pr(\mathbf{y} | X, W) + \log \Pr(W) \quad (10)$$

where,  $W = (\mathbf{w}_1, \mathbf{w}_2, \dots, \mathbf{w}_K)$ . The updating equations in (9) are almost unchanged except that the equation for  $\mathbf{w}_k$  is changed to the following equation

$$\mathbf{w}_k = \left( \sum_{i=1}^m \phi_{i,k} [\bar{\mathbf{x}}_i \bar{\mathbf{x}}_i^T + S_i] + \lambda I \right)^{-1} \left( \sum_{i=1}^m \phi_{i,k} y_i \bar{\mathbf{x}}_i \right) \quad (11)$$

Evidently, the introduction of the uninformative prior is in general to reduce the magnitude of the regression weights. As a result, the small weights will become smaller and even zeros, which will result in sparse solution for  $W$ .

### 5.2.3 Incorporation of GO information in the similarity matrix

To incorporate the GO information into the regression model, we first represent each gene by the set of GO codes that are associated with the gene. We further expand the GO profile of each gene by including the parent nodes of each associated GO code. We then compute the similarity between two genes based on the overlap between their GO profiles. Since some GO codes may be more important than others, we adopt the term frequency independent document frequency (TF.IDF) weighting scheme of information

retrieval and weight each GO code by the IDF factor when computing the gene similarity. More specifically, the IDF factor for a GO code  $g$  is computed as

$$\text{IDF}(g) = \log \left( \frac{N + 0.5}{N(g)} \right) \quad (12)$$

where  $N$  is the total number of genes and  $N(g)$  is the number of genes whose profile include the GO code  $g$ . We denote the pairwise gene similarity by the matrix  $T = [T_{i,j}]_{n \times n}$  where element  $T_{i,j}$  represents the similarity between the  $i$ th gene and the  $j$ th gene.

In order to regulate the regression weights using the GO information, we assume that two genes are likely to share similar weights when they share a large number of common GO functions. In other words, two genes tend to have similar regression weights if they share large similarity in their GO profiles. Based on this assumption, we can construct the following energy function to measure the consistency between the assigned regression weights  $\mathbf{w}$  and the gene similarity  $T$

$$l(\mathbf{w}, T) = \sum_{i,j=1}^n T_{i,j} (w_i - w_j)^2 = \mathbf{w}^T L \mathbf{w} \quad (13)$$

where  $L$  is the graph Laplacian of similarity matrix  $T$ . Evidently, the smaller the  $l(\mathbf{w}, T)$  is, the more consistent the regression weight  $\mathbf{w}$  is to the gene similarity  $T$ . We can then incorporate the gene similarity  $T$  into the regression model as a Bayesian prior for regression weights  $W$ , i.e.,

$$\begin{aligned} \Pr(\mathbf{w}) &\propto \exp\left(-\lambda \sum_{i=1}^n w_i^2 - \tau \sum_{i,j=1}^n T_{i,j} (w_i - w_j)^2\right) \\ &= \exp\left(-\mathbf{w}^T [\lambda I + \tau L] \mathbf{w}\right) \end{aligned} \quad (14)$$

Note that in the above, in addition to the prior for the gene similarity  $T$ , we also include the uninformative prior through the factor  $\lambda I$ . The updating equations for the integrated Bayesian regression mixture model are almost identical to the ones in (10) except that the equation for  $\mathbf{W}_k$  is changed to the following equation

$$\mathbf{w}_k = \left( \sum_{i=1}^m \phi_{i,k} [\bar{\mathbf{x}}_i \bar{\mathbf{x}}_i^T + S_i] + \lambda I + \tau L \right)^{-1} \left( \sum_{i=1}^m \phi_{i,k} y_i \bar{\mathbf{x}}_i \right) \quad (15)$$

#### 5.2.4 Formation of the Integrative Mixture GO (IMGO) model

The two key parameters to our mixture model are  $\lambda$  and  $\tau$ . Parameter  $\lambda$  is related to the uninformative prior, and its role is to reduce the variance in the regression weights. Given that we have a large number of genes ( $\sim 700$ ) and relatively small number of experimental conditions ( $\sim 14$ ), there will be infinite number of ways to regress the cell response that are equally valid. The introduction of uninformative prior  $\lambda I$  will allow us to distinguish among the regression models that have the same regression error. In particular, by increasing the value of the parameter  $\lambda$ , we require the regression model to favor the regression model where only a small number of genes are assigned large weights and most genes are assigned very small weights even zero weights. The parameter  $\tau$  is related to the Bayesian prior for GO information. The larger the  $\tau$ , the more we require the

regression weights to be consistent with the GO information of genes. Apparently, we need to choose the appropriate value for  $\tau$  such that the regression weights can be consistent with both the GO information and the cell response.

#### **5.2.5 Discriminating ability of the IMG0**

The ability of the IMG0 to discriminate between the different phenotypes (e.g., cytotoxic vs. non-toxic conditions or high ketogenic vs. low ketogenic conditions) was measured as the difference in the probabilities of the two models for the palmitate without TNF- $\alpha$  (P-0) condition. This condition was chosen because it defined a threshold value for the toxic phenotype and showed maximum variation with the parameters. Therefore, an ideal condition is one where the probability of one model is unity and the other zero. Thus, the separation would have a range of 0 to 1, with 0 meaning both model are equally good and 1 meaning one of the models is superior over the other in modeling the condition of choice.

#### **5.2.6 Identification of discriminating genes**

In order to identify the genes which contribute the greatest to the difference in the two models (sub-populations), a concept similar to that used in the filter methods was employed. The absolute differences of the weights for the two models were calculated and the genes were ranked in decreasing order. The genes which showed greatest values of the absolute weight differences were identified to have contributed the most in separating the two models.

## 5.3 Results and Discussion

### 5.3.1 Cytotoxicity and ketone body release of the treatments

The cytotoxicity of various treatments is shown in Figure 5.1a. Among the different FFAs studied, the saturated FFA palmitate caused the greatest toxicity. TNF- $\alpha$  co-supplementation exacerbated the toxicity of the SFA, but TNF- $\alpha$  had no cytotoxic effect by itself or in the presence of UFAs. In addition to the cytotoxic effects of the fatty acids, the oxidation of FFAs was measured as the release of acetoacetate into the medium. It was observed that palmitate was oxidized to a greater extent than the other FFA treatments (Figure 5.1b) and TNF- $\alpha$  had no significant effect on the release of acetoacetate.

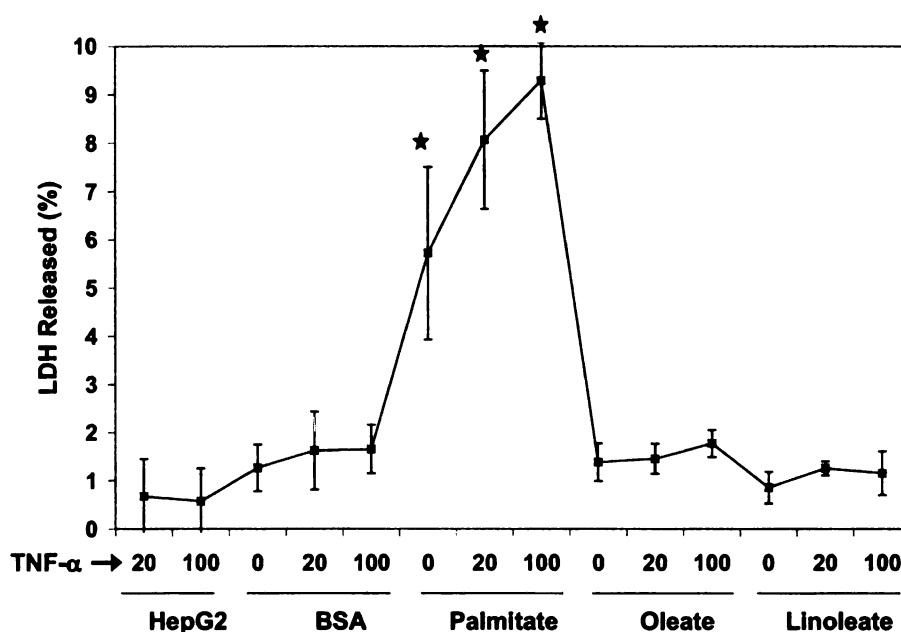


**Figure 5.1a Cytotoxicity of the treatments.** Confluent HepG2 cells were treated for 24 h with 0.7 mM of the indicated FFA complexed to 4% (w/v) BSA, in presence or absence of TNF- $\alpha$  (0, 20 or 100 ng/ml). The cytotoxicity was measured as the % LDH released, as defined in the methods section. Data presented as mean  $\pm$  s.d. of three independent experiments. \*, significant FFA effect,  $p < 0.01$ , #, significant TNF- $\alpha$  effect,  $p < 0.01$ .



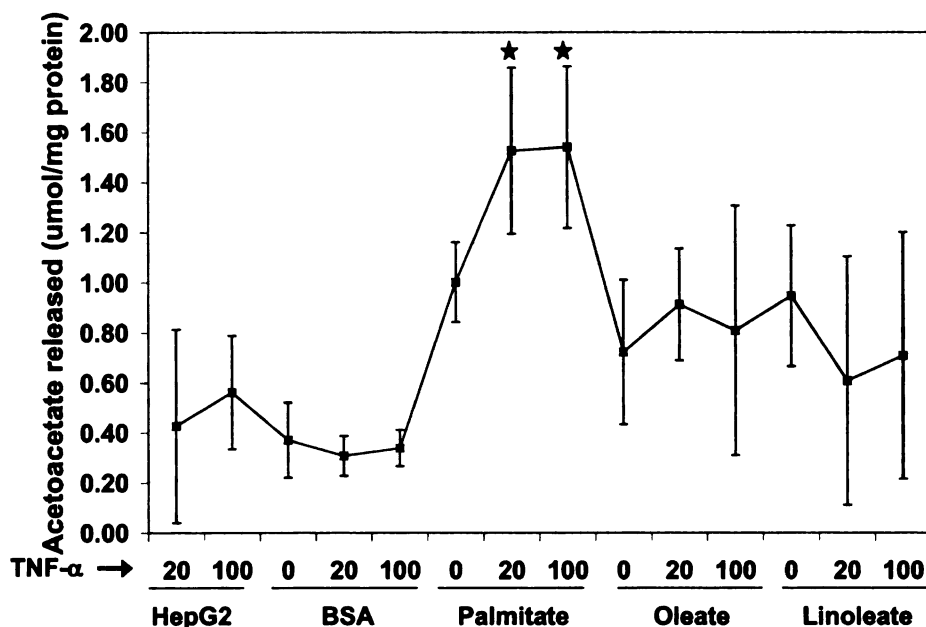


**Figure 5.1b Profile of acetoacetate release by various treatments.** The acetoacetate production in response to various treatments. Confluent HepG2 cells were treated for 24 h with 0.7 mM of the indicated FFA complexed to 4% (w/v) BSA, in presence or absence of TNF- $\alpha$  (0, 20 or 100 ng/ml). Acetoacetate was measured by enzymatic assay. Data presented as mean  $\pm$  s.d. of three independent experiments. \*, significant FFA effect,  $p < 0.01$ , #, significant TNF- $\alpha$  effect,  $p < 0.01$ .

### 5.3.2 Integrative Mixture Model Gene Ontology (IMGO) analysis

The genes which were affected by the treatments (FFA or TNF- $\alpha$  or their interaction) were identified by two-way ANOVA analysis. In order to identify the genes which contribute to the cytotoxicity of palmitate and TNF- $\alpha$  from the other treatments, the IMGO analysis was performed on the differentially expressed genes. To achieve separation of palmitate (toxic and ketogenic) conditions from the rest (non-toxic and non-ketogenic), a two-population mixed model was employed. The discrimination between the populations was calculated as the difference in the probabilities of the two models. Because the discrimination by the model is sensitive to the two parameters  $\lambda$  and  $\tau$ , the effect of these parameters on the ability of the mixture model to separate the cytotoxic

and non-toxic conditions was studied. The results of this analysis are shown in Figure 5.2. For very small  $\lambda$  (of 0.1), the separation increased with  $\tau$ . For higher  $\lambda$ , the separation displayed maxima with  $\tau = 3$ . This indicated that incorporation of prior knowledge ( $\tau$ ) improves the discriminating ability of the IMGO, but as the uninformative prior ( $\lambda$ ) is increased, only a small incorporation of  $\tau$  is needed to improve the separation. For higher values of  $\lambda$ , further increase of  $\tau$  weakens the discrimination of toxic vs. non-toxic conditions. The optimal values of  $\lambda$  and  $\tau$  vary, depending upon the sub-populations as well as the responses studied. Therefore, optimal values of these parameters can not be identified *a priori*.

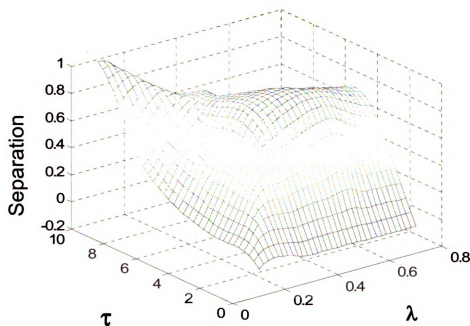


**Figure 5.2** Variation of the discriminating ability of the mixture model with the smoothing constant ( $\lambda$ ) and the weight to GO ( $\tau$ ). The probability of the model for the cytotoxic condition is plotted as a function of the two parameters  $\lambda$  and  $\tau$ .

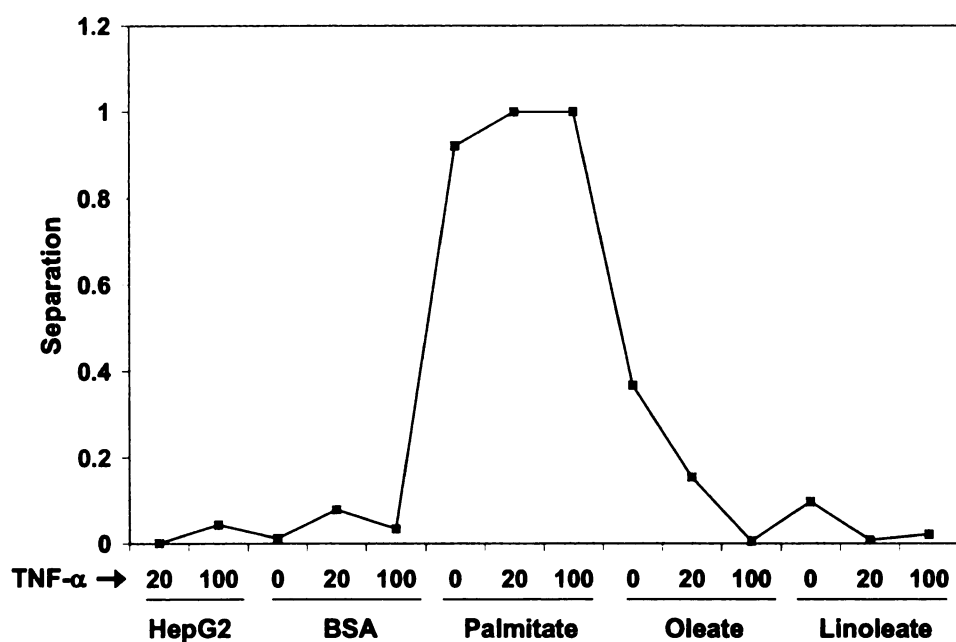


**Figure 5.3a Discrimination of the cytotoxic conditions from the non-toxic conditions for  $\lambda = 0.5$ ,  $\tau = 3$ .** A two sub-population model was fit for cytotoxicity and the ability of model to distinguish the cytotoxic (high LDH release) conditions was tested.

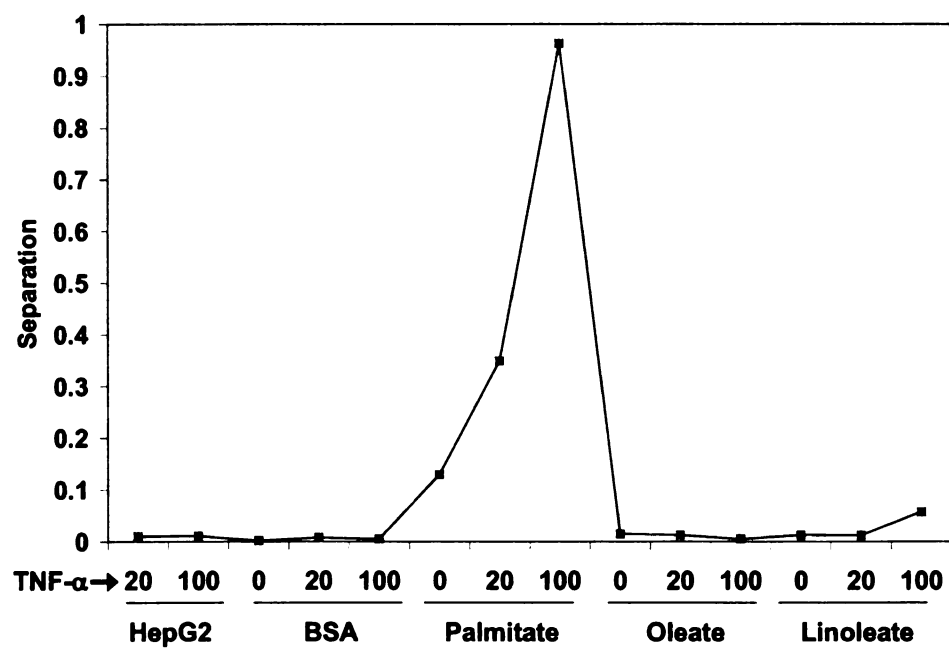


**Figure 5.3b Discrimination of the ketogenesis for  $\lambda = 0.5$ ,  $\tau = 3$ .** A two sub-population model was fit for cytotoxicity and the ability of model to distinguish the ketogenic (high acetoacetate release) conditions was tested.

As a preliminary screen of IMGO, its discriminating ability to differentiate the cytotoxic and metabolically distinct subpopulations was studied. The IMGO analysis was indeed able to separate the cytotoxic conditions from the non-toxic ones. Figure 5.3a shows the separation of the cytotoxic conditions for the parameter values of  $\lambda = 0.3$  and  $\tau = 3$  (the optimum value of  $\tau$  for  $\lambda = 0.3$ ). The IMGO analysis was also able to distinguish the conditions which had higher acetoacetate release, namely the palmitate-treated samples, from the others (Figure 5.3b). It must be emphasized that the two responses of LDH and acetoacetate release were simultaneously analyzed in a single run of the program. In fact, multiple metabolic and phenotypic responses can be analyzed simultaneously using this procedure, making it a truly parallel analysis method.

### **5.3.3 Identification of the genes responsible for separating the toxic vs. non-toxic phenotype**

In order to identify the genes that could discriminate between the toxic and non-toxic phenotypes, a two-population mixture model was fit and the genes with the greatest differences in their weights for the two models were identified. Detailed results of this analysis are available in additional file 1. This analysis identified that lysosomal ATPase V0 subunit a isoform 1 (ATP6V0A1, accession number NM\_005177) and adenylate cyclase 9 (AC9, accession number H64281) were the genes which had the greatest differences in their weights for the two models. Another lysosomal ATPase, the 13kDa, V1 subunit G isoform 1 (ATP6V1G1, accession number AA608567) also had very high difference in weights for the two models. These genes also had the greatest individual weights for the second mixture model (which fit the toxic phenotypes better), further

emphasizing the important role of these proteins in the FFA-toxicity. The location of these genes in the ranked list for greatest difference in weights for the two models is shown in Table 5.1. While the two lysosomal ATPases had consistently higher ranks irrespective of the separation achieved in the two mixture models (defined as probability for the model which fit the cytotoxic condition), AC9 had very low rank when the separation was poor (about 0.5), but its rank became very high (= 2) for higher separation (0.6 or higher).

$\lambda$	$\tau$	Probability	Rank (AC9)	Rank (ATP6V0A1)	Rank(ATP6V1G1)
0.1	0	0.5	N/A	N/A	N/A
	3	0.5454	3	1	4
	7	0.6696	2	1	4
	10	0.9917	2	1	4
0.3	0	0.5	453	2	5
	3	0.8991	2	1	4
	7	0.8857	2	1	4
	10	0.8186	2	1	5
0.5	0	0.5	455	2	5
	3	0.9604	2	1	4
	7	0.7963	2	1	5
	10	0.7479	2	1	5
0.7	0	0.5	460	2	5
	3	0.8835	2	1	4
	7	0.7508	2	1	5
	10	0.6914	2	1	5

**Table 5.1 The ranks of the three genes, adenylate cyclase 9 (AC9) and lysosomal ATPases (ATP6V0A1 and ATP6V1G1) as a function of  $\lambda$  and  $\tau$ .** Two subpopulation mixture model was fit to the data using various values of the parameters  $\lambda$  and  $\tau$ . The probability is defined as the probability of associated with the model that fit the cytotoxic conditions better. The absolute differences of weights assigned for a gene by the two models were ranked in decreasing order. The location of the three genes in the ranked list was identified and is shown. All the genes had same weights for the two models when  $\lambda = 0.1$  and  $\tau = 0$ , thus the differences were all 0 and ranking was not possible.

### 5.3.4 Experimental validation of lysosomal ATPase genes

In order to investigate the role of lysosomal ATPases in the cytotoxicity of palmitate, the effect of Bafilomycin A1 (Bfl, an inhibitor specific for lysosomal ATPases) on the cytotoxicity was studied. Treating cells with palmitate in the presence of 5 nM Bfl significantly increased the toxicity of this fatty acid (Figure 5.4). Similar concentration of Bfl was not toxic by itself. These results indicated that the functioning of lysosomal ATPases is affected by palmitate and may mediate the toxicity of this FFA.

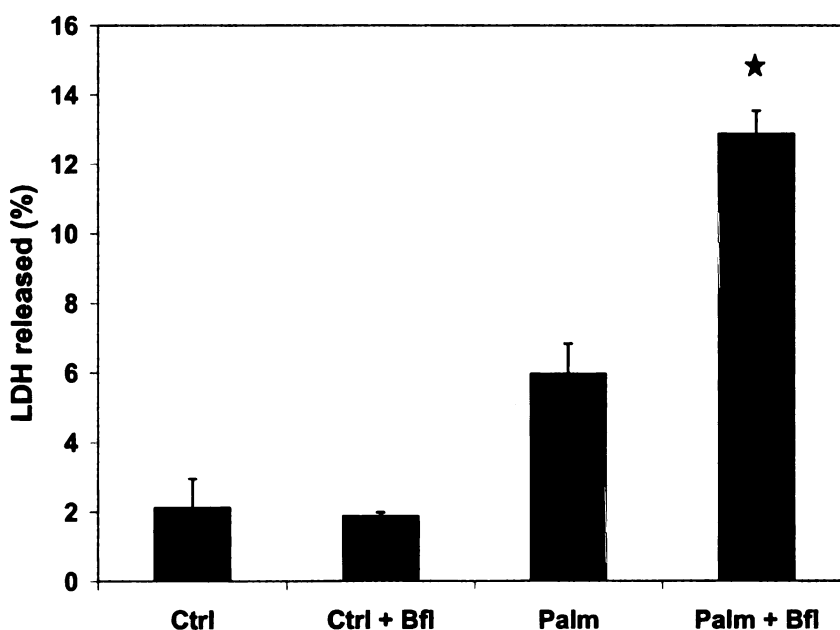


**Figure 5.4** Effect of inhibitor of lysosomal ATPase, bafilomycin (Bfl) on the toxicity of palmitate. Cells were treated with 0.7 mM palmitate or control medium in the presence of 5 nM Bfl for 24 h and the LDH release was measured. Data presented as mean  $\pm$  s.d. of six samples from two independent experiments.

### 5.3.5 Experimental validation of adenylate cyclase

Caspase-3 is an effector/ terminal caspase, which mediates the changes leading to apoptosis. Cells exposed to palmitate had about 7-fold higher greater caspase-3 activities than controls. In order to identify the role of AC in the cytotoxicity of the FFAs, we

tested the effect of increasing the cAMP levels of the cells on the activation of caspase-3 by palmitate. Treating the cells with palmitate in the presence of IBMX and forskolin (chemicals known to increase cAMP levels) further increased the caspase-3 activation in response to palmitate (Figure 3b), but did not affect caspase-3 activation in controls (not shown). In fact, after 24 h of exposure to palmitate + forskolin and IBMX, the caspase activity was about twice than that observed in palmitate alone. This indicated that elevated cAMP levels could worsen the apoptotic effects of palmitate, corroborating with the model predictions of the importance of AC9 in the cytotoxicity of palmitate.

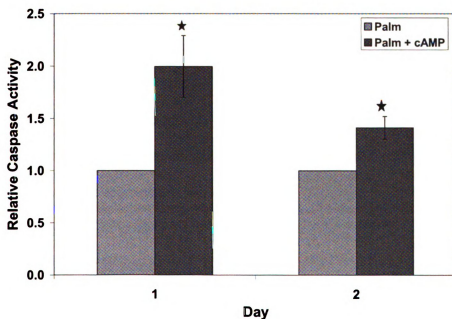


**Figure 5.5 Effect of increasing cAMP levels on the caspase-3 activation by palmitate.** Cells were treated with 0.7 mM palmitate or control medium in the presence of 5 nM Bfl for 48 h. Media were replaced daily. The relative caspase-3 activity was measured. Data presented as mean  $\pm$  s.d. of nine samples from three independent experiments.

## 5.4 Discussion

Incorporation of the functional information of genes in the microarray analysis is a new and active area of research. However, most of the currently available methods utilize the prior functional (GO) information to generate pre-defined sets of genes (Subramanian et al., 2005 and Beisvag et al., 2006). The underlying assumption in these analyses is that a phenotype is altered by concerted change in the expression of many genes of a GO-category (Subramanian et al., 2005). The approach presented here is conceptually somewhat similar to these approaches, but with major differences: (a) The similarity matrix employed in the analysis is based on the overlap in the GO profiles among every pair of genes in the data-set. Therefore, there are no strict gene sets and the possibility of interaction/ coregulation of any pair of genes is incorporated as well as weighted, i.e., genes with greater overlap (even if they lie within a same GO-group) have greater coefficient in the similarity matrix and vice versa. (b) The contribution of individual gene (or maximum a pair of genes) in discriminating between the populations can be identified. Many times the goal is to identify a few discriminating genes that could be further tested. This technique offers the possibility of objectively identifying such genes by suggesting the topmost discriminatory genes. (c) One can control the contribution of the GO information in the model. In our study, the contribution of the similarity matrix (GO information) is weighted by the factor  $\tau$ , which can be varied. This is in contrast to other methods where the GO information takes precedence over the data and the subsequent processing. The advantage of controlling the contribution of GO information is best shown by Figure 3, where it is shown that even though GO improves the discrimination, but for better discrimination, the contribution of GO must be regulated. It



is likely that at higher values of  $\lambda$ , the constraints imposed by higher  $\tau$  adversely affect the discrimination. In addition to these advantages, the model offers possibility of discriminating multiple subpopulations, though this needs to be further tested and validated.

The genes selected for the FFA-toxicity identified an important role of lysosomes in the toxicity of palmitate to the HepG2 cells. Lysosomal ATPases regulate the import of  $H^+$  ions and regulate the function of these organelles. These ATPases have two domains, the cytosolic V1 and the transmembrane V0. The V1 domain contains the ATP catalytic site. ATP6V0A1 encodes one of three A subunit proteins and the encoded protein is associated with clathrin-coated vesicles, while ATP6V1G1 encodes for one of three V1 domain G subunit proteins. The selection of these genes indicates an alteration in the functioning of lysosomes. Indeed, a recent study has identified an important role of lysosomal permeabilization in the toxicity of palmitate to HepG2 cells (Feldstein et al., 2006). This study showed that in hepatocytes and HepG2 cells, exposure to palmitate leads to translocation of Bax (a pro-apoptotic Bcl-2 family protein) to lysosomes, which leads to the rupture of lysosomes. The exact mechanism of how Bax causes permeabilization of lysosomes is not clear.

Another important target identified by the analysis is adenylate cyclase 9 (AC9). AC's are membrane bound enzymes that catalyses the formation of cyclic AMP from ATP and are regulated by a family of G protein-coupled receptors, protein kinases, and calcium. AC9 is stimulated by beta-adrenergic receptor activation but is insensitive to forskolin,

calcium, and somatostatin. It has previously been identified that the activity of adenylate cyclase is regulated by palmitoylation (Mollner 1995), as is the activity of G-proteins (Linder et al. 1993 and Degtyarev et al. 1993). It is likely that the elevated palmitate levels lead to palmitoylation and greater activity of AC9, causing increased intracellular cAMP levels, which in turn, would activate other signaling pathways by activating cAMP-dependent protein kinase (PKA). PKA would then phosphorylate and activate membrane channels and contractile proteins, as well as affect transcription of various genes by phosphorylating transcription factors, like C/EBP. Activation of AC and PKA has been suggested to mediate cell death in response to stimuli such as ethanol (Maas et al. 2005), morphine (Lim et al. 2005) and pathogens (Hewlett et al. 2006 and Voth et al. 2005). On the contrary, cytoprotective role of this pathway has been indicated in anoikis (Joseph et al. 2005), spinal-injury (Chen and Tzeng 2005), CD-34+ cytotoxicity (Negretto 2006) and myocardial infarction (Takahashi et al. 2006, etc.).

Another gene that had consistently high weight was nuclear factor of kappa light polypeptide gene enhancer in B-cells inhibitor, alpha (NFKBIA). NFKBIA encodes for the inhibitor of NF- $\kappa$ B (I $\kappa$ B-alpha). The activity of NF- $\kappa$ B is regulated through I $\kappa$ B-alpha. NF- $\kappa$ B is an important transcription factor that regulates the expression of a variety of genes, such as those involved in the regenerative (Taub, 1996), anti-apoptotic (Schuchmann and Galle, 2002 and Bradham et al., 1998) and anti-oxidant (Huang et al., 2001) response of the cells. In addition, the rapid activation of NF- $\kappa$ B has been suggested to protect the hepatocytes and hepatoma cells from the cytotoxic action of TNF- $\alpha$  (Bradham et al., 1998). Based on these roles of NFKBIA, it should have a positive

association with the cytotoxicity. Indeed, the regression coefficient of this gene to cytotoxicity was positive.

Other genes which are known to play important role in cellular physiology were also identified to be very important in relation to the FFA toxicity. It was identified that NADH dehydrogenase (ubiquinone) Fe-S protein 1 (NDUFS1) was the most important protein, especially for conditions with small separation of the models (i.e., both model had very similar weights and so were almost equally good). Our previous study has identified the important role that NADH dehydrogenases play in regulating the FFA-toxicity (Srivastava and Chan, 2007). Another gene that was identified as important for certain conditions was cytochrome P450, subfamily 46 (cholesterol 24-hydroxylase) (CYP46). CYP46 is involved in the synthesis of cholesterol metabolite 24S-hydroxycholesterol. Alterations in cholesterol metabolism are associated with various disorders, and may even lead to cell death (Tabas 2002 and Cutler et al. 2002). Some conditions also identified chloride channel 4 (CLCN4 / CIC4). CIC4 exhibits chloride-coupled proton transport activity and transport a significant amount of protons across the plasma membrane, even against the electrochemical gradient, when activated by positive voltages (Picollo and Pusch 2005). A redox-regulation of its activity has been suggested (Mazzanti et al. 2005). However, the role played by this gene in the FFA-toxicity is currently not clear.

Thus, the IMGO analysis identified proteins that play important role in the toxicity of FFAs. While some of these proteins have already been shown to play important roles in

the toxicity of FFAs, others have been indicated to play important roles in cellular physiology and thus could contribute to the FFA. Our results indicate the IMGGO is a useful approach to incorporate ontology information in the selection process to identify important genes that regulate certain functions of interest.

## CHAPTER 6. CONCLUSIONS AND FUTURE DIRECTIONS

### 6.1 Conclusions

The objectives of this research were to investigate the physiological, metabolic and genomic alterations caused by FFA, more specifically saturated FFA, which were associated with its toxicity. This study has revealed complex changes in multiple cellular levels on exposure to saturated FFA. It was shown that the toxicity was caused by excessive production of reactive oxygen species (ROS), specially hydrogen peroxide and hydroxyl radicals. It was also shown that mitochondrial complexes I and III were the primary sources of the cytotoxic ROS. This information may help in the development of novel treatment strategies which employ scavengers specific to these radicals, or inhibitors that reduce ROS generation at the mitochondrial complexes. Such scavengers/inhibitors may be more effective in protecting liver against the cytotoxic action of FFAs. The saturated FFAs not only lead to greater ROS generation, but also reduce cellular antioxidant ability by reducing the levels of cystine transporter, which leads to reduced synthesis of GSH, the primary anti-oxidant molecule. Thus, the saturated FFA causes deleterious alterations at multiple levels of cellular redox balance, which perhaps amplifies its cytotoxic potential. In addition to ROS, various signaling pathways play important roles in the alterations caused by palmitate. In particular, the roles of JNK and ERK in the toxicity of these fatty acids were identified.

Chronic exposure to FFAs is known to be associated with development of insulin resistance as well as lipotoxicity. This study suggests that saturated FFAs cause much greater lipotoxicity than the unsaturated FFAs. Additionally, the gene-expression data

suggests that the genes with known functions in inhibiting insulin signaling, e.g., INPPL1, are upregulated only in the saturated FFA. Thus, it is likely that saturated FFAs also inhibit insulin signaling to a greater extent than the unsaturated FFAs in hepatocytes, as has been shown in other types of cells.

The studies in this thesis have indicated that integration of multi-source high-throughput information may help identify novel targets that could be more potent in regulating the progression of metabolic disorders. A case in point is of glutamate-cysteine synthetase/ligase (GCS/L). The GA/PLS analysis for TG-only had identified GCS as an important gene. However, GCS was not selected by the dual-response analysis, suggesting that it was not important to regulate TG and LDH. In fact, in chapter 2 it was identified that GCS was elevated in palmitate-treated cells and thus, would not be a limitation for the glutathione synthesis. Therefore, overexpression of GCS is unlikely to improve palmitate-toxicity. The integrative analyses could help quell such false-positives and suggest more robust targets than individual analyses. Finally, it was shown that incorporation of the prior (gene ontology) information of genes could lead to better discrimination among the sub-populations and can help identify targets with important roles in the underlying cellular processes.

## **6.2 Future Directions**

The studies presented in this thesis have provided information on multiple alterations by FFAs and identified some which play important role in lipotoxicity. Greater insights may be achieved by performing some of the following studies.

### **6.2.1 *In vivo* studies**

The ‘acid-tests’ of the findings of this study would be the application of the knowledge learned in an *in vivo* system. For example, the effects of specific hydroxyl radical or peroxide scavengers, or the effects of partial inhibition of complexes I and III on the development of lipotoxicity in an animal model may be tested and compared to those of superoxide-specific scavengers. Similarly, the effects of ERK inhibitors or ERK-null rodents on a high saturated fat diet should be investigated. Because ERK and JNK can also regulate the expression of multiple genes, the roles played by these in regulating the responses of interest could identify novel mechanisms of alterations by FFAs. The mechanisms behind greater TG accumulation in response to the JNK inhibitor requires further investigation. Because JNK has been touted as a potent anti-obesity target, such studies are important to differentiate the whole-body-level and individual-cell-level effects of this protein.

### **6.2.2 Insulin signaling in response to different FFAs**

While some amount of literature is available on the effect of different types of FFAs on insulin signaling in beta cells and myocytes, similar studies in hepatocytes are lacking. The effects of the different types of FFAs on insulin signaling in hepatocytes should be studied to identify if there are differences in the effects of different types of FFAs on insulin signaling. Such studies would decipher the association between lipotoxicity and insulin signaling. If the saturated FFAs emerge as having greater deleterious effect on

insulin signaling as well, they could become the primary culprits among the FFAs which cause various metabolic disorders associated with obesity.

### **6.2.3 Application of the frameworks developed to other diseases/ data sets**

The integrative frameworks developed in chapters 4 and 5 should be applied and tested in other diseases and compared to available methods. Such analyses would help to generalize the validity of the approaches as well as to find robust targets to regulate a cellular response of interest.

I believe that the information, data and frameworks generated in the current thesis would help advance the field of obesity and lipotoxicity research and have the potential to be applied to other diseases.



# APPENDIX

## 1. Table of metabolic fluxes for day 1

Rxn No.	Equation	BSA		Palm		Ole	
1	G+ATP --> G-6-P	27.58	1.82	27.84	1.36	26.61	0.77
2	G-6-P -> F-6-P	28.40	1.40	28.07	1.30	26.99	0.75
	F-6-P +ATP --> Glyceraldehyde-3-P +						
3	DHAP	28.40	1.40	28.07	1.30	26.99	0.75
4	DHAP --> Glyceraldehyde-3-P	28.40	1.40	28.07	1.30	27.00	0.75
5	Glyceraldehyde-3-P --> 3-PGA	57.83	2.71	56.64	2.51	54.80	1.46
6	3PGA --> PEP + NADH (+ 2ATP)	57.83	2.71	56.64	2.51	54.80	1.46
7	PEP --> Pyr	57.83	2.71	56.64	2.51	54.80	1.46
8	Pyruvate + NADH --> (Lactate)	53.13	3.43	52.81	4.50	50.89	2.81
9	Pyruvate --> Acetyl-CoA + NADH +CO2	3.09	3.40	3.07	4.69	2.06	2.90
10	Acetyl-CoA + OAA --> Citrate	8.67	2.54	8.03	1.79	7.92	2.24
	Citrate --> a-KetoGlutarate + NADPH						
11	+CO2	8.55	2.54	7.94	1.79	7.74	2.24
	a-Ketoglutarate --> Succinyl-CoA +						
12	NADH + CO2	9.01	2.57	8.28	1.79	8.48	2.24
	Succinyl-CoA --> Fumarate + FADH2 +						
13	ATP	9.29	2.54	8.52	1.77	8.70	2.23
14	Fumarate --> OAA + NADH	8.80	2.54	8.11	1.79	8.11	2.24
15	G-6-P --> 12 NADPH + 6 CO2	-0.81	0.77	-0.23	0.19	-0.38	0.15
16	CO2 out	16.35	4.69	17.98	5.03	16.72	4.71
17	2 Acetyl-CoA --> Acetoacetyl-CoA	-1.03	0.84	-0.39	0.69	-0.68	0.37
18	Acetoacetyl-CoA --> Acetoacetate	0.17	0.21	0.29	0.15	0.29	0.10
19	Acac out	0.05	0.04	0.09	0.03	0.07	0.02
	Acetoacetate + NADH --> (B-OH						
20	butyrate)	0.03	0.01	0.13	0.05	0.08	0.02
21	O2 (In)	20.75	3.29	22.15	3.79	21.83	5.38
22	NADH + 0.5 O2 --> 2.5 ATP	32.87	5.35	34.76	6.28	35.47	8.86
23	FADH2 + 0.5 O2 --> 2 ATP	10.28	2.54	9.61	1.80	9.74	2.24
24	Glycerol + ATP --> Glycerol-3-P	0.75	0.06	0.47	0.05	0.80	0.06
	Glycerol-3-P --> Glyceraldehyde-3-P +						
25	NADH	1.03	0.28	0.49	0.29	0.81	0.20
26	Palm-CoA --> 8 Acetyl-CoA + 14 NADH	-0.32	0.50	0.42	0.52	0.39	0.32
27	Palm-CoA + DAG --> TG	0.00	0.00	0.03	0.01	0.04	0.02
28	Ser (In)	0.50	0.12	0.50	0.18	0.48	0.05
29	Ser --> NH3 + Pyr	0.27	0.41	0.48	0.28	-0.01	0.11
30	Gln In	2.43	0.30	2.23	0.10	2.48	0.11
31	His --> Glu + NH4	0.42	0.09	0.29	0.08	0.48	0.07
32	Asp (In)	-0.10	0.05	-0.11	0.02	0.00	0.00
33	Glu (In)	-0.83	0.43	-0.68	0.29	-0.63	0.09
34	Gly (In)	0.09	0.29	-0.17	0.20	0.72	0.07
35	Glycine --> 2 CO2 + NADH + NH3	-0.40	0.29	-0.52	0.20	0.06	0.08
36	NH4 (In)	-2.54	0.82	-2.53	0.54	-2.47	0.21
37	Arg In	0.55	0.09	0.39	0.08	0.35	0.03
38	Thr (In)	0.12	0.21	0.19	0.14	0.18	0.07
39	Ala (In)	-1.89	0.82	-1.31	0.45	-1.85	0.28

40	Glu + Pyr --> Ala + aKG	1.94	0.75	1.41	0.41	1.92	0.25
41	Pro In	-0.42	0.16	-0.51	0.11	0.03	0.05
42	Cys In	0.19	0.01	0.15	0.02	0.17	0.02
43	Tyr (In)	0.08	0.17	-0.07	0.11	0.16	0.09
	Tyr + aKG + 2 O2 --> Glu + CO2 +						
44	Acetoacetate + Fumarate	-0.08	0.20	-0.06	0.14	-0.14	0.09
45	Val (In)	0.55	0.32	0.25	0.24	0.45	0.16
46	Om IN	-0.03	0.03	-0.05	0.02	0.04	0.01
47	Lys (In)	0.33	0.33	0.34	0.24	0.31	0.09
48	Ile (IN)	0.20	0.20	0.45	0.18	0.48	0.09
49	Leu (In)	0.30	0.17	0.55	0.16	0.41	0.08
50	Phe (In)	0.18	0.05	0.37	0.07	0.22	0.03
51	Glu + Cys + Gly --> GSH	0.43	0.10	0.35	0.07	0.54	0.04
	HCO3- + NH4 + Om + 2 ATP -->						
52	Citrulline	-0.18	0.21	-0.16	0.14	-0.07	0.06
	Citrulline + Asp + ATP --> Fumarate +						
53	Arg	-0.29	0.13	-0.27	0.09	-0.26	0.04
54	Arg --> Om + Urea	0.22	0.16	0.01	0.12	0.02	0.05
55	Urea Out	0.22	0.16	0.01	0.12	0.02	0.05
56	Gln --> Glu + NH4	2.20	0.27	2.04	0.10	2.10	0.10
	Om + a-KG + 0.5 NADPH + 0.5 NADH --						
57	> Pro	0.31	0.27	0.02	0.18	0.06	0.09
58	Asp + NH4 --> Asn	0.12	0.06	0.08	0.04	0.19	0.02
	Thr --> Pyr + CO2 + NH4 + 2 NADH +						
59	FADH2	0.06	0.21	0.18	0.14	0.06	0.07
	Val + aKG --> Glu + CO2 + 2NADH +						
60	FADH2 + Succ-CoA	0.37	0.30	0.06	0.23	0.19	0.14
	Lys + 2 aKG + NADPH --> 2Glu +						
	Acetoacetyl-CoA + 2CO2 + 4 NADH +						
61	FADH2	0.23	0.27	0.13	0.18	0.16	0.08
	Ile + aKG --> Glu + Succ-CoA + Acetyl-						
62	CoA + NADH + FADH2	0.03	0.20	0.26	0.17	0.22	0.08
	Leu + aKG --> Glu + HMG-CoA + NADH						
63	+ FADH2	0.25	0.18	0.45	0.16	0.34	0.08
64	Phe + O2 --> Tyr	0.01	0.09	0.19	0.08	-0.04	0.04
	Ser + 2 Palm-CoA + NADPH --> CO2						
65	+Ceramide + FADH2	0.00	0.08	0.06	0.01	0.05	0.11
	Ceramide + PhosphatidylCholine -->						
66	Sphingomyelin	0.01	0.04	0.00	0.03	0.02	0.01
	Acetoacetyl-CoA + Acetyl-CoA --> HMG-						
67	CoA	-0.96	0.72	-0.55	0.62	-0.80	0.34
68	HMG-CoA + 2 NADPH (+ 3ATP) --> IPP	-0.71	0.68	-0.10	0.59	-0.46	0.32
69	2 IPP --> Geranyl-PP	-0.24	0.23	-0.03	0.20	-0.16	0.11
70	Geranyl-PP + IPP --> Farnesyl-PP	-0.23	0.22	-0.03	0.19	-0.15	0.11
	2 Farnesyl-PP + 0.5 NADPH + 0.5 NADH						
71	--> Squalene	-0.11	0.10	-0.02	0.09	-0.07	0.05
72	Squalene + O2 + NADPH --> Lanosterol	-0.08	0.08	-0.01	0.07	-0.06	0.04
	Lanosterol + 10.5 NADPH + 4.5 NADH +						
73	10 O2 --> Chol + 3 CO2	-0.06	0.06	-0.01	0.05	-0.04	0.03
74	Cholesterol Ester --> Chol + FA-CoA	0.04	0.03	0.01	0.03	0.02	0.02
	2 Palm-CoA + Glycerol-3-P -->						
75	Phosphatidate	-0.18	0.20	0.00	0.21	0.06	0.14
76	Phosphatidate --> DAG	-0.10	0.11	0.01	0.08	-0.10	0.04

77	Phosphatidate --> CDP-DAG	-0.06	0.17	-0.01	0.16	0.18	0.11
78	CDP-DAG + Ser --> PhosphatidylSerine PhosphatidylSerine -->	0.12	0.22	0.01	0.15	0.31	0.07
79	PhosphatidylEthanolamine + CO2 CDP-DAG + G-3-P -->	0.09	0.15	0.01	0.10	0.21	0.05
80	PhosphatidylGlycerol	-0.15	0.14	-0.02	0.13	-0.11	0.08
81	2 PG --> Cardiolipin + Glycerol DAG + CDP-Choline -->	-0.06	0.06	-0.01	0.05	-0.04	0.03
82	PhosphatidylCholine DAG + CDP-Ethanolamine -->	-0.01	0.02	0.00	0.02	0.00	0.01
83	PhosphatidylEthanolamine	-0.06	0.09	-0.01	0.06	-0.12	0.03
84	Glu + 2 NADPH --> Pro	0.28	0.35	0.67	0.23	0.17	0.11
85	Palm (In)	N.D.	N.D.	0.44	0.11	0.57	0.03

## 2. Values of the metabolic fluxes for day 2

Rxn No.	Equation	BSA		Palm		Ole	
1	G+ATP --> G-6-P	27.10	1.13	26.68	2.27	26.86	2.75
2	G-6-P --> F-6-P	27.94	0.98	26.99	2.16	27.19	2.63
3	F-6-P +ATP --> Glyceraldehyde-3-P + DHAP	27.94	0.98	27.00	2.16	27.19	2.63
4	DHAP --> Glyceraldehyde-3-P	27.94	0.98	27.00	2.16	27.19	2.63
5	Glyceraldehyde-3-P --> 3-PGA	56.89	2.00	54.59	4.15	55.05	5.01
6	3PGA --> PEP + NADH (+ 2ATP)	56.89	2.00	54.59	4.15	55.05	5.01
7	PEP --> Pyr	56.89	2.00	54.60	4.15	55.05	5.01
8	Pyruvate + NADH --> (Lactate)	51.20	3.47	50.11	5.33	50.64	5.51
9	Pyruvate --> Acetyl-CoA + NADH +CO2	4.23	2.85	3.20	6.29	2.74	7.01
10	Acetyl-CoA + OAA --> Citrate	9.99	2.44	7.03	2.78	7.83	2.00
11	Citrate --> a-KetoGlutarate + NADPH +CO2	9.87	2.44	6.92	2.77	7.66	2.00
12	a-Ketoglutarate --> Succinyl-CoA + NADH + CO2	10.24	2.47	7.50	2.97	8.28	2.02
13	Succinyl-CoA --> Fumarate + FADH2 + ATP	10.56	2.44	7.58	2.86	8.56	2.01
14	Fumarate --> OAA + NADH	10.11	2.44	7.14	2.79	7.99	2.00
15	G-6-P --> 12 NADPH + 6 CO2	-0.83	0.66	-0.31	0.30	-0.32	0.23
16	CO2 out	19.56	4.30	15.52	7.12	16.82	7.00
17	2 Acetyl-COA --> Acetoacetyl-CoA	-1.01	0.69	0.26	1.11	-0.74	0.85
18	Acetoacetyl-CoA --> Acetoacetate	0.27	0.20	1.57	0.40	0.38	0.43
19	Acac out	0.06	0.04	0.68	0.11	0.14	0.02
20	Acetoacetate + NADH --> (B-OH butyrate)	0.05	0.02	0.79	0.22	0.04	0.04
21	O2 (In)	23.78	3.69	19.48	5.89	20.91	4.15
22	NADH + 0.5 O2 --> 2.5 ATP	38.24	5.92	32.10	9.86	34.26	6.99
23	FADH2 + 0.5 O2 --> 2 ATP	11.59	2.45	8.51	2.87	9.63	2.04
24	Glycerol + ATP --> Glycerol-3-P	0.71	0.08	0.44	0.06	0.66	0.05
25	Glycerol-3-P --> Glyceraldehyde-3-P + NADH	1.01	0.24	0.60	0.41	0.67	0.40
26	Palm-CoA --> 8 Acetyl-CoA + 14 NADH	-0.32	0.42	0.37	0.72	0.28	0.69
27	Palm-CoA + DAG --> TG	0.00	0.00	0.04	0.01	0.07	0.02
28	Ser (In)	0.45	0.11	0.52	0.61	0.55	0.08
29	Ser --> NH3 + Pyr	0.16	0.33	0.04	0.71	0.02	0.29
30	Gln In	2.65	0.40	2.68	1.32	2.64	0.34
31	His --> Glu + NH4	0.35	0.07	0.30	0.14	0.43	0.01
32	Asp (In)	0.00	0.01	-0.11	0.02	0.00	0.01
33	Glu (In)	-0.73	0.22	-0.78	0.55	-0.59	0.32
34	Gly (In)	0.08	0.17	-0.15	0.22	0.11	0.13
35	Glycine --> 2 CO2 + NADH + NH3	-0.46	0.20	-0.63	0.40	-0.56	0.18
36	NH4 (In)	-2.31	0.61	-2.03	0.71	-1.87	0.64
37	Arg In	0.50	0.16	0.25	0.11	0.29	0.13
38	Thr (In)	0.13	0.17	0.17	0.57	0.15	0.12
39	Ala (In)	-1.61	0.68	-1.34	0.73	-1.64	0.63
40	Glu + Pyr --> Ala + aKG	1.67	0.63	1.40	0.67	1.72	0.58
41	Pro In	-0.66	0.31	-0.53	0.41	-0.30	0.36

42	Cys In	0.20	0.00	0.11	0.03	0.17	0.02
43	Tyr (In)	0.07	0.12	-0.04	0.22	0.14	0.49
	Tyr + aKG + 2 O2 --> Glu + CO2 +						
44	Acetoacetate + Fumarate	-0.16	0.19	-0.10	0.31	-0.20	0.43
45	Val (In)	0.53	0.27	0.13	0.22	0.52	0.16
46	Orn IN	0.00	0.02	-0.03	0.03	0.02	0.01
47	Lys (In)	0.36	0.29	0.23	0.24	0.35	0.20
48	Ile (IN)	0.29	0.24	0.39	0.18	0.41	0.13
49	Leu (In)	0.31	0.24	0.48	0.18	0.42	0.12
50	Phe (In)	0.14	0.11	0.26	0.10	0.14	0.06
51	Glu + Cys + Gly --> GSH	0.46	0.09	0.38	0.22	0.54	0.09
	HCO3- + NH4 + Orn + 2 ATP -->						
52	Citrulline	-0.03	0.17	-0.06	0.24	0.01	0.16
	Citrulline + Asp + ATP --> Fumarate +						
53	Arg	-0.17	0.10	-0.23	0.14	-0.20	0.11
54	Arg --> Orn + Urea	0.26	0.19	-0.04	0.21	0.01	0.18
55	Urea Out	0.26	0.19	-0.04	0.21	0.01	0.18
56	Gln --> Glu + NH4	2.38	0.34	2.41	1.13	2.27	0.30
	Orn + a-KG + 0.5 NADPH + 0.5 NADH -->						
57	> Pro	0.21	0.26	-0.05	0.31	-0.05	0.22
58	Asp + NH4 --> Asn	0.12	0.05	0.11	0.09	0.17	0.05
	Thr --> Pyr + CO2 + NH4 + 2 NADH +						
59	FADH2	0.06	0.17	0.07	0.53	0.02	0.13
	Val + aKG --> Glu + CO2 + 2NADH +						
60	FADH2 + Succ-CoA	0.34	0.25	-0.03	0.23	0.28	0.16
	Lys + 2 aKG + NADPH --> 2Glu +						
61	Acetoacetyl-CoA + 2CO2 + 4 NADH +						
	FADH2	0.22	0.24	0.13	0.22	0.19	0.18
	Ile + aKG --> Glu + Succ-CoA + Acetyl-						
62	CoA + NADH + FADH2	0.10	0.23	0.22	0.21	0.17	0.14
	Leu + aKG --> Glu + HMG-CoA + NADH						
63	+ FADH2	0.25	0.23	0.43	0.19	0.35	0.13
64	Phe + O2 --> Tyr	-0.04	0.12	0.10	0.15	-0.10	0.09
	Ser + 2 Palm-CoA + NADPH --> CO2						
65	+Ceramide + FADH2	0.06	0.09	0.12	0.18	0.06	0.04
	Ceramide + PhosphatidylCholine -->						
66	Sphingomyelin	0.02	0.03	0.04	0.07	0.02	0.02
	Acetoacetyl-CoA + Acetyl-CoA --> HMG-						
67	CoA	-1.06	0.61	-1.18	1.09	-0.92	0.74
68	HMG-CoA + 2 NADPH (+ 3ATP) --> IPP	-0.81	0.56	-0.75	1.07	-0.57	0.71
69	2 IPP --> Geranyl-PP	-0.27	0.19	-0.25	0.36	-0.19	0.24
70	Geranyl-PP + IPP --> Farnesyl-PP	-0.26	0.18	-0.24	0.35	-0.18	0.23
	2 Farnesyl-PP + 0.5 NADPH + 0.5						
71	NADH --> Squalene	-0.12	0.09	-0.11	0.16	-0.09	0.11
72	Squalene + O2 + NADPH --> Lanosterol	-0.10	0.07	-0.09	0.13	-0.07	0.08
	Lanosterol + 10.5 NADPH + 4.5 NADH +						
73	10 O2 --> Chol + 3 CO2	-0.07	0.05	-0.06	0.09	-0.05	0.06
74	Cholesterol Ester --> Chol + FA-CoA	0.04	0.03	0.04	0.06	0.03	0.04
	2 Palm-CoA + Glycerol-3-P -->						
75	Phosphatidate	-0.19	0.17	-0.05	0.29	0.06	0.30
76	Phosphatidate --> DAG	-0.11	0.09	-0.09	0.17	-0.09	0.10
77	Phosphatidate --> CDP-DAG	-0.05	0.14	0.07	0.25	0.18	0.24
78	CDP-DAG + Ser --> PhosphatidylSerine	0.15	0.17	0.26	0.36	0.34	0.19

79	PhosphatidylSerine --> PhosphatidylEthanolamine + CO2 CDP-DAG + G-3-P -->	0.11	0.12	0.18	0.25	0.23	0.13
80	PhosphatidylGlycerol	-0.17	0.12	-0.16	0.23	-0.13	0.17
81	2 PG --> Cardiolipin + Glycerol DAG + CDP-Choline -->	-0.07	0.05	-0.06	0.09	-0.05	0.07
82	PhosphatidylCholine DAG + CDP-Ethanolamine -->	-0.01	0.02	0.01	0.03	0.00	0.02
83	PhosphatidylEthanolamine	-0.07	0.07	-0.11	0.14	-0.13	0.07
84	Glu + 2 NADPH --> Pro	0.64	0.39	0.75	0.53	0.59	0.39
85	Palm (In)	N.D.	N.D.	0.49	0.10	0.56	0.03

### 3. Values of the metabolic fluxes for day 3

Rxn No.	Equation	BSA		Palm		Ole	
1	G+ATP → G-6-P	26.81	1.18	26.40	6.06	28.18	1.25
2	G-6-P → F-6-P	27.43	0.95	26.73	5.74	28.79	1.21
	F-6-P +ATP → Glyceraldehyde-3-P +						
3	DHAP	27.43	0.95	26.73	5.74	28.79	1.21
4	DHAP → Glyceraldehyde-3-P	27.44	0.95	26.73	5.74	28.80	1.21
5	Glyceraldehyde-3-P → 3-PGA	55.67	1.87	54.06	10.89	58.26	2.32
6	3PGA → PEP + NADH (+ 2ATP)	55.67	1.87	54.06	10.89	58.26	2.32
7	PEP → Pyr	55.67	1.87	54.06	10.89	58.26	2.32
8	Pyruvate + NADH → (Lactate)	49.58	2.68	48.47	7.49	49.89	2.81
9	Pyruvate → Acetyl-CoA + NADH +CO2	4.60	2.42	4.78	12.66	6.64	3.45
10	Acetyl-CoA + OAA → Citrate	8.41	2.21	8.05	3.17	9.16	2.07
	Citrate → a-KetoGlutarate + NADPH						
11	+CO2	8.29	2.20	7.95	3.17	8.98	2.07
	a-Ketoglutarate → Succinyl-CoA +						
12	NADH + CO2	8.85	2.23	8.56	3.17	9.60	2.07
	Succinyl-CoA → Fumarate + FADH2 +						
13	ATP	9.00	2.21	8.67	3.16	9.84	2.07
14	Fumarate → OAA + NADH	8.53	2.21	8.14	3.18	9.34	2.07
15	G-6-P → 12 NADPH + 6 CO2	-0.62	0.57	-0.32	0.41	-0.60	0.17
16	CO2 out	18.56	3.81	19.02	12.01	21.87	4.70
17	2 Acetyl-COA → Acetoacetyl-CoA	-0.75	0.65	0.15	1.51	-1.89	0.62
18	Acetoacetyl-CoA → Acetoacetate	0.23	0.10	1.19	0.47	0.21	0.28
19	Acac out	0.04	0.01	0.45	0.39	0.03	0.07
	Acetoacetate + NADH → (B-OH						
20	butyrate)	0.05	0.02	0.50	0.14	0.09	0.07
21	O2 (In)	21.50	3.45	22.05	5.67	21.83	4.83
22	NADH + 0.5 O2 → 2.5 ATP	34.81	5.52	36.68	9.40	36.16	8.01
23	FADH2 + 0.5 O2 → 2 ATP	9.85	2.19	9.53	3.15	10.89	2.09
24	Glycerol + ATP → Glycerol-3-P	0.60	0.04	0.49	0.41	0.63	0.19
	Glycerol-3-P → Glyceraldehyde-3-P +						
25	NADH	0.79	0.21	0.59	0.83	0.66	0.27
26	Palm-CoA → 8 Acetyl-CoA + 14 NADH	-0.20	0.37	0.31	1.36	-0.38	0.37
27	Palm-CoA + DAG → TG	0.00	0.00	0.04	0.01	0.64	0.12
28	Ser (In)	0.45	0.11	0.59	0.32	0.49	0.06
29	Ser → NH3 + Pyr	0.26	0.40	0.14	0.41	0.08	0.24
30	Gln In	2.34	0.47	2.63	0.37	2.66	0.13
31	His → Glu + NH4	0.41	0.08	0.24	0.13	0.39	0.05
32	Asp (In)	-0.01	0.01	-0.11	0.02	0.00	0.01
33	Glu (In)	-0.73	0.24	-0.63	0.43	-0.59	0.28
34	Gly (In)	0.05	0.07	-0.16	0.22	0.58	0.10
35	Glycine → 2 CO2 + NADH + NH3	-0.39	0.19	-0.63	0.24	-0.11	0.14
36	NH4 (In)	-2.48	0.81	-2.08	0.60	-2.33	0.55
37	Arg In	0.41	0.11	0.32	0.09	0.32	0.06
38	Thr (In)	0.15	0.18	0.24	0.38	0.14	0.10
39	Ala (In)	-1.83	0.26	-1.01	0.58	-1.75	0.62
40	Glu + Pyr → Ala + aKG	1.85	0.24	1.10	0.53	1.84	0.57
41	Pro In	-0.46	0.07	-0.51	0.20	-0.16	0.17

42	Cys In	0.19	0.01	0.09	0.03	0.15	0.00
43	Tyr (In)	0.06	0.04	-0.05	0.20	0.24	0.30
44	Tyr + aKG + 2 O2 --> Glu + CO2 + Acetoacetate + Fumarate	-0.14	0.10	-0.23	0.22	-0.09	0.27
45	Val (In)	0.41	0.01	0.21	0.24	0.47	0.16
46	Om IN	0.01	0.00	-0.04	0.03	0.02	0.01
47	Lys (In)	0.34	0.09	0.27	0.24	0.37	0.10
48	Ile (IN)	0.15	0.06	0.35	0.18	0.48	0.11
49	Leu (In)	0.17	0.05	0.39	0.16	0.48	0.10
50	Phe (In)	0.09	0.03	0.18	0.07	0.19	0.04
51	Glu + Cys + Gly --> GSH HCO3- + NH4 + Om + 2 ATP -->	0.39	0.10	0.37	0.10	0.55	0.06
52	Citrulline Citrulline + Asp + ATP --> Fumarate +	-0.13	0.14	-0.02	0.17	-0.01	0.14
53	Arg	-0.21	0.08	-0.20	0.11	-0.23	0.09
54	Arg --> Om + Urea	0.18	0.14	0.03	0.15	0.00	0.11
55	Urea Out	0.18	0.14	0.03	0.15	0.00	0.11
56	Gln --> Glu + NH4 Om + a-KG + 0.5 NADPH + 0.5 NADH --	2.14	0.40	2.35	0.32	2.26	0.12
57	> Pro	0.30	0.14	-0.08	0.21	-0.07	0.17
58	Asp + NH4 --> Asn Thr --> Pyr + CO2 + NH4 + 2 NADH +	0.12	0.03	0.09	0.05	0.18	0.04
59	FADH2 Val + aKG --> Glu + CO2 + 2NADH +	0.10	0.18	0.15	0.35	0.01	0.11
60	FADH2 + Succ-CoA Lys + 2 aKG + NADPH --> 2Glu +	0.27	0.04	0.03	0.23	0.20	0.15
61	Acetoacetyl-CoA + 2CO2 + 4 NADH + FADH2	0.30	0.09	0.10	0.20	0.19	0.13
62	Ile + aKG --> Glu + Succ-CoA + Acetyl- CoA + NADH + FADH2	0.00	0.07	0.17	0.18	0.21	0.11
63	Leu + aKG --> Glu + HMG-CoA + NADH + FADH2	0.15	0.06	0.30	0.17	0.40	0.11
64	Phe + O2 --> Tyr Ser + 2 Palm-CoA + NADPH --> CO2	-0.06	0.05	0.00	0.10	-0.07	0.07
65	+Ceramide + FADH2 Ceramide + PhosphatidylCholine -->	0.04	0.10	0.11	0.12	0.03	0.03
66	Sphingomyelin Acetoacetyl-CoA + Acetyl-CoA --> HMG-	0.01	0.04	0.04	0.05	0.00	0.01
67	CoA	-0.68	0.61	-0.94	1.41	-1.90	0.51
68	HMG-CoA + 2 NADPH (+ 3ATP) --> IPP	-0.53	0.59	-0.63	1.38	-1.50	0.49
69	2 IPP --> Geranyl-PP	-0.18	0.20	-0.21	0.46	-0.50	0.16
70	Geranyl-PP + IPP --> Farnesyl-PP 2 Farnesyl-PP + 0.5 NADPH + 0.5 NADH	-0.17	0.19	-0.20	0.45	-0.49	0.16
71	--> Squalene	-0.08	0.09	-0.10	0.21	-0.23	0.08
72	Squalene + O2 + NADPH --> Lanosterol Lanosterol + 10.5 NADPH + 4.5 NADH +	-0.06	0.07	-0.07	0.16	-0.18	0.06
73	10 O2 --> Chol + 3 CO2	-0.04	0.05	-0.05	0.12	-0.13	0.04
74	Cholesterol Ester --> Chol + FA-CoA 2 Palm-CoA + Glycerol-3-P -->	0.03	0.03	0.03	0.07	0.08	0.03
75	Phosphatidate	-0.12	0.15	-0.02	0.56	0.18	0.16
76	Phosphatidate --> DAG	-0.07	0.10	-0.07	0.15	0.42	0.12
77	Phosphatidate --> CDP-DAG	-0.03	0.13	0.08	0.40	-0.17	0.17
78	CDP-DAG + Ser --> PhosphatidylSerine	0.10	0.21	0.24	0.21	0.25	0.15



79	PhosphatidylSerine --> PhosphatidylEthanolamine + CO2 CDP-DAG + G-3-P -->	0.08	0.15	0.17	0.14	0.19	0.10
80	PhosphatidylGlycerol	-0.11	0.13	-0.13	0.29	-0.35	0.11
81	2 PG --> Cardiolipin + Glycerol DAG + CDP-Choline -->	-0.04	0.05	-0.05	0.12	-0.14	0.05
82	PhosphatidylCholine DAG + CDP-Ethanolamine -->	0.00	0.01	0.01	0.05	-0.03	0.01
83	PhosphatidylEthanolamine	-0.05	0.08	-0.10	0.08	-0.13	0.06
84	Glu + 2 NADPH --> Pro	0.31	0.17	0.77	0.30	0.50	0.25
85	Palm (In)	N.D.	N.D.	0.48	0.15	0.58	0.03

#### 4. Matlab Program Used for Flux Calculations

```
function mfa(S,M)
% S: stoichiometric matrix
% M: measurement matrix
% where M has the following format:
% column 1: Index vector specifying measured reactions.
% column 2 to k: measurements
% column k + 1: measurement average
% column k + 2: measurement sd
clear;
S = load('StoichOle.txt');
M_in = load('MsrOleD2.txt');

% Get data size
[data_rows,data_columns] = size(M_in);
num_groups = data_columns-3;

%-----
% Identifying Measurement Errors
%-----

M = MsmtErr3(S,M_in);
tot_eqns = length(S);

list = M(:,1);
Gc = S;
Gc(:,list) = [];
disp('The condition no. of Gc matrix is');
disp(cond(Gc));
CN_GC = cond(Gc);
if CN_GC > 10^6
    disp('condition number too high, QUITTING !!!');
    return;
end
Gm = S(:,list);

output = [];
for i = 1:(num_groups+1)
    vm = M(:,i+1);
    temp = mppi(Gc,Gm,vm,S,M);
    output = [output,temp(:,2)];
end;
sd = M(:,data_columns);
var_vm = power(sd,2);
Gc_pi = inv(Gc.*Gc)*Gc.';
B = -Gc_pi*Gm;
[B_row,B_col] = size(B);
for i = 1:B_row
    coeff = B(i,:);
    coeff_2 = power(coeff,2);
    var_vc(i) = coeff_2*var_vm;
end;
var_vc = var_vc.';
```

```

var_top = [compidx(S,M),var_vc];
var_bottom = [list,var_vm];
var = [var_top;var_bottom];
var = sortrows(var,1);
sd = power(var(:,2),0.5);
output = [output,sd];

%write the output matrix
output

% Save?
% save = input('Save? yes or no.\n>','s');
% while (strcmp(save,'yes') | strcmp(save,'no')) == 0
%     save = input('Invalid response. Enter yes or no.\n>','s');
% end;
% if strcmp(save,'no') == 0
%     [fname, pathname] = uiputfile('* .txt','Save Fit Results As');
%     cd(pathname);
%     %save fname output;
%     mwrite(output,fname);
%     disp('Fit results saved.')
% else
%     disp('Fit results not saved.')
% end;

```

## 5. Matlab Program Used for Gross Measurement Identification according to Wang and Stephanopoulos

```
function [MsmtAfterDeln] = MsmtErr3(S,M)

%clear;

list = M(:,1);
n_msr = length(list); %-----Total number of measurements-----
[row_S, colm_S] = size(S);
not_msr = colm_S - n_msr;
x = M(:,2);
%xu = x;
%-----
% Partition the S matrix (bring to the 1st columns those fluxes which are NOT measured)
%-----
Gc = S;
Gc(:,list) = [];
%size(Gc);
Gm = S(:,list);
G = [Gc Gm];

%-----
% Eliminate the unmeasured columns and obtain the 'A' matrix
%-----
G_red = rrefSS(G, n_msr);
%size(G_red)
for i = (not_msr+1) : row_S
    for j = (not_msr+1) : colm_S
        A(i-not_msr,j-not_msr) = G_red(i,j);
    end
end;
[nrow_A, ncol_A] = size(A);

min_msr = ncol_A-nrow_A; %-----Min # of msrmt of just determination-----

%-----
% Obtain the Psi, Epsilon, Phi matrices
%-----

Err = M(:,3);
Xbar = M(:,2);

Psi = diag(Err.*Err);
Eps = -A*Xbar;
Phi = A*Psi*A';
Inv_Phi = pinv(Phi);
h = Eps*Inv_Phi*Eps;

%-----
% Calculate Chi-Square Parameter and compare h with it
%-----
n_fluxEq = length(S);
chi_sq_param = chi2inv(0.9, n_fluxEq-n_msr);
```

```

% disp('Chi_Sq_param = ');
% disp(chi_sq_param);

Msmt4Deln = [];

if h > chi_sq_param
    disp('!!! Error in Measurements: Adjusting values !!!');

    %-----
    %STEP 1 : Initialize
    %-----
    xc = [];
    Ac = [];
    Psi_c = [];
    xu = x;
    Au = A;
    Psi_u = Psi;

    %-----
    % Run the deletion multiple times until h < ChiSqr, or i = n_msr-1
    %-----
    for i = 1:n_msr-1
        [h_a, test_pass, GrossErr] = DelMsmt2(nrow_A, Au, Ac, xu, xc, Psi_u, Psi_c, Eps, Inv_Phi,
n_msr, min_msr,i);

        if test_pass == 1
            Msmt4Deln = [Msmt4Deln, GrossErr];
            index = [];
            for row = 1:n_msr
                for j = 1:length(Msmt4Deln)
                    if (Xbar(row) == Msmt4Deln(j))
                        index = [index,row];
                    end
                end
            end
            disp('The following measurements have gross errors');
            disp(M(index,:));
            M(index,:) = [];
            MsmtAfterDeln = M;
            disp('Success !!!, Errors reduced');
            return
        else
            %-----Find the Index of msmt whose deletion produces the
            %min value of h_a
            l_ha = length(h_a);
            for j = 1:l_ha
                if h_a(j) == min(h_a)
                    %
                    disp('Deleting the foll measurement produces least h');
                    %
                    disp(xu(j));
                    Msmt4Deln = [Msmt4Deln, xu(j)];
                    xc = [xc, xu(j)];
                    xu(j) = [];
                    Ac = [Ac Au(:,j)];
                    Au(:,j) = [];
                    %
                    Au(j,:) = [];
                end
            end
        end
    end
end

```

```

        Psi_c = diag(xc.*xc);
        Psi_u(j,:) = [];
        Psi_u(:,j) = [];
    end %-----End of If h_a == mmin(h_a)
end %-----End of for j = 1:l_ha
end %-----End of If-Else
end %-----End of For Looping

else %-----That is, if h <= chi2param
disp('Good Measurements--Calculating Fluxes .....');
MsmtAfterDeln = M;
end %-----End of If h_a > chi2param

```

```

function [A] = rrefSS(A, n_msr, tol)

```

```

% A modification of the RREF command/ program in Matlab

```

```

[m,n] = size(A);

```

```

% Does it appear that elements of A are ratios of small integers?

```

```

[num, den] = rat(A);

```

```

rats = isequal(A,num./den);

```

```

% Compute the default tolerance if none was provided.

```

```

if (nargin < 3), tol = max(m,n)*eps(class(A))*norm(A,'inf'); end

```

```

% Loop over the entire matrix.

```

```

i = 1;

```

```

j = 1;

```

```

jb = [];

```

```

while (i <= m) && (j <= n_msr)

```

```

% Just change the n here if you want to eliminate

```

```

<n cols

```

```

% Find value and index of largest element in the remainder of column j.

```

```

[p,k] = max(abs(A(i:m,j))); k = k+i-1;

```

```

if (p <= tol)

```

```

% The column is negligible, zero it out.

```

```

A(i:m,j) = zeros(m-i+1,1);

```

```

j = j + 1;

```

```

else

```

```

% Remember column index

```

```

jb = [jb j];

```

```

% Swap i-th and k-th rows.

```

```

A([i k],j:n) = A([k i],j:n);

```

```

% Divide the pivot row by the pivot element.

```

```

A(i,j:n) = A(i,j:n)/A(i,j);

```

```

% Subtract multiples of the pivot row from all the other rows.

```

```

for k = [1:i-1 i+1:m]

```

```

A(k,j:n) = A(k,j:n) - A(k,j)*A(i,j:n);

```

```

end

```

```

i = i + 1;

```

```

j = j + 1;

```

```

end

```

```

end

```

```
% Return "rational" numbers if appropriate.  
if rats  
    [num,den] = rat(A);  
    A=num./den;  
end
```

## 6. Matlab Program Used for the Perturbation Analyses

```
function mfa_Perturb_SS(S,M)

% S: stoichiometric matrix
% M: measurement matrix
% where M has the following format:
% column 1: Index vector specifying measured reactions.
% column 2 to k: measurements
% column k + 1: measurement average
% column k + 2: measurement sd
clear;

S = load('StoichPalm.txt');
M_in = load('MsrPalmD1.txt');

% Get data size
[data_rows,data_columns] = size(M_in);
num_groups = data_columns-3;

%-----
% Identifying Measurement Errors
%-----

M = MsmtErr3(S,M_in);
tot_eqns = length(S);

list = M(:,1);
Gc = S;
Gc(:,list) = [];
disp('The condition no. of Gc matrix is');
disp(cond(Gc));
CN_GC = cond(Gc);
if CN_GC > 10^6
    disp('condition number too high, QUITTING !!!');
    return;
end
Gm = S(:,list);

Varbl = M(27,2);          %Change here for the variable
FluxVals = [];
for Glu = -2*Varbl:0.5*Varbl:2*Varbl
    output = [];
    var_vc = [];
    M(27,2) = Glu;        % Change the index of M corresp to msmt
    for i = 1:(num_groups+1)
        vm = M(:,i+1);
        temp = mppi(Gc,Gm,vm,S,M);
        output = [output,temp(:,2)];
    end;
    sd = M(:,data_columns);
    var_vm = power(sd,2);
    Gc_pi = inv(Gc.*Gc)*Gc.';
    B = -Gc_pi*Gm;
```



```

[B_row,B_col] = size(B);
for i = 1:B_row
    coeff = B(i,:);
    coeff_2 = power(coeff,2);
    var_vc(i) = coeff_2*var_vm;
end;
var_vc = var_vc';
var_top = [compidx(S,M), var_vc];
var_bottom = [list,var_vm];
var = [var_top;var_bottom];
var = sortrows(var,1);
sd = power(var(:,2),0.5);
output = [output,sd];
FluxVals = [FluxVals, output];
end

%-----Change the file name Acc to the Amino Acid-----
dlmwrite('EffectPalmVarnD1.txt', FluxVals, 'delimiter', '\t');

```

## BIBLIOGRAPHY

1. Agafonov A, Gritsenko E, Belosludtsev K, Kovalev A, Gateau-Roesch O, Saris NE, Mironova GD. A permeability transition in liposomes induced by the formation of Ca<sup>2+</sup>/palmitic acid complexes. *Biochim Biophys Acta*. 2003 Jan 31;1609(2):153-60.
2. Ahuja HS, Szanto A, Nagy L, and Davies PJ. The retinoid X receptor and its ligands: versatile regulators of metabolic function, cell differentiation and cell death. *J Biol Regul Homeost Agents*. 2003 Jan-Mar;17(1):29-45.
3. Ajuwon KM, Spurlock ME. Palmitate activates the NF-kappaB transcription factor and induces IL-6 and TNFalpha expression in 3T3-L1 adipocytes. *J Nutr*. 2005 Aug;135(8):1841-6.
4. Al-Shahrour F, Minguez P, Vaquerizas JM, Conde L and Dopazo J. Babelomics: a suite of web-tools for functional annotation and analysis of group of genes in high-throughput experiments, *Nucleic Acids Research* 2005; 33(Web Server issue): W460-W464.
5. Anderson ME and Meister A. Intracellular delivery of cysteine. *Methods Enzymol*. 1987;143: 313-326.
6. Andrieu-Abadie N, Gouaze V, Salvayre R, Levade T. Ceramide in apoptosis signaling: relationship with oxidative stress. *Free Radic Biol Med*. 2001 Sep 15;31(6):717-28.
7. Angulo P, Lindor KD. Non-alcoholic fatty liver disease. *J Gastroenterol Hepatol*. 2002 Feb;17 Suppl:S186-90.
8. Armstrong JS. Mitochondrial membrane permeabilization: the sine qua non for cell death. *Bioessays*. 2006 Mar;28(3):253-60.
9. Astrup A. The role of dietary fat in obesity. *Semin Vasc Med*. 2005 Feb;5(1):40-7.
10. Bandyopadhyay S, Zhan R, Wang Y, Pai SK, Hirota S, Hosobe S, Takano Y, Saito K, Furuta E, Iizumi M, Mohinta S, Watabe M, Chalfant C, and Watabe K. Mechanism of apoptosis induced by the inhibition of fatty acid synthase in breast cancer cells. *Cancer Res*. 2006 Jun 1;66(11):5934-40.
11. Barnard, M. L. and S. Matalon. Mechanisms of extracellular reactive oxygen species injury to the pulmonary microvasculature. *J Appl Physiol*. 1992 May; 72(5): 1724-9.
12. Basnakian AG, Ueda N, Hong X, Galitovsky VE, Yin X, Shah SV. Ceramide synthase is essential for endonuclease-mediated death of renal tubular epithelial

- cells induced by hypoxia-reoxygenation. *Am J Physiol Renal Physiol*. 2005 Feb;288(2):F308-14..
13. Beehler CJ, Ely ME, Rutledge KS, Simchuk ML, Reiss OK, Shanley PF, Repine JE. Toxic effects of dimethylthiourea in rats. *J Lab Clin Med*. 1994 Jan;123(1):73-80.
  14. Beisvag V, Junge FK, Bergum H, Jolsum L, Lydersen S, Gunther CC, Ramampiaro H, Langaas M, Sandvik AK, Laegreid A. GeneTools--application for functional annotation and statistical hypothesis testing. *BMC Bioinformatics*. 2006 Oct 24;7:470.
  15. Bennett BL, Satoh Y, and Lewis AJ. JNK: a new therapeutic target for diabetes. *Curr Opin Pharmacol*. 2003 Aug;3(4):420-5.
  16. Bernardi P, Penzo D, Wojtczak L. Mitochondrial energy dissipation by fatty acids. Mechanisms and implications for cell death. *Vitam Horm*. 2002;65:97-126.
  17. Bernardi P, Broekemeier KM, Pfeiffer DR. Recent progress on regulation of the mitochondrial permeability transition pore; a cyclosporin-sensitive pore in the inner mitochondrial membrane. *J Bioenerg Biomembr*. 1994 Oct;26(5):509-17.
  18. Berridge MJ. The endoplasmic reticulum: a multifunctional signaling organelle. *Cell Calcium*. 2002 Nov-Dec;32(5-6):235-49.
  19. Bligh, E. G. and W. J. Dyer. A rapid method of total lipid extraction and purification. *Can J Biochem Physiol* 1959 Aug;37(8): 911-7.
  20. Boden G, She P, Mozzoli M, Cheung P, Gumireddy K, Reddy P, Xiang X, Luo Z, and Ruderman N. Free fatty acids produce insulin resistance and activate the proinflammatory nuclear factor-kappaB pathway in rat liver. *Diabetes*. 2005 Dec;54(12):3458-65.
  21. Boden G. Role of fatty acids in the pathogenesis of insulin resistance and NIDDM. *Diabetes*. 1997 Jan;46(1):3-10.
  22. Boden G, Chen X, Capulong E, Mozzoli M. Effects of free fatty acids on gluconeogenesis and autoregulation of glucose production in type 2 diabetes. *Diabetes*. 2001 Apr;50(4):810-6.
  23. Bradham CA, Plumpe J, Manns MP, Brenner DA, Trautwein C. Mechanisms of hepatic toxicity. I. TNF-induced liver injury. *Am J Physiol*. 1998 Sep;275(3 Pt 1):G387-92.
  24. Brown M.P.S., Grundy W.N., Lin D., Cristianini N., Sugnet C., Furey T.S., Ares M., Jr., Haussler D. Knowledge-based analysis of microarray gene expression data using support vector machines. *Proc. Natl. Acad. Sci. USA* 2000 97(1):262-267.

25. Browning JD, Szczepaniak LS, Dobbins R, Nuremberg P, Horton JD, Cohen JC, et al. Prevalence of hepatic steatosis in an urban population in the United States: impact of ethnicity. *Hepatology* 2004; 40: 1387-1395.
26. Brownsey RW, Boone AN, Elliott JE, Kulpa JE, and Lee WM. Regulation of acetyl-CoA carboxylase. *Biochem Soc Trans.* 2006 Apr;34(Pt 2):223-7.
27. Bruce CR, Dyck DJ. Cytokine regulation of skeletal muscle fatty acid metabolism: effect of interleukin-6 and tumor necrosis factor-alpha. *Am J Physiol Endocrinol Metab.* 2004 Oct;287(4):E616-21.
28. Bruck R, Aeed H, Shirin H, Matas Z, Zaidel L, Avni Y, Halpern Z. The hydroxyl radical scavengers dimethylsulfoxide and dimethylthiourea protect rats against thioacetamide-induced fulminant hepatic failure. *J Hepatol.* 1999 Jul;31(1):27-38.
29. Brun T, Assimacopoulos-Jeannet F, Corkey BE, and Prentki M. Long-chain fatty acids inhibit acetyl-CoA carboxylase gene expression in the pancreatic beta-cell line INS-1. *Diabetes.* 1997 Mar;46(3):393-400.
30. Brusselmans K, De Schrijver E, Verhoeven G, and Swinnen JV. RNA interference-mediated silencing of the acetyl-CoA-carboxylase-alpha gene induces growth inhibition and apoptosis of prostate cancer cells. *Cancer Res.* 2005 Aug 1;65(15):6719-25.
31. Cai LQ, Imperato-McGinley J, and Zhu YS. Regulation of prostate 5alpha-reductase-2 gene expression and prostate weight by dietary fat and caloric intake in the rat. *Prostate.* 2006 May 15;66(7):738-48.
32. Cantley LC. The phosphoinositide 3-kinase pathway. *Science.* 2002 May 31;296(5573):1655-7.
33. Cederbaum AI, Dicker E, Rubin E, Cohen G. The effect of dimethylsulfoxide and other hydroxyl radical scavengers on the oxidation of ethanol by rat liver microsomes. *Biochem Biophys Res Commun.* 1977 Oct 24;78(4):1254-62.
34. Chajes V, Cambot M, Moreau K, Lenoir GM, and Joulin V. Acetyl-CoA carboxylase alpha is essential to breast cancer cell survival. *Cancer Res.* 2006 May 15;66(10):5287-94.
35. Chan C, Berthiaume F, Lee K, Yarmush ML. Metabolic flux analysis of cultured hepatocytes exposed to plasma. *Biotechnol Bioeng.* 2003 Jan 5;81(1):33-49.
36. Chan C, Berthiaume F, Lee K, Yarmush ML. Metabolic flux analysis of hepatocyte function in hormone- and amino acid-supplemented plasma. *Metab Eng.* 2003 Jan;5(1):1-15.

37. Chan C, Hwang D, Stephanopoulos GN, Yarmush ML, Stephanopoulos G. Application of multivariate analysis to optimize function of cultured hepatocytes. *Biotechnol Prog.* 2003 Mar-Apr;19(2):580-98.
38. Chan SL, Yu VC. Proteins of the bcl-2 family in apoptosis signalling: from mechanistic insights to therapeutic opportunities. *Clin Exp Pharmacol Physiol.* 2004 Mar;31(3):119-28.
39. Chang Y, Wang J, Lu X, Thewke DP, Mason RJ. KGF induces lipogenic genes through a PI3K and JNK/SREBP-1 pathway in H292 cells. *J Lipid Res.* 2005 Dec;46(12):2624-35.
40. Cheema SK and Agellon LB. Metabolism of cholesterol is altered in the liver of C3H mice fed fats enriched with different C-18 fatty acids. *J Nutr.* 1999 Sep;129(9):1718-24.
41. Chen T, Guo L, Zhang L, Shi L, Fang H, Sun Y, Fuscoe JC, Mei N. Gene Expression Profiles Distinguish the Carcinogenic Effects of Aristolochic Acid in Target (Kidney) and Non-target (Liver) Tissues in Rats. *BMC Bioinformatics.* 2006 Sep 26;7 Suppl 2:S20
42. Chen WH, Tzeng SF. Pituitary adenylate cyclase-activating polypeptide prevents cell death in the spinal cord with traumatic injury. *Neurosci Lett.* 2005 Aug 12-19;384(1-2):117-21.
43. Chen Q, Vazquez EJ, Moghaddas S, Hoppel CL, Lesnefsky EJ. Production of reactive oxygen species by mitochondria: central role of complex III. *J Biol Chem.* 2003 Sep 19;278(38):36027-31.
44. Chia DJ, Boston BA. Childhood obesity and the metabolic syndrome. *Adv Pediatr.* 2006;53:23-53.
45. Cho JH, Lee D, Park JH, Lee IB. Gene selection and classification from microarray data using kernel machine. *FEBS Lett.* 2004 Jul 30;571(1-3):93-8.
46. Cnop M, Hannaert JC, Hoorens A, Eizirik DL, Pipeleers DG. Inverse relationship between cytotoxicity of free fatty acids in pancreatic islet cells and cellular triglyceride accumulation. *Diabetes.* 2001 Aug;50(8):1771-7.
47. Coleman RA, Lee DP. Enzymes of triacylglycerol synthesis and their regulation. *Prog Lipid Res.* 2004 Mar;43(2):134-76.
48. Cossarizza A, Ceccarelli D, Masini A. Functional heterogeneity of an isolated mitochondrial population revealed by cytofluorometric analysis at the single organelle level. *Exp Cell Res.* 1996 Jan 10;222(1):84-94.
49. Cousin SP, Hugl SR, Wrede CE, Kajio H, Myers MG Jr, and Rhodes CJ. Free fatty acid-induced inhibition of glucose and insulin-like growth factor I-induced

- deoxyribonucleic acid synthesis in the pancreatic beta-cell line INS-1. *Endocrinology*. 2001 Jan;142(1):229-40.
50. Cutler RG, Pedersen WA, Camandola S, Rothstein JD, Mattson MP. Evidence that accumulation of ceramides and cholesterol esters mediates oxidative stress-induced death of motor neurons in amyotrophic lateral sclerosis. *Ann Neurol*. 2002 Oct;52(4):448-57.
  51. D'Ambrosio SM, Gibson-D'Ambrosio RE, Brady T, Oberyszyn AS, Robertson FM. Mechanisms of nitric oxide-induced cytotoxicity in normal human hepatocytes. *Environ Mol Mutagen* 2001;37:46-54.
  52. Dashti N, Feng Q, Franklin FA. Long-term effects of cis and trans monounsaturated (18:1) and saturated (16:0) fatty acids on the synthesis and secretion of apolipoprotein A-I- and apolipoprotein B-containing lipoproteins in HepG2 cells. *Journal of Lipid Research* 2000;41:1980-1990.
  53. Dave S, Farrance DP, Whitehead SA. Evidence that nitric oxide inhibits steroidogenesis in cultured rat granulosa cells. *Clin Sci (Lond)* 1997;92:277-284.
  54. Day CP, James OF. Steatohepatitis: a tale of two "hits"? *Gastroenterology*. 1998 Apr;114(4):842-5.
  55. DeFronzo RA. Dysfunctional fat cells, lipotoxicity and type 2 diabetes. *Int J Clin Pract Suppl*. 2004 Oct;(143):9-21.
  56. Degtyarev MY, Spiegel AM, Jones TL. The G protein alpha s subunit incorporates [3H]palmitic acid and mutation of cysteine-3 prevents this modification. *Biochemistry*. 1993 Aug 17;32(32):8057-61.
  57. Devireddy LR, Teodoro JG, Richard FA, and Green MR. Induction of apoptosis by a secreted lipocalin that is transcriptionally regulated by IL-3 deprivation. *Science*. 2001 Aug 3;293(5531):829-34.
  58. Dickson LM, and Rhodes CJ. Pancreatic beta-cell growth and survival in the onset of type 2 diabetes: a role for protein kinase B in the Akt? *Am J Physiol Endocrinol Metab*. 2004 Aug;287(2):E192-8.
  59. Ding W-X, Shen H-M, Ong C-N. Critical role of reactive oxygen species and mitochondrial permeability transition in microcystin-induced rapid apoptosis in rat hepatocytes. *Hepatology (Philadelphia)* 2000;32:547-555.
  60. Draghici S, Khatri P, Bhavsar P, Shah A, Krawetz SA, Tainsky MA. Onto-Tools, the toolkit of the modern biologist: Onto-Express, Onto-Compare, Onto-Design and Onto-Translate. *Nucleic Acids Res*. 2003;31:3775-3781.

61. Dringen R, Hamprecht B. Involvement of glutathione peroxidase and catalase in the disposal of exogenous hydrogen peroxide by cultured astroglial cells. *Brain Res* 1997;759:67-75.
62. Dymkowska D, Szczepanowska J, Wieckowski MR, Wojtczak L. Short-term and long-term effects of fatty acids in rat hepatoma AS-30D cells: the way to apoptosis. *Biochim Biophys Acta*. 2006 Feb;1763(2):152-63.
63. Edelstein LC, Lagos L, Simmons M, Tirumalai H, and Gelinas C. NF-kappa B-dependent assembly of an enhanceosome-like complex on the promoter region of apoptosis inhibitor Bfl-1/A1. *Mol Cell Biol*. 2003 Apr;23(8):2749-61.
64. El-Assaad W, Buteau J, Peyot M-L, Nolan C, Roduit R, Hardy S, Joly E, et al. Saturated fatty acids synergize with elevated glucose to cause pancreatic b-cell death. *Endocrinology* 2003;144:4154-4163.
65. Farrell GC, Larter CZ. Nonalcoholic fatty liver disease: from steatosis to cirrhosis. *Hepatology*. 2006 Feb;43(2 Suppl 1):S99-S112.
66. Felber JP, Golay A. Pathways from obesity to diabetes. *Int J Obes Relat Metab Disord*. 2002 Sep;26 Suppl 2:S39-45.
67. Feldstein AE, Werneburg NW, Canbay A, Guicciardi ME, Bronk SF, Rydzewski R, Burgart LJ, et al. Free fatty acids promote hepatic lipotoxicity by stimulating TNF-alpha expression via a lysosomal pathway. *Hepatology* 2004;40:185-194.
68. Feldstein AE, Werneburg NW, Li Z, Bronk SF, Gores GJ. Bax inhibition protects against free fatty acid-induced lysosomal permeabilization. *Am J Physiol Gastrointest Liver Physiol*. 2006 Jun;290(6):G1339-46.
69. Fernanda Cury-Boaventura M, Cristine Kanunfre C, Gorjao R, Martins de Lima T, Curi R. Mechanisms involved in Jurkat cell death induced by oleic and linoleic acids. *Clin Nutr*. 2006 Dec;25(6):1004-14.
70. France-Lanord V, Brugg B, Michel PP, Agid Y, Ruberg M. Mitochondrial free radical signal in ceramide-dependent apoptosis: a putative mechanism for neuronal death in Parkinson's disease. *J Neurochem* 1997;69:1612-1621.
71. Fujita N and Tsuruo T. Survival-signaling pathway as a promising target for cancer chemotherapy. *Cancer Chemother Pharmacol*. 2003 Jul;52 Suppl 1:S24-8.
72. Fukui K, Wada T, Kagawa S, Nagira K, Ikubo M, Ishihara H, Kobayashi M, Sasaoka T. Impact of the liver-specific expression of SHIP2 (SH2-containing inositol 5'-phosphatase 2) on insulin signaling and glucose metabolism in mice. *Diabetes*. 2005 Jul;54(7):1958-67.
73. Gardner DK, Lane M. Amino acids and ammonium regulate mouse embryo development in culture. *Biol Reprod*. 1993 Feb;48(2):377-85.

74. Gibbons GF, Khurana R, Odwell A, Seelaender MC. Lipid balance in HepG2 cells: active synthesis and impaired mobilization. *J Lipid Res.* 1994 Oct;35(10):1801-8.
75. Glosli H, Gudbrandsen OA, Mullen AJ, Halvorsen B, Rost TH, Wergedahl H, Prydz H, Aukrust P, and Berge RK. Down-regulated expression of PPARalpha target genes, reduced fatty acid oxidation and altered fatty acid composition in the liver of mice transgenic for hTNFalpha. *Biochim Biophys Acta.* 2005 Jun 1;1734(3):235-46.
76. Glosli H, Tronstad KJ, Wergedal H, Muller F, Svardal A, Aukrust P, Berge RK, Prydz H. Human TNF-alpha in transgenic mice induces differential changes in redox status and glutathione-regulating enzymes. *FASEB J.* 2002 Sep;16(11):1450-2.
77. Gogvadze V, Walter PB, Ames BN. The role of Fe<sup>2+</sup>-induced lipid peroxidation in the initiation of the mitochondrial permeability transition. *Arch Biochem Biophys* 2003;414:255-260.
78. Gomez EO, Mendoza-Milla C, Ibarra-Sanchez MJ, Ventura-Gallegos JL, Zentella A. Ceramide reproduces late appearance of oxidative stress during TNF-mediated cell death in L929 cells. *Biochem Biophys Res Commun* 1996;228:505-509.
79. Gong P, Cederbaum AI. Transcription factor Nrf2 protects HepG2 cells against CYP2E1 plus arachidonic acid-dependent toxicity. *J Biol Chem.* 2006 May 26;281(21):14573-9.
80. Greutter CA and Lemke SM (1985) Dissociation of cysteine and glutathione levels from nitroglycerin-induced relaxation. *Eur J Pharmacol* 111: 85-95.
81. Griffin JL, Bonney SA, Mann C, Hebbachi AM, Gibbons GF, Nicholson JK, Shoulders CC, Scott J. An integrated reverse functional genomic and metabolic approach to understanding orotic acid-induced fatty liver. *Physiol Genomics.* 2004 Apr 13;17(2):140-9. Grivennikova VG, Vinogradov AD. Generation of superoxide by the mitochondrial Complex I. *Biochim Biophys Acta* 2006.
82. Guo L, Zhang L, Sun Y, Muskhelishvili L, Blann E, Dial S, Shi L, Schroth G, Dragan YP. Differences in hepatotoxicity and gene expression profiles by anti-diabetic PPAR gamma agonists on rat primary hepatocytes and human HepG2 cells. *Mol Divers.* 2006 Aug;10(3):349-60.
83. Halestrap AP, Connern CP, Griffiths EJ, Kerr PM. Cyclosporin A binding to mitochondrial cyclophilin inhibits the permeability transition pore and protects hearts from ischaemia/reperfusion injury. *Mol Cell Biochem* 1997;174:167-172.
84. Halestrap AP, Woodfield KY, Connern CP. Oxidative stress, thiol reagents, and membrane potential modulate the mitochondrial permeability transition by affecting nucleotide binding to the adenine nucleotide translocase. *J Biol Chem* 1997;272:3346-3354.



85. Hamacher-Brady A, Brady NR, Logue SE, Sayen MR, Jinno M, Kirshenbaum LA, Gottlieb RA, and Gustafsson AB. Response to myocardial ischemia/reperfusion injury involves Bnip3 and autophagy. *Cell Death Differ*. 2006 Apr 28.
86. Hansen HO, Grunnet I, and Knudsen J. Triacylglycerol synthesis in goat mammary gland. Factors influencing the esterification of fatty acids synthesized de novo. *Biochem J*. 1984 Jun 1;220(2):521-7.
87. Hansen HO, Grunnet I, and Knudsen J. Triacylglycerol synthesis in goat mammary gland. The effect of ATP, Mg<sup>2+</sup> and glycerol 3-phosphate on the esterification of fatty acids synthesized de novo. *Biochem J*. 1984 Jun 1;220(2):513-9.
88. Hashimoto K, Farrow BJ, Evers BM. Activation and role of MAP kinases in 15d-PGJ2-induced apoptosis in the human pancreatic cancer cell line MIA PaCa-2. *Pancreas*. 2004 Mar;28(2):153-9.
89. Hennig B, Lei W, Arzuaga X, Ghosh DD, Saraswathi V, Toborek M. Linoleic acid induces proinflammatory events in vascular endothelial cells via activation of PI3K/Akt and ERK1/2 signaling. *J Nutr Biochem*. 2006 Nov;17(11):766-72.
90. Hewlett EL, Donato GM, Gray MC. Macrophage cytotoxicity produced by adenylate cyclase toxin from *Bordetella pertussis*: more than just making cyclic AMP! *Mol Microbiol*. 2006 Jan;59(2):447-59.
91. Higa M, Shimabukuro M, Shimajiri Y, Takasu N, Shinjyo T, and Inaba T. Protein kinase B/Akt signalling is required for palmitate-induced beta-cell lipotoxicity. *Diabetes Obes Metab*. 2006 Mar;8(2):228-33.
92. Hirosumi J, Tuncman G, Chang L, Gorgun CZ, Uysal KT, Maeda K, Karin M, and Hotamisligil GS. A central role for JNK in obesity and insulin resistance. *Nature*. 2002 Nov 21;420(6913):333-6.
93. Hong-Ping G, Bao-Shan KU. Neuroprotective effect of L-lysine monohydrochloride on acute iterative anoxia in rats with quantitative analysis of electrocorticogram. *Life Sci*. 1999;65(2):PL19-25.
94. [http://www.ncbi.nlm.nih.gov/entrez/query.fcgi?db=gene&cmd=Retrieve&dopt=full\\_report&list\\_uids=1183](http://www.ncbi.nlm.nih.gov/entrez/query.fcgi?db=gene&cmd=Retrieve&dopt=full_report&list_uids=1183)
95. [http://www.ncbi.nlm.nih.gov/entrez/query.fcgi?db=gene&cmd=Retrieve&dopt=full\\_report&list\\_uids=535](http://www.ncbi.nlm.nih.gov/entrez/query.fcgi?db=gene&cmd=Retrieve&dopt=full_report&list_uids=535)
96. [http://www.ncbi.nlm.nih.gov/entrez/query.fcgi?db=gene&cmd=Retrieve&dopt=full\\_report&list\\_uids=9550](http://www.ncbi.nlm.nih.gov/entrez/query.fcgi?db=gene&cmd=Retrieve&dopt=full_report&list_uids=9550)
97. Huang ZZ, Chen C, Zeng Z, Yang H, Oh J, Chen L, Lu SC. Mechanism and significance of increased glutathione level in human hepatocellular carcinoma and liver regeneration. *FASEB J*. 2001 Jan;15(1):19-21.

98. Hwang D, Alevizos I, Schmitt WA, Misra J, Ohyama H, Todd R, Mahadevappa M, Warrington JA, Stephanopoulos G, Wong DT, Stephanopoulos G. Genomic dissection for characterization of cancerous oral epithelium tissues using transcription profiling. *Oral Oncol.* 2003 Apr;39(3):259-68.
99. Ichihara K, and Tanaka C. Some properties of progesterone 5 alpha-reductase solubilized from rat liver microsomes. *Biochem Int.* 1987 Nov;15(5):1005-11.
100. Imazu T, Shimizu S, Tagami S, Matsushima M, Nakamura Y, Miki T, Okuyama A, and Tsujimoto Y. Bcl-2/E1B 19 kDa-interacting protein 3-like protein (Bnip3L) interacts with bcl-2/Bcl-xL and induces apoptosis by altering mitochondrial membrane permeability. *Oncogene.* 1999 Aug 12;18(32):4523-9.
101. Isenberg JS, Klaunig JE. Role of the mitochondrial membrane permeability transition (MPT) in rotenone-induced apoptosis in liver cells. *Toxicol Sci* 2000;53:340-351.
102. Issandou M, Guillard R, Boullay AB, Linhart V, Lopez-Perez E. Up-regulation of low-density lipoprotein receptor in human hepatocytes is induced by sequestration of free cholesterol in the endosomal/lysosomal compartment. *Biochem Pharmacol.* 2004 Jun 15;67(12):2281-9.
103. Ji J, Zhang L, Wang P, Mu YM, Zhu XY, Wu YY, Yu H, Zhang B, Chen SM, and Sun XZ. Saturated free fatty acid, palmitic acid, induces apoptosis in fetal hepatocytes in culture. *Exp Toxicol Pathol.* 2005 Apr;56(6):369-76.
104. Jimenez-Lopez JM, Carrasco MP, Marco C, and Segovia JL. Hexadecylphosphocholine disrupts cholesterol homeostasis and induces the accumulation of free cholesterol in HepG2 tumour cells. *Biochem Pharmacol.* 2006 Apr 14;71(8):1114-21.
105. Joffe BI, Goldberg RB, Seftel HC, Distiller LA. Insulin, glucose and triglyceride relationships in obese African subjects. *Am J Clin Nutr.* 1975 Jun;28(6):616-20.
106. Joseph RR, Yazer E, Hanakawa Y, Stadnyk AW. Prostaglandins and activation of AC/cAMP prevents anoikis in IEC-18. Apoptosis. 2005 Dec;10(6):1221-33.
107. Jove M, Planavila A, Sanchez RM, Merlos M, Laguna JC, Vazquez-Carrera M. Palmitate induces tumor necrosis factor-alpha expression in C2C12 skeletal muscle cells by a mechanism involving protein kinase C and nuclear factor-kappaB activation. *Endocrinology.* 2006 Jan;147(1):552-61.
108. Kadenbach B. Intrinsic and extrinsic uncoupling of oxidative phosphorylation. *Biochim Biophys Acta* 2003;1604:77-94.
109. Karin M and Gallagher E. From JNK to pay dirt: jun kinases, their biochemistry, physiology and clinical importance. *IUBMB Life.* 2005 Apr-May;57(4-5):283-95.

110. Kennedy BP and Ramachandran C. Protein tyrosine phosphatase-1B in diabetes. *Biochem Pharmacol.* 2000 Oct 1;60(7):877-83.
111. Kim BJ, Forbes NS. Flux analysis shows that hypoxia-inducible-factor-1-alpha minimally affects intracellular metabolism in tumor spheroids. *Biotechnol Bioeng.* 2006 Sep 28;
112. Kim BJ, Ryu SW, Song BJ. JNK- and p38 kinase-mediated phosphorylation of Bax leads to its activation and mitochondrial translocation and to apoptosis of human hepatoma HepG2 cells. *J Biol Chem.* 2006 Jul 28;281(30):21256-65.
113. Kim Y-M, de Vera ME, Watkins SC, Billiar TR. Nitric oxide protects cultured rat hepatocytes from tumor necrosis factor-a-induced apoptosis by inducing heat shock protein 70 expression. *Journal of Biological Chemistry* 1997;272:1402-1411.
114. Kim Y-M, Kim T-H, Chung H-T, Talanian RV, Yin X-M, Billiar TR. Nitric oxide prevents tumor necrosis factor a-induced rat hepatocyte apoptosis by the interruption of mitochondrial apoptotic signaling through S-nitrosylation of caspase-8. *Hepatology (Philadelphia)* 2000;32:770-778.
115. Kisseleva MV, Cao L, and Majerus PW. Phosphoinositide-specific inositol polyphosphate 5-phosphatase IV inhibits Akt/protein kinase B phosphorylation and leads to apoptotic cell death. *J Biol Chem.* 2002 Feb 22;277(8):6266-72.
116. Kojima H, Sakurai S, Uemura M, Takekawa T, Morimoto H, Tamagawa Y, Fukui H. Difference and similarity between non-alcoholic steatohepatitis and alcoholic liver disease. *Alcohol Clin Exp Res.* 2005 Dec;29(12 Suppl):259S-63S.
117. Kong JY, Rabkin SW. Palmitate-induced apoptosis in cardiomyocytes is mediated through alterations in mitochondria: prevention by cyclosporin A. *Biochimica et Biophysica Acta* 2000;1485:45-55.
118. Kroemer G, Dallaporta B, Resche-Rigon M. The mitochondrial death/life regulator in apoptosis and necrosis. *Annu Rev Physiol* 1998;60:619-642.
119. Laurent A, Nicco C, Tran Van Nhieu J, Borderie D, Chereau C, Conti F, Jaffray P, et al. Pivotal role of superoxide anion and beneficial effect of antioxidant molecules in murine steatohepatitis. *Hepatology* 2004;39:1277-1285.
120. Le Phillip P, Bahl A, Ungar LH. Using prior knowledge to improve genetic network reconstruction from microarray data. *In Silico Biol.* 2004;4(3):335-53.
121. Lee JI, Kang J, and Stipanuk MH. Differential regulation of glutamate-cysteine ligase subunit expression and increased holoenzyme formation in response to cysteine deprivation. *Biochem J.* 2006 January 1; 393(Pt 1): 181-190.
122. Lee JS, Pinnamaneni SK, Eo SJ, Cho IH, Pyo JH, Kim CK, Sinclair AJ, Febbraio MA, Watt MJ. Saturated, but not n-6 polyunsaturated, fatty acids induce insulin

- resistance: role of intramuscular accumulation of lipid metabolites. *J Appl Physiol*. 2006 May;100(5):1467-74.
123. Lee K, Berthiaume F, Stephanopoulos GN, Yarmush ML. Profiling of dynamic changes in hypermetabolic livers. *Biotechnol Bioeng*. 2003 Aug 20;83(4):400-15.
  124. Lee M, Bae MA. Docosahexaenoic acid induces apoptosis in CYP2E1-containing HepG2 cells by activating the c-Jun N-terminal protein kinase related mitochondrial damage. *J Nutr Biochem*. 2006 Sep 7.
  125. Leo C, Horn LC, and Hockel M. Hypoxia and expression of the proapoptotic regulator BNIP3 in cervical cancer. *Int J Gynecol Cancer*. 2006 May-Jun;16(3):1314-20.
  126. Li J, Li LJ, Chao HC, Yang Q, Liu XL, Sheng JF, Yu HY, Huang JR. Isolation and short term cultivation of swine hepatocytes for bioartificial liver support system. *Hepatobiliary Pancreat Dis Int*. 2005 May;4(2):249-53.
  127. Li Z, and Chan C. Integrating gene expression and metabolic profiles. *J Biol Chem*. 2004 Jun 25;279(26):27124-37.
  128. Liang T and Liao S. Inhibition of steroid 5 alpha-reductase by specific aliphatic unsaturated fatty acids. *Biochem J*. 1992 Jul 15;285 ( Pt 2):557-62.
  129. Lim G, Wang S, Lim JA, Mao J. Activity of adenylyl cyclase and protein kinase A contributes to morphine-induced spinal apoptosis. *Neurosci Lett*. 2005 Dec 2;389(2):104-8.
  130. Linder et al., *Proc. Natl. Acad. Sci. USA* 90 (1993) 3675-3679.
  131. Listenberger LL, Han X, Lewis SE, Cases S, Farese RV Jr, Ory DS, and Schaffer JE. Triglyceride accumulation protects against fatty acid-induced lipotoxicity. *Proc Natl Acad Sci U S A*. 2003 Mar 18;100(6):3077-82.
  132. Listenberger LL, Ory DS, Schaffer JE. Palmitate-induced apoptosis can occur through a ceramide-independent pathway. *J Biol Chem*. 2001 May 4;276(18):14890-5.
  133. Littler DR, Assaad NN, Harrop SJ, Brown LJ, Pankhurst GJ, Luciani P, Aguilar MI, Mazzanti M, Berryman MA, Breit SN, Curmi PM. Crystal structure of the soluble form of the redox-regulated chloride ion channel protein CLIC4. *FEBS J*. 2005 Oct;272(19):4996-5007.
  134. Liu JJ, Cutler G, Li W, Pan Z, Peng S, Hoey T, Chen L, Ling XB. Multiclass cancer classification and biomarker discovery using GA-based algorithms. *Bioinformatics*. 2005 Jun 1;21(11):2691-7.

135. Liu Y, Fiskum G, Schubert D. Generation of reactive oxygen species by the mitochondrial electron transport chain. *J Neurochem* 2002;80:780-787.
136. Lu SC, Huang HY. Comparison of sulfur amino acid utilization for GSH synthesis between HepG2 cells and cultured rat hepatocytes. *Biochem Pharmacol.* 1994 Mar 2;47(5):859-69.
137. Lu SC. Regulation of hepatic glutathione synthesis: current concepts and controversies. *FASEB J.* 1999 Jul;13(10):1169-83.
138. Lu YF, Chiang CF. Effect of dietary cholesterol and fat levels on lipid peroxidation and the activities of antioxidant enzymes in rats. *Int J Vitam Nutr Res* 2001;71:339-346.
139. Lu Z-H, Mu Y-M, Wang B-A, Li X-L, Lu J-M, Li J-Y, Pan C-Y, et al. Saturated free fatty acids, palmitic acid and stearic acid, induce apoptosis by stimulation of ceramide generation in rat testicular Leydig cell. *Biochemical and Biophysical Research Communications* 2003;303:1002-1007.
140. Maas JW Jr, Indacochea RA, Muglia LM, Tran TT, Vogt SK, West T, Benz A, Shute AA, Holtzman DM, Mennerick S, Olney JW, Muglia LJ. Calcium-stimulated adenylyl cyclases modulate ethanol-induced neurodegeneration in the neonatal brain. *J Neurosci.* 2005 Mar 2;25(9):2376-85.
141. Maestre I, Jordan J, Calvo S, Reig JA, Cena V, Soria B, Prentki M, et al. Mitochondrial dysfunction is involved in apoptosis induced by serum withdrawal and fatty acids in the b-cell line INS-1. *Endocrinology* 2003;144:335-345.
142. Malhi H, Bronk SF, Werneburg NW, Gores GJ. Free fatty acids induce JNK-dependent hepatocyte lipoapoptosis. *J Biol Chem.* 2006 Apr 28;281(17):12093-101.
143. Manco M, Mingrone G, Greco AV, Capristo E, Gniuli D, De Gaetano A, and Gasbarrini G. Insulin resistance directly correlates with increased saturated fatty acids in skeletal muscle triglycerides. *Metabolism.* 2000 Feb;49(2):220-4.
144. McCullough AJ. Pathophysiology of nonalcoholic steatohepatitis. *J Clin Gastroenterol.* 2006 Mar;40(3 Suppl 1):S17-29.
145. Menendez JA, Mehmi I, Atlas E, Colomer R, and Lupu R. Novel signaling molecules implicated in tumor-associated fatty acid synthase-dependent breast cancer cell proliferation and survival: Role of exogenous dietary fatty acids, p53-p21WAF1/CIP1, ERK1/2 MAPK, p27KIP1, BRCA1, and NF-kappaB. *Int J Oncol.* 2004 Mar;24(3):591-608.
146. Mensink M, Blaak EE, van Baak MA, Wagenmakers AJ, Saris WH. Plasma free Fatty Acid uptake and oxidation are already diminished in subjects at high risk for developing type 2 diabetes. *Diabetes* 2001;50:2548-2554.

147. Miglietta A, Bozzo F, Bocca C, Gabriel L, Trombetta A, Belotti S, Canuto RA. Conjugated linoleic acid induces apoptosis in MDA-MB-231 breast cancer cells through ERK/MAPK signalling and mitochondrial pathway. *Cancer Lett.* 2006 Mar 28;234(2):149-57.
148. Minnich A, Tian N, Byan L, Bilder G. A potent PPARalpha agonist stimulates mitochondrial fatty acid beta-oxidation in liver and skeletal muscle. *Am J Physiol Endocrinol Metab.* 2001 Feb;280(2):E270-9.
149. Mitsui H, Takuwa N, Maruyama T, Maekawa H, Hirayama M, Sawatari T, Hashimoto N, Takuwa Y, Kimura S. The MEK1-ERK map kinase pathway and the PI 3-kinase-Akt pathway independently mediate anti-apoptotic signals in HepG2 liver cancer cells. *Int J Cancer.* 2001 Apr 1;92(1):55-62.
150. Miyazaki M, Kim YC, and Ntambi JM. A lipogenic diet in mice with a disruption of the stearoyl-CoA desaturase 1 gene reveals a stringent requirement of endogenous monounsaturated fatty acids for triglyceride synthesis. *J Lipid Res.* 2001 Jul;42(7):1018-24.
151. Miyazaki M, Kim YC, Gray-Keller MP, Attie AD, and Ntambi JM. The biosynthesis of hepatic cholesterol esters and triglycerides is impaired in mice with a disruption of the gene for stearoyl-CoA desaturase 1. *J Biol Chem.* 2000 Sep 29;275(39):30132-8.
152. Mollner S, Beck K, Pfeuffer T. Acylation of adenylyl cyclase catalyst is important for enzymic activity. *FEBS Lett.* 1995 Sep 11;371(3):241-4.
153. Morrison JL, Breitling R, Higham DJ, Gilbert DR. GeneRank: using search engine technology for the analysis of microarray experiments. *BMC Bioinformatics.* 2005 Sep 21;6:233.
154. Musashi M, Ota S, Shiroshita N. The role of protein kinase C isoforms in cell proliferation and apoptosis. *Int J Hematol.* 2000 Jul;72(1):12-9.
155. Negrotto S, Pacienza N, D'Atri LP, Pozner RG, Malaver E, Torres O, Lazzari MA, Gomez RM, Schattner M. Activation of cyclic AMP pathway prevents CD34(+) cell apoptosis. *Exp Hematol.* 2006 Oct;34(10):1420-8.
156. Newsholme P, Keane D, Welters HJ, Morgan NG. Life and death decisions of the pancreatic beta-cell: the role of fatty acids. *Clin Sci (Lond).* 2007 Jan;112(1):27-42.
157. Nguyen GH, French R, Radhakrishna H. Protein kinase A inhibits lysophosphatidic acid induction of serum response factor via alterations in the actin cytoskeleton. *Cell Signal.* 2004 Oct;16(10):1141-51.
158. Ni TC and Savageau MA. Application of biochemical systems theory to metabolism in human red blood cells. Signal propagation and accuracy of representation. *Journal of biological chemistry* 1996;271:7927-41.

159. Ni TC and Savageau MA. Model assessment and refinement using strategies from biochemical systems theory: application to metabolism in human red blood cells. *Journal of theoretical biology* 1996;179:329-68.
160. Niknahad H, Khan S, O'Brien PJ. Hepatocyte injury resulting from the inhibition of mitochondrial respiration at low oxygen concentrations involves reductive stress and oxygen activation. *Chem Biol Interact* 1995;98:27-44.
161. Nohl H, Gille L, Staniek K. Intracellular generation of reactive oxygen species by mitochondria. *Biochem Pharmacol* 2005;69:719-723.
162. Okuyama R, Fujiwara T, Ohsumi J. High glucose potentiates palmitate-induced NO-mediated cytotoxicity through generation of superoxide in clonal b-cell HIT-T15. *FEBS Letters* 2003;545:219-223.
163. Oliver MF, Opie LH. Effects of glucose and fatty acids on myocardial ischaemia and arrhythmias. *Lancet*. 1994;343:155-158.
164. Olsen C. An enzymatic fluorimetric micromethod for the determination of acetoacetate, -hydroxybutyrate, pyruvate and lactate. *Clin Chim Acta*. 1971 Jul;33(2):293-300.
165. Ono H, Shimano H, Katagiri H, Yahagi N, Sakoda H, Onishi Y, Anai M, Ogihara T, Fujishiro M, Viana AY, Fukushima Y, Abe M, Shojima N, Kikuchi M, Yamada N, Oka Y, and Asano T. Hepatic Akt activation induces marked hypoglycemia, hepatomegaly, and hypertriglyceridemia with sterol regulatory element binding protein involvement. *Diabetes*. 2003 Dec;52(12):2905-13.
166. Ostrander DB, Sparagna GC, Amoscato AA, McMillin JB, Dowhan W. Decreased cardiolipin synthesis corresponds with cytochrome c release in palmitate-induced cardiomyocyte apoptosis. *Journal of Biological Chemistry* 2001;276:38061-38067.
167. Pan W. Incorporating biological information as a prior in an empirical bayes approach to analyzing microarray data. *Stat Appl Genet Mol Biol*. 2005;4:Article12.
168. Petronilli V, Cola C, Massari S, Colonna R, Bernardi P. Physiological effectors modify voltage sensing by the cyclosporin A-sensitive permeability transition pore of mitochondria. *J Biol Chem* 1993;268:21939-21945.
169. Picollo A, Pusch M. Chloride/proton antiporter activity of mammalian CLC proteins CLC-4 and CLC-5. *Nature*. 2005 Jul 21;436(7049):420-3.
170. Qanungo S, Wang M, and Nieminen AL. N-Acetyl-L-cysteine Enhances Apoptosis through Inhibition of Nuclear Factor- $\kappa$ B in Hypoxic Murine Embryonic Fibroblasts. *J. Biol. Chem.*, Vol. 279, Issue 48, 50455-50464, November 26, 2004.

171. Randle PJ. The interrelationships of hormones, fatty acid and glucose in the provision of energy. *Postgrad Med J*. 1964 Aug;40:457-63.
172. Raynaud JP, Cousse H, and Martin PM. Inhibition of type 1 and type 2 5alpha-reductase activity by free fatty acids, active ingredients of Permixon. *J Steroid Biochem Mol Biol*. 2002 Oct;82(2-3):233-9.
173. Remizov O, Jakubov R, Dufer M, Krippeit Drews P, Drews G, Waring M, Brabant G, Wienbergen A, Rustenbeck I, Schofl C. Palmitate-induced Ca<sup>2+</sup>-signaling in pancreatic beta-cells. *Mol Cell Endocrinol*. 2003 Dec 30;212(1-2):1-9.
174. Resh MD. Palmitoylation of ligands, receptors, and intracellular signaling molecules. *Sci STKE*. 2006 Oct 31;2006(359):re14.
175. Roden M. Muscle triglycerides and mitochondrial function: possible mechanisms for the development of type 2 diabetes. *Int J Obes (Lond)*. 2005 Sep;29 Suppl 2:S111-5.
176. Ruvolo PP. Intracellular signal transduction pathways activated by ceramide and its metabolites. *Pharmacol Res*. 2003 May;47(5):383-92.
177. Rys-Sikora KE and Gill DL. Fatty acid-mediated calcium sequestration within intracellular calcium pools. *J Biol Chem*. 1998 Dec 4;273(49):32627-35.
178. Sandler S, Andersson A. The partial protective effect of the hydroxyl radical scavenger dimethyl urea on streptozotocin-induced diabetes in the mouse in vivo and in vitro. *Diabetologia* 1982;23:374-378.
179. Sanyal AJ, Campbell-Sargent C, Mirshahi F, Rizzo WB, Contos MJ, Sterling RK, Luketic VA, Shiffman ML, and Clore JN. Nonalcoholic steatohepatitis: association of insulin resistance and mitochondrial abnormalities. *Gastroenterology*. 2001 Apr;120(5):1183-92.
180. Sasaoka T, Wada T, and Tsuneki H. Lipid phosphatases as a possible therapeutic target in cases of type 2 diabetes and obesity. *Pharmacol Ther*. 2006 Jul 12
181. Sato H, Shiiya A, Kimata M, Maebara K, Tamba M, Sakakura Y, Makino N, Sugiyama F, Yagami K, Moriguchi T, Takahashi S, Bannai S. Redox imbalance in cystine/glutamate transporter-deficient mice. *J Biol Chem*. 2005 Nov 11;280(45):37423-9.
182. Schattenberg JM, Singh R, Wang Y, Lefkowitz JH, Rigoli RM, Scherer PE, Czaja MJ. JNK1 but not JNK2 promotes the development of steatohepatitis in mice. *Hepatology*. 2006 Jan;43(1):163-72.
183. Scheen AJ, Luyckx FH. Obesity and liver disease. *Best Pract Res Clin Endocrinol Metab*. 2002 Dec;16(4):703-16.



184. Schonfeld P, Bohnensack R. Fatty acid-promoted mitochondrial permeability transition by membrane depolarization and binding to the ADP/ATP carrier. *FEBS Lett* 1997;420:167-170.
185. Schuchmann M, Galle PR. Dead or alive -- NF-kappaB, the guardian which tips the balance. *J Hepatol.* 2002 Jun;36(6):827-8.
186. Shi CS and Kehrl JH. Tumor necrosis factor (TNF)-induced germinal center kinase-related (GCKR) and stress-activated protein kinase (SAPK) activation depends upon the E2/E3 complex Ubc13-Uev1A/TNF receptor-associated factor 2 (TRAF2). *J Biol Chem.* 2003 Apr 25;278(17):15429-34.
187. Shimabukuro M, Ohneda M, Lee Y, Unger RH. Role of nitric oxide in obesity-induced beta cell disease. *J Clin Invest* 1997;100:290-295.
188. Shimabukuro M, Zhou YT, Levi M, Unger RH. Fatty acid-induced beta cell apoptosis: a link between obesity and diabetes. *Proc Natl Acad Sci U S A.* 1998 Mar 3;95(5):2498-502.
189. Simbula G, Columbano A, Ledda-Columbano GM, Sanna L, Deidda M, Diana A, Pibiri M. Increased ROS generation and p53 activation in alpha-lipoic acid-induced apoptosis of hepatoma cells. *Apoptosis.* 2006 Nov 21
190. Skowronski R, Hollenbeck CB, Varasteh BB, Chen YD, Reaven GM. Regulation of non-esterified fatty acid and glycerol concentration by insulin in normal individuals and patients with type 2 diabetes. *Diabet Med* 1991;8:330-333.
191. Skurk T, Alberti-Huber C, Herder C, Hauner H. Relationship between adipocyte size and adipokine expression and secretion. *J Clin Endocrinol Metab.* 2006.
192. Sleeman MW, Wortley KE, Lai KM, Gowen LC, Kintner J, Kline WO, Garcia K, Stitt TN, and Yancopoulos GD, Wiegand SJ, and Glass DJ. Absence of the lipid phosphatase SHIP2 confers resistance to dietary obesity. *Nat Med.* 2005 Feb;11(2):199-205.
193. Srivastava S and Chan C. Hydrogen peroxide and hydroxyl radicals mediate palmitate toxicity to human hepatoma cells: relation to mitochondrial permeability transition. *Free Rad Res.* 2007 Jan; 41(1):38-49.
194. Starkov AA, Fiskum G. Regulation of brain mitochondrial H<sub>2</sub>O<sub>2</sub> production by membrane potential and NAD(P)H redox state. *J Neurochem.* 2003 Sep;86(5):1101-7.
195. Strange K, Denton J, and Nehrke K. Ste20-type kinases: evolutionarily conserved regulators of ion transport and cell volume. *Physiology (Bethesda).* 2006 Feb;21:61-8.

196. Stroemblad G, Bjoerntorp P. Reduced hepatic insulin clearance in rats with dietary-induced obesity. *Metabolism, Clinical and Experimental* 1986;35:323-327.
197. Su F, Schneider RJ. Hepatitis B virus HBx protein sensitizes cells to apoptotic killing by tumor necrosis factor alpha. *Proc Natl Acad Sci U S A* 1997;94:8744-8749.
198. Subramanian A, Tamayo P, Mootha VK, Mukherjee S, Ebert BL, Gillette MA, Paulovich A, Pomeroy SL, Golub TR, Lander ES, Mesirov JP. Gene set enrichment analysis: a knowledge-based approach for interpreting genome-wide expression profiles. *Proc Natl Acad Sci U S A*. 2005 Oct 25;102(43):15545-50.
199. Swagell CD, Henly DC, Morris CP. Expression analysis of a human hepatic cell line in response to palmitate. *Biochem Biophys Res Commun*. 2005 Mar 11;328(2):432-41.
200. Tabas I. Consequences of cellular cholesterol accumulation: basic concepts and physiological implications. *J Clin Invest*. 2002 Oct;110(7):905-11.
201. Takahashi T, Tang T, Lai NC, Roth DM, Rebolledo B, Saito M, Lew WY, Clopton P, Hammond HK. Increased cardiac adenylyl cyclase expression is associated with increased survival after myocardial infarction. *Circulation*. 2006 Aug 1;114(5):388-96.
202. Tan Y, Shi L, Tong W, Hwang GT, Wang C. Multi-class tumor classification by discriminant partial least squares using microarray gene expression data and assessment of classification models. *Comput Biol Chem*. 2004 Jul;28(3):235-44.
203. Tan Y, Shi L, Tong W, Wang C. Multi-class cancer classification by total principal component regression (TPCR) using microarray gene expression data. *Nucleic Acids Res*. 2005 Jan 7;33(1):56-65.
204. Tanaka N, Aoyama T. Mechanism of the onset and development of hepatic steatosis and PPAR. *Cell (Tokyo, Japan)* 2001;33:289-292.
205. Taub R. Liver regeneration 4: transcriptional control of liver regeneration. *FASEB J*. 1996 Mar;10(4):413-27.
206. Tietge UJ, Sun G, Czarnecki S, Yu Q, Lohse P, Du H, Grabowski GA, Glick JM, Rader DJ. Phenotypic correction of lipid storage and growth arrest in wolman disease fibroblasts by gene transfer of lysosomal acid lipase. *Hum Gene Ther*. 2001 Feb 10;12(3):279-89.
207. Tiwari M, Kumar A, Sinha RA, Shrivastava A, Balapure AK, Sharma R, Bajpai VK, et al. Mechanism of 4-HPR induced apoptosis in glioma cells: evidences suggesting role of mitochondrial-mediated pathway and endoplasmic reticulum stress. *Carcinogenesis* 2006.

208. Troyanskaya OG, Garber ME, Brown PO, Botstein D, Altman RB. Nonparametric methods for identifying differentially expressed genes in microarray data. *Bioinformatics*. 2002 Nov;18(11):1454-61.
209. Tuttle RL, Gill NS, Pugh W, Lee JP, Koeberlein B, Furth EE, Polonsky KS, Naji A, and Birnbaum MJ. Regulation of pancreatic beta-cell growth and survival by the serine/threonine protein kinase Akt1/PKBalpha. *Nat Med*. 2001 Oct;7(10):1133-7.
210. Ueki K, Kondo T, Tseng YH, Kahn CR. Central role of suppressors of cytokine signaling proteins in hepatic steatosis, insulin resistance, and the metabolic syndrome in the mouse. *Proc Natl Acad Sci U S A*. 2004 Jul 13;101(28):10422-7.
211. Van Der Westhuizen L, Shephard GS, Snyman SD, Abel S, Swanevelder S, Gelderblom WCA. Inhibition of sphingolipid biosynthesis in rat primary hepatocyte cultures by fumonisin B1 and other structurally related compounds. *Food and Chemical Toxicology* 1998;36:497-503.
212. Van ISC, Van Der Wouden JM, Liebisch G, Schmitz G, Hoekstra D. Polarized membrane traffic and cell polarity development is dependent on dihydroceramide synthase-regulated sphinganine turnover. *Mol Biol Cell* 2004;15:4115-4124.
213. Verbsky J and Majerus PW. Increased levels of inositol hexakisphosphate (InsP6) protect HEK293 cells from tumor necrosis factor (alpha)- and Fas-induced apoptosis. *J Biol Chem*. 2005 Aug 12;280(32):29263-8.
214. Verbsky JW, Chang SC, Wilson MP, Mochizuki Y, and Majerus PW. The pathway for the production of inositol hexakisphosphate in human cells. *J Biol Chem*. 2005 Jan 21;280(3):1911-20.
215. Voth DE, Hamm EE, Nguyen LG, Tucker AE, Salles II, Ortiz-Leduc W, Ballard JD. *Bacillus anthracis* oedema toxin as a cause of tissue necrosis and cell type-specific cytotoxicity. *Cell Microbiol*. 2005 Aug;7(8):1139-49.
216. Vugmeyster Y, Borodovsky A, Maurice MM, Maehr R, Furman MH, and Ploegh HL. The ubiquitin-proteasome pathway in thymocyte apoptosis: caspase-dependent processing of the deubiquitinating enzyme USP7 (HAUSP). *Mol Immunol*. 2002 Nov;39(7-8):431-41.
217. Wagman AS and Nuss JM. Current therapies and emerging targets for the treatment of diabetes. *Curr Pharm Des*. 2001 Apr;7(6):417-50.
218. Wang A, Xia T, Ran P, Chen X, Nuessler AK. Qualitative study of three cell culture methods. *J Huazhong Univ Sci Technolog Med Sci*. 2002;22(4):288-91.
219. Wang D and Sul HS. (1998) Insulin stimulation of the fatty acid synthase promoter is mediated by the phosphatidylinositol 3-kinase pathway: involvement of protein kinase B/Akt. *J Biol Chem*. 1998 Sep 25;273(39):25420-6.

220. Wang D, Wei Y, Pagliassotti MJ. Saturated fatty acids promote endoplasmic reticulum stress and liver injury in rats with hepatic steatosis. *Endocrinology*. 2006 Feb;147(2):943-51.
221. Wang Z, Wang Y, Xuan J, Dong Y, Bakay M, Feng Y, Clarke R, Hoffman EP. Optimized multilayer perceptrons for molecular classification and diagnosis using genomic data. *Bioinformatics*. 2006 Mar 15;22(6):755-61.
222. Wei Y, Wang D, Topczewski F, Pagliassotti MJ. Saturated fatty acids induce endoplasmic reticulum stress and apoptosis independently of ceramide in liver cells. *Am J Physiol Endocrinol Metab*. 2006 Aug;291(2):E275-81.
223. Weinberg JM. Lipotoxicity. *Kidney Int*. 2006 Nov;70(9):1560-6.
224. Weiss JN, Korge P, Honda HM, Ping P. Role of the mitochondrial permeability transition in myocardial disease. *Circ Res* 2003;93:292-301.
225. Whiteman M, Rose P, Siau JL, Cheung NS, Tan GS, Halliwell B, Armstrong JS. Hypochlorous acid-mediated mitochondrial dysfunction and apoptosis in human hepatoma HepG2 and human fetal liver cells: role of mitochondrial permeability transition. *Free Radic Biol Med* 2005;38:1571-1584.
226. Wieckowski MR, Wojtczak L. Fatty acid-induced uncoupling of oxidative phosphorylation is partly due to opening of the mitochondrial permeability transition pore. *FEBS Lett* 1998;423:339-342.
227. Wild AC, Moinova HR, and Mulcahy RT. Regulation of gamma -Glutamylcysteine Synthetase Subunit Gene Expression by the Transcription Factor Nrf2. *J Biol Chem*, Vol. 274, Issue 47, 33627-33636, November 19, 1999.
228. Woerle HJ, Popa E, Dostou J, Welle S, Gerich J, Meyer C. Exogenous insulin replacement in type 2 diabetes reverses excessive hepatic glucose release, but not excessive renal glucose release and impaired free fatty acid clearance. *Metabolism* 2002;51:1494-1500.
229. Wojtczak L, Schonfeld P. Effect of fatty acids on energy coupling processes in mitochondria. *Biochim Biophys Acta* 1993;1183:41-57.
230. Yamagishi S-i, Okamoto T, Amano S, Inagaki Y, Koga K, Koga M, Choei H, et al. Palmitate-induced apoptosis of microvascular endothelial cells and pericytes. *Molecular Medicine (Baltimore, MD, United States)* 2002;8:179-184.
231. Yamaguchi M, Miyashita Y, Kumagai Y, Kojo S. Change in liver and plasma ceramides during D-galactosamine-induced acute hepatic injury by LC-MS/MS. *Bioorg Med Chem Lett* 2004;14:4061-4064.

232. Yu MU, Yoo JM, Lee YS, Lee YM, Hong JT, Oh KW, Song S, et al. Altered de novo sphingolipid biosynthesis is involved in the serum deprivation-induced cell death in LLC-PK1 cells. *J Toxicol Environ Health A* 2004;67:2085-2094.
233. Yuan YV, Kitts DD, Godin DV. Variations in dietary fat and cholesterol intakes modify antioxidant status of SHR and WKY rats. *J Nutr* 1998;128:1620-1630.
234. Zegura B, Sedmak B, Filipic M. Microcystin-LR induces oxidative DNA damage in human hepatoma cell line HepG2. *Toxicon* 2003;41:41-48.

MICHIGAN STATE UNIVERSITY LIBRARIES



3 1293 02845 8762